



TECHNICKÁ UNIVERZITA V LIBERCI
Fakulta textilní



NANOFILTRATION MEMBRANES BASED ON NANOFIBROUS MATERIAL

Baturalp YALCINKAYA

2016

ABSTRACT

Fabrication of nanofibrous material has become the center of attraction by the researchers due to their unique physical properties for instance high porosity and super thin fiber diameter. Electrospinning of various polymers has gained advanced chemical properties to the nanofibrous materials besides physical ones. During the last decade, the interest in the use of the nanofibrous material, in particular, has emerged in water treatment. However, even now, the main limitation of using the nanofibrous material, especially in liquid filtration, is their weak properties and low adhesion to the other surface. Hence, the motivation of this thesis was to overcome the mechanical properties issue of nanofibers layer and prepare them as a nanofiltration membrane for separation of salt.

The main goal of this dissertation was fabrication and optimization of thin film composite membranes based on laminated nanofibrous and nonwoven composite materials and investigation of their filtration performance against to mono and divalent salt solution. The best filtration (selectivity and flux) by the active barrier layer was achieved by optimizing four parameters: the monomer solution concentration, the reaction time for monomer polymerization, the drying time and the post-treatment temperature (Chapter 3). At each step of the process, one of the optimum conditions, indicated by filtration performance, was selected and the investigation proceeded to the next step. The filtration performance of the fabricated thin film nanofibrous composite (TFNC) membranes was compared to the performance of reference samples, including commercial ones. The TFNC (2) membrane based on *m*-phenylenediamine monomers showed a higher rejection of NaCl salt ions (93.57%) at a lower flux when compared to commercial NF90 membranes. The flux performances of the piperazine monomer-based TFNC (1) and (3) membranes, were about 10 and 100% higher, respectively, than that of a commercial NF270 membrane, while maintaining the same MgSO₄ salt rejection rate (95.6 and 93.5%, respectively).

Once, the optimization of thin film nanofibrous composite membrane was done for liquid filtration and salt separation, the enhancement of filtration performance carried out using additives (Chapter 4). Surfactants were used to increase hydrophilicity and flux performance of TFNC membranes whereas acid acceptors were used to increase salt rejection performance. The filtration performance was performed using four different salt solutions with dead-end filtration cell in chapter 4. Piperazine monomer-based membranes that were prepared by adding acid acceptor were able to reject 98.8 % MgSO₄ and 97.4% Na₂SO₄ with high flux 40.5 L m⁻²

h^{-1} and $23.2 \text{ L m}^{-2} \text{ h}^{-1}$ respectively. The rejection rates of monovalent salts were lower than divalent salts using PIP-based membranes such as 25.9 % CaCl_2 and 18.3 % NaCl . *M*-phenylenediamine monomer-based membranes, which were prepared by adding surfactants and acid acceptor, showed higher rejection performance in four kinds of salts solutions in comparison with PIP based membranes. The rejection rates of MgSO_4 , Na_2SO_4 , CaCl_2 and NaCl salts solution were 98.5 %, 98.3 %, 97.4 % and 96.3 % respectively while the flux performance was increased four times higher, than that of TFNC (2).

The filtration of real seawater showed that the combination of prepared PIP and MPD based TFNC membranes were performed good salt ions rejection from seawater. However, to retain the salt ions from the seawater was impossible all at once. The first filtration attempt was not able retained sufficient amount of salt ions from seawater. For this reason, the same feed seawater was circulated and was used more than once while the same membrane fixed on the dead-end cell. For instance, the same feed seawater circulated six times with same PIP-based membrane and two times with same MPD-based membrane. Finally, TFNC membranes were succeeded retain 80 % of salt ions from seawater.

All the laminated membranes were showed high mechanical strength under the applied pressure, and there was no breakdown during the filtration process. Therefore, this study gave insight on the industrial role of nanofibrous and nonwoven fabric as a supporting membrane to fabricate high mechanical performance nanofiltration membranes.

Keywords: Nanofiltration, nanofibers, reverse osmosis, polyamide, lamination, desalination, thin film nanofibrous composite, interfacial polymerization.

ANOTACE

Tato práce se zabývá studiem procesů odsolování roztoků solí pomocí vodné filtrace. Konkrétně se zabývá konstrukcí a výrobou filtračních membrán s využitím nanovláknenných materiálů.

Výroba a použití nanovláknenných materiálů se stala díky svým vlastnostem, jako je například poróznost, zájmem vědců v mnoha oblastech. Během poslední doby je jednou z oblastí zájmu také problematika úpravy vlastností vody. Avšak, do této doby hlavním problémem použití nanovláknenných materiálů pro filtraci vody, jsou špatné mechanické vlastnosti zmíněných materiálů. Proto motivací této práce bylo zlepšení mechanických vlastností nanovláknenných materiálů a příprava nanovláknenných membrán vhodných pro filtraci vody, konkrétně pro odsolování vody.

Hlavním cílem práce byla příprava a optimalizace kompozitních membrán, složených z nanovláknenných materiálů, netkané textilie a tenkého polymerního filmu. U takto připravených filtračních membrán byla studována a sledována schopnost filtrovat jednomocné a dvojmocné soli z vodního roztoku. Nejlepších filtračních vlastností připravovaných membrán, bylo dosaženo optimalizací vlastností polymerního filmu, který lze nazvat jako aktivní bariérová vrstva. Toho bylo dosaženo optimalizací čtyř základních parametrů: koncentrací roztoků monomerů, reakčním časem polymerizace, časem sušení a teplotou, které jsou membrány vystaveny po sušení. Každý z těchto parametrů měl vliv na konečné vlastnosti membrány a optimální parametry byly stanovovány krok po kroku.

Vlastnosti všech připravených membrán, nanovláknenných kompozitů s tenkým polymerním filmem (TFNC), byly porovnány s komerčně dostupnými membránami, které sloužily jako referenční vzorky. Jako solné roztoky byly použity roztoky $MgSO_4$, Na_2SO_4 , $CaCl_2$, $NaCl$.

TFNC membrána vyrobená za použití monomerů m-fenyl diaminu vykazovala vyšší efektivitu záchytu $NaCl$ iontů a vyšší průtok než komerční membrána NF90. Dosažený průtok membrán s polymerním filmem připraveným z monomerů piperazinu byl o 10-100% vyšší než u komerční membrány NF 270 při zachování podobné efektivitě záchytu soli $MgSO_4$.

Pro dosažení ještě lepších výsledků, zvýšení efektivitě záchytu a většího průtoku, bylo přidáváno několik typů aditiv do roztoků monomerů před mezifázovou polymerizací. Touto úpravou je dosaženo až 96 % záchytu iontů $NaCl$. Výsledky jsou uvedeny v práci.

V experimentální části se práce dále zabývá problematikou odsolování skutečné mořské vody. Výsledkem je membrána TFNC, která je schopna odstranit 80 % iontů soli z mořské vody. Práce se také zabývá opakovaným použitím membrán a jejich mechanickými vlastnostmi.

Klíčová slova:

Nanofiltrace, Nanovlákna, reversní osmóza, polyamid, laminace, odsolování vody, kompozit, mezifázová polymerizace

ACKNOWLEDGEMENT

I would like to thank my supervisor **Ing. Jiří Chaloupek Ph.D.** for his assistance, guidance and friendship throughout my study and research. Thanks also go to my colleague at the Department of the Nonwoven and Nanofibrous materials.

I would like to express my gratitude to **Prof. RNDr. Oldřich Jirsák, CSc.** for his inestimable advice and support during my research activity.

I express my deepest love and gratitude to my family and my wife, **Fatma** who put her faith in me and urged me to do better.

I thank profusely to Bc. Filip Sanetrník for his kind help and co-operation throughout my study period.

Many thanks go to Student Grant Competition financed by Ministry of Education, Youth and Sport (No: 21041, Manufacture of polymeric membranes based on nanofibrous layers, 2014) for funding my experimental expenses.

Special thanks go to, Ing. Jana Müllerová, Ph.D., Mgr, Pavel Hrabak, Ph.D., Mrs. Hana Pohlreichova and Mrs. Daniela Myšáková for their great support in analytic experimental of my dissertation.

My thanks and appreciations go to **Ing. Hana Musilová** and **Mrs. Bohumila Keilová** who have willingly helped me out with their abilities.

CONTENT

Abstract	i
Anotace.....	iii
Acknowledgement.....	v
Content	vi
List of symbols	ix
List of Figures	xiii
List of Tables.....	xvi
Chapter 1	17
General Introduction	17
Chapter 2	20
Theoretical Part	20
2.1. Nanofibers	20
2.2. Electrospinning.....	20
2.3. Membranes	21
2.3.1. Membrane Structure.....	21
2.3.1.1. Symmetric membranes.....	22
2.3.1.2. Asymmetric membranes	22
2.3.2. Interfacial polymerization	23
2.3.3. Filtration methods	23
2.3.4. Membrane separation properties.....	24
2.4. Parameters of interfacial polymerized membranes	24
2.4.1. Interactions of dependent parameters and independent parameters.....	25
2.4.1.1. Type of monomer and its solutions.....	25
2.4.1.2. Reaction time of monomer solutions	27
2.4.1.3. Drying method and time	27
2.4.1.4. Post reactions and treatments.....	27
2.5. Membrane Transport Theory.....	28
2.6. Application of nanofibrous scaffolds in liquid filtration.....	30
2.6.1. Nanofibers in microfiltration	30
2.6.2. Nanofibers in ultrafiltration	32
2.6.3. Nanofibers in nanofiltration	33
2.6.4. Nanofibers in reverse osmosis	35
2.6.5. Nanofibers in forward osmosis	35
2.6.6. Improved mechanical strength of nanofibers in liquid filtration	35
2.6.7. Effects of additives on the thin film composite membranes.....	37

2.7. Application of lamination process for nanofibers	38
2.8. Motivation and scope of this thesis	39
Chapter 3	40
Fabrication and optimization of thin film nanofibrous composite membranes for removal of salts.....	40
3.1. Introduction	40
3.2. Experimental.....	40
3.2.1. Materials	40
3.2.2. Preparation of electrospun PA6 porous nanofibrous layer	41
3.2.3. Lamination of nonwoven and nanofibrous materials.....	41
3.2.4. Preparation and optimization of active barrier layer.....	42
3.2.5. TFNC membrane performance evaluation.....	43
3.2.6. Characterization of NNC scaffold and TFNC membrane.....	44
3.3. Results and discussion	45
3.3.1. Characteristic of NNC scaffolds and TFNC membranes.....	45
3.3.2. Optimization and evaluation of TFNC membranes	47
3.3.2.1. Various concentration of monomer solutions	48
3.3.2.2. Reaction time in monomer solutions (contact time)	55
3.3.2.3. Determination of drying method and time	58
3.3.2.4. Determination of curing temperature	60
3.3.2.5. Comparison with commercial membranes.....	61
3.4. Conclusion.....	63
Chapter 4	65
Enhancement filtration properties of thin film nanofibrous composite membranes	65
4.1. Introduction	65
4.2. Experimental.....	66
4.2.1. Materials	66
4.2.2. Preparation of enhanced TFNC membranes	66
4.2.3. Liquid chromatography analysis	67
4.2.4. Characterization of enhanced TFNC membranes	67
4.2.5. Molecular weight cut-off (MWCO) test using aqueous PEG solutions	68
4.2.6. Evaluation of filtration performance.....	68
4.3. Results and discussion	68
4.3.1. Characteristic of enhanced TFNC membranes	68
4.3.2. Filtration Performance of Enhanced PIP-based TFNC membranes	74
4.3.3. Filtration Performance of Enhanced MPD-based TFNC membranes	81
4.3.4. Determination of Molecular weight cut-off of the TFNC membranes	86

4.3.5. Analysis of real seawater filtration	87
4.3.6. Conclusion	90
Chapter 5	93
General Conclusion	93
Referances	96

LIST OF SYMBOLS

Symbol	Long name	Unit
PP/PE	Polypropylene / Polyethylene nonwoven	
PA6	Polyamide 6	
NNC	Nonwoven and nanofibrous composite	
TFC	Thin film composite	
TFNC (1 - 2 – 3)	Thin film nanofibrous composite (1 – 2 – 3)	
PIP	Piperazine	
MPD	<i>m</i> -pheylenediamine	
TMC	Trimesoylchloride	
TEA	Triethylamine	
	Nanometer	nm
	Micrometer	μm
IP	Interfacial polymerization	
MF	Microfiltration	
UF	Ultrafiltration	
NF	Nanofiltration	
FO	Forward osmosis	

d	Diameter	m
ΔP ; ΔC ; ΔE	Driving force	
ppm	Parts per million	
NaOH	Sodium hydroxide	
Na ₂ SO ₄	Sodium sulfite	
MgSO ₄	Magnesium sulfate	
CaCl ₂	Calcium chloride	
NaCl	Sodium chloride	
<i>J_i</i>	Flux	L/m ² h
<i>D_i</i>	Diffusion coefficient	
<i>dc_i/dx</i>	Concentration gradient	
<i>dp/dx</i>	Pressure gradient	
<i>C_i</i>	Concentration of component	
<i>K'</i>	Coefficient reflecting the nature of the medium	
BSA	Bovine serum albumin	
RC	Regenerated cellulose	
EM	Electrospun Membrane	
PTT	Poly trimethylene terephthalate	

PVA	Polyvinyl alcohol	
TiO ₂	Titanium dioxide	
PAN	Polyacrylonitrile	
PES	Polyethersulfone	
PSf	Polysulfone	
PANI	Polyaniline	
PVDF	Polyvinylidene fluoride	
PEG	Polyethylene glycol	
PI	Polyimide	
CA	Cellulose acetate	
DMF	Dimethylformamide	
NMP	N-Methyl-2-pyrrolidone	
PET	Polyethylene terephthalate	
PDA	Polydopamine	
	Kilovolt	kV
cf	Conductivity of feed water	S
cp	Conductivity of permeate water	S
Ra	Average roughness	nm

RMS	Root mean square	nm
Rt	Peak to valley roughness	nm
w/v	Weight divided volume	%
	Applied pressure	bar
rpm	Revolutions per minute	
PIP+TEA	Piperazine and triethylamine based	
MPD+TEA	<i>m</i> -phenylenediamine and triethylamine based	
MPD+TEA+Tr-X	<i>m</i> -phenylenediamine, triethylamine and Triton-X 100based	
MPD+TEA+Sy-AH	<i>m</i> -phenylenediamine, triethylamine and Synferol-AH based	

LIST OF FIGURES

Figure 2.1. Schematic representation of a two-phase system separates by a membrane.	21
Figure 2.2. Schematic diagrams of the types of membrane	22
Figure 2.3. Schematic drawing of the formation of a composite membrane via IP	23
Figure 2.4. Different filtration methods	24
Figure 2.5. Permeants transport by pore flow and solution diffusion	28
Figure 2.6 Schematic representation of the nominal pore size of membranes (Baker 2012)..	29
Figure 3.1. Electrospinning of PA6 nanofibers using Nanospider™ Production Line NS 1WS500U	41
Figure 3.2. Lamination method and equipment.	42
Figure 3.3. Schematic of dead-end filtration unit.....	43
Figure 3.4. SEM images of (A) top view (nanofibers) and (B) cross-sectioned NNC scaffolds	45
Figure 3.5. ATR-FTIR of NNC scaffold (1) and (2) 2.0–0.2 (w/v)% MPD–TMC, (3) 2.0–0.2 (w/v)% PIP–TMC	46
Figure 3.6. An Aromatic polyamide formed with trimesoyl chloride and <i>m</i> -phenylenediamine	48
Figure 3.7. Reaction of piperazine and trimesoyl chloride to aliphatic PA	49
Figure 3.8. SEM images of TFNC membranes (A) 2.0–0.2 (w/v)% MPD–TMC, (B) 2.0–0.2 (w/v)% PIP–TMC, (C) cross-sectioned 2.0–0.2 (w/v)% PIP–TMC, (D) Unsuccessful polymerization of active layer on nonwoven fabric.....	49
Figure. 3.9. Dependence of the flux and rejection on MPD concentration for various TMC concentrations with TFNC-based membranes using feed solutions of 2000ppm (A) NaCl and (B) MgSO ₄	51
Figure 3.10. Hydrolysis of acid halides and formation of carboxylic acid	52
Figure 3.11. The dependence of flux and rejection on PIP concentration at various TMC concentrations in TFNC-based membranes using feed solutions of 2000ppm (A) NaCl and (B) MgSO ₄	53
Figure 3.12. The reaction time dependence of (A) flux and (B) rejection of MPD-based TFNC membranes using the NaCl feed solutions for various reaction times.	56
Figure 3.13. The reaction time dependence of (A) flux and (B) rejection of PIP-based TFNC membranes using the MgSO ₄ feed solutions for various reaction times	57
Figure 3.14. The drying method and time dependence of flux and rejection based TFNC membranes using the feed solutions MgSO ₄	59

Figure 3.15. Crack(A) and unformed active layer (B) onto NNC scaffold (C) thorn-like structure on active layer	59
Figure 3.16. The temperature dependence of flux and rejection of (A) MPD-based membranes using the feed solutions of 2000ppm NaCl, (B) PIP-based membranes using the feed solutions of 2000ppm MgSO ₄	61
Figure 3.17. Comparison of filtration performance (A-NaCl, B-MgSO ₄) between TFNC and commercial membranes at 2000ppm and 4.8 bar with dead-end filtration cell	62
Figure 4.1. Surface images of PIP-based membranes which were prepared (A) 4 % w/v TEA, (B) TEA+NaOH and (C) TEA+ Na ₃ PO ₄ in aqueous solutions.....	69
Figure 4.2. Surface images of MPD-based membranes which were prepared (A) 2 % w/v TEA, (B) TEA+Synferol AH and (C) TEA+Triton-X in aqueous solutions.	70
Figure 4.3. The chemical structure of surfactants.	71
Figure 4.4. ATR-FTIR of PIP-based TFNC membranes active layer prepared using additives.	71
Figure 4.5. ATR-FTIR of MPD-based TFNC membranes active layer prepared using additives.	72
Figure 4.6. Effects of TEA concentration on MgSO ₄ rejection and flux performance of PIP-based membranes at 2000ppm and 4.8 bar with dead-end filtration cell.	75
Figure 4.7. Effects of TEA concentration on Na ₂ SO ₄ rejection and flux performance of PIP-based membranes at 2000ppm and 4.8 bar with dead-end filtration cell.	75
Figure 4.8. Effects of the different reaction time of organic solution on (A) MgSO ₄ , (B) Na ₂ SO ₄ rejection and flux performance of PIP+TEA based membranes at 2000ppm and 4.8 bar with dead-end filtration cell.	76
Figure 4.9. Cross-sectioned images of PIP+TEA based membranes that were prepared (A) 1m-5m and (B) 1m-45sec reaction time.	77
Figure 4.10. Effects of different acid acceptor on MgSO ₄ rejection and flux performance of PIP-based membranes at 2000 ppm and 4.8 bar with dead-end filtration cell.....	78
Figure 4.11. Observation of filtration process in an extended period of PIP+TEA+NaOH membrane using pure water at 4.8 bar.	79
Figure 4.12. Extended filtration of (A) MgSO ₄ , (B) Na ₂ SO ₄ , (C) CaCl ₂ and (D) NaCl feed solutions at 2000ppm and 4.8 bar using dead-end cell.	80
Figure 4.13. Pure water fluxes performance for MPD-based membranes.	81
Figure 4.14. Effects of different additive on (A NaCl, (B) CaCl ₂ rejection and flux performance of MPD-based membranes at 2000ppm and 4.8 bar with dead-end filtration cell.....	83
Figure 4.15. A nanosize crack on the surface of MPD+TEA based membrane.....	84
Figure 4.16. Observation of filtration process in extended period of MPD+TEA+Sy-AH membrane using pure water at 4.8 bar.	85

Figure 4.17. Extended filtration of (A) NaCl, (B) CaCl₂, (C) MgSO₄ and (D) Na₂SO₄ feed solutions at 2000ppm and 4.8 bar using dead-end cell. 86

Figure 4. 18. The filtration experiment of seawater using different membrane and dead-end cell at 4.8 bar..... 88

Figure 4.19. Circulated filtration of seawater using (A) PIP and (B) MPD based membranes 89

LIST OF TABLES

Table 2.1. Independent and dependent parameters of IP membranes	25
Table 3.1. Properties of NNC scaffold	45
Table 3.2. AFM properties of specimens	47
Table 3.3. Contact angle measurement of species	47
Table 3.4. Flux and rejection performance of MPD and PIP based membranes.....	53
Table 3.5. The drying method and time dependence of flux and rejection of PIP-based membranes using feed solutions of 2000ppm MgSO ₄	58
Table 4.1. Contact angle properties of TFNC membranes (type of membrane specified with reaction time).....	73
Table 4.2. Properties of salt that were used for feed solutions.....	80
Table 4.3. The rejection values of TFNC membranes using PEG feed solutions	86
Table 4.4. Main dissolved ions in Mediterranean seawater sample	87
Table 4.5. Amount of ions in the filtered seawater sample [permeate (2.) in Figure 4.19].....	90

CHAPTER 1

GENERAL INTRODUCTION

Essential nutrient for all living being is water. Living things are made up 50% to 95% water, and it covers more than 70% of Earth's surface that 96.5% of it found in oceans and seas, 1.7% in groundwater, 1.7% in ice caps and glaciers, rest of it in the air as the vapor or clouds. Only 3% of the Earth's water is freshwater, and 1% of freshwater is drinkable (Wikipedia 2015). Regrettably, the ratio of potable water is decreased day by day because of intense industrialization, increasing of population, over-urbanization.

Many countries or regions are under threat of water scarcity. The effects of water scarcity have been prompted to many governments to search for new drinkable water alternatives. However, alternatives are not always available for some countries, and therefore, desalination has been the center of interest for them.

Desalination refers to a water treatment process that separates salty water into a high salt concentration and a fresh water stream of low concentration and is one of the principal alternative sources for potable water available today. In the early 1970s, semipermeable membranes which are permeable to water but which reject salts and suspended solid that are located in the heart of the desalination process (Ribeiro 1996).

Last four decades, filter medias based on synthetic polymers have been proved themselves on liquid filtration, especially reverse osmosis membranes with hi-performance (99.5% - 99.8% of salt ions rejection). Fibrous materials have been considered as a filter media in recent years of the twentieth century. Especially, nonwoven materials are used for air and liquid filtration such as car filter, medical filtration process and swimming pool filters.

Nonwovens include a wide variety of technology, and the classification of nonwovens-related to the production process is based on the selection of specific operations in each of the three steps; dry laid, wet laid and spun laid. Drylaid is distinguished from the four different forming methods such as carded, air laid, a combination of carded and air, and electrostatic laid while spun laid is distinguished three and they are spun laid, melt blown and electrostatic spun (Jirsák and Wadsworth 1999).

Nonwoven filter media are ideal for filtration applications due to highly internal surface area and porosity that provides high liquid flux and dirt load capacity. Usage of nonwovens in water

treatment is one of the fastest growing segment in the filtration industry. Nowadays, they are mainly used as pre-filter or supporting material and replaced other forms of media such as paper, glass, and carbon due to low cost and increased efficiency. However, the nonwoven filter media is remained incapable against the submicron particle due to the large pore size.

With the new era in material science so-called nanotechnology, the finer fibers which have lower diameter than any conventional fiber and higher porosity of fabrics are possible to produce from polymeric materials. Nanofibers became a popular term in past decades and are rapidly growing in the application of filtration technology. Donaldson Company, USA has already commercialized nanofiber filter media consisted of 10 μ m size cellulose fibers and 250 nm size nanofibers, so-called Ultra-Web (Timothy and Kristine 2003). Usage of nanofibrous materials is still a big challenge in liquid filtration. They have been exhibited good filtration performance in micro dimension particles. However, when it comes to nano or sub nano dimension, unaided nanofibrous layers are failed to satisfy. It will take to next decade or two to realize if nanofibrous filter materials are the serious rescuer of drought in the world.

In the light of all the facts mentioned above, the primary objective of this study is to fabricate a composite membrane by forming active barrier layer onto a fibrous material such as nonwoven and nanofiber layers for liquid filtration. The nonwoven and nanofibrous fabrics are gathered by lamination method to achieve excellent adhesion. The optimization of active barrier layer which is produced by interfacial polymerization (IP) method are involved four different basically step. For instance, various concentration of monomer solutions, reaction or contact time of monomer solutions, determination of drying time and method, and determination of curing temperature are that to achieve best filtration performance (selectivity and flux). Characterization of membranes was done to evaluate their properties such as morphology, mechanical strength, contact angle. The filtration performance of TFNC membranes was compared with commercial membranes (i.e., NF90 and NF270). The nanofiltration test was carried out using monovalent and divalent salt solutions (NaCl and MgSO₄, 2000ppm) and a dead-end filtration cell. Moreover, the filtration performance (rejection and flux) was tried to increase by adding acid acceptor or surfactants (e.g. TEA, NaOH, Na₃PO₄, Synferol-AH, Triton-X 100). Extended period filtration performance of enhanced membranes were evaluated by dead-end filtration using deionized water and NaCl, MgSO₄, CaCl₂ and Na₂SO₄ as feed solutions. The existence of the residual chemical in permeate water were investigated to ensure that any chemical component (PIP, MPD, TMC, TEA, surfactants) of the TFNC membranes

released into permeate water or not. Finally, the filtration process was carried out using real seawater which was obtained from the mediterranean sea.

CHAPTER 2

THEORETICAL PART

2.1. NANOFIBERS

Fiber is a raw material that the beginning point of all production of textile surface. Fibers are bunch together to create yarn, woven or nonwoven fabrics. The textile industry had one's share from nanotechnology, and the thinnest form of the fiber so-called nanofiber has been produced by electrospinning method. Fibers with a diameter of the range $d=10-900$ nm can readily be electrospun into mats (Darrell and Iksoo 1996).

2.2. ELECTROSPINNING

In the 15th century, Sir William Gilbert carried out the first observation so-called electrospaying that when a suitably electrically charged piece of amber was brought near a droplet of water, it would form a cone shape and small droplets would be ejected from the tip of the cone (Gilbert 2010).

First nanofibers deposition from viscous polymeric solution using charged electrode was obtained and patented by Cooley and Morton in 1902 (Cooley 1902; Morton 1902). However, the fibrous material was inadequate for practical uses.

Zeleny investigated the behavior of fluid at the end of capillaries in 1914 [Zeleny 1914]. The electrospinning of the melt solution that used an air-blast to assist fiber formation was patent by Norton [Norton 1936]. However, this work did not gain technical performance due to the poor understanding of the process.

Needle electrospinning was patented by Formhals firstly in 1930 years (Anton 1934; Yalcinkaya and Cengiz-Callioglu 2011) and at present, needle electrospinning still one of the most important methods to produce nanofibers for lab application.

The biggest step in the production methods of nanofiber was the invention of roller electrospinning methods (Jirsak et al. 2005). This method is the unique to produce nanofibers at industrial scale and was commercialized by Elmarco under the Nanospider trade name. Nanospider equipment can produce membranes collected fibers in a range from 50 to 600 nm in diameter. The quality or productivity of nanofibers fabrics are affected by the parameters which are involved; condition process, solution, and environmental parameters. There are

numerous of research for investigating of impacts of parameters on the nanofibers quality during electrospinning. For instance, the solution concentration, applied voltage, the distance between the electrode, humidity of chamber, and additive in solution have a direct effect on the nanofibers morphology and productivity (Yalcinkaya et al. 2014; Yalcinkaya et al. 2012; Yalcinkaya et al. 2015; Yener and Yalcinkaya 2013).

2.3. MEMBRANES

An exact definition of membranes always becomes difficult, a general definition may be a selective barrier between two phases, the term selective being inherent to a membrane or a membrane process (Mulder 1996). The one side of phases is called as feed whereas other is called as permeate. Species float into membranes from one phase to another under the effect of a driving force (Fig 2.1).

Driving force can be pressure, temperature or differences in concentration that acting on the components in the feed.

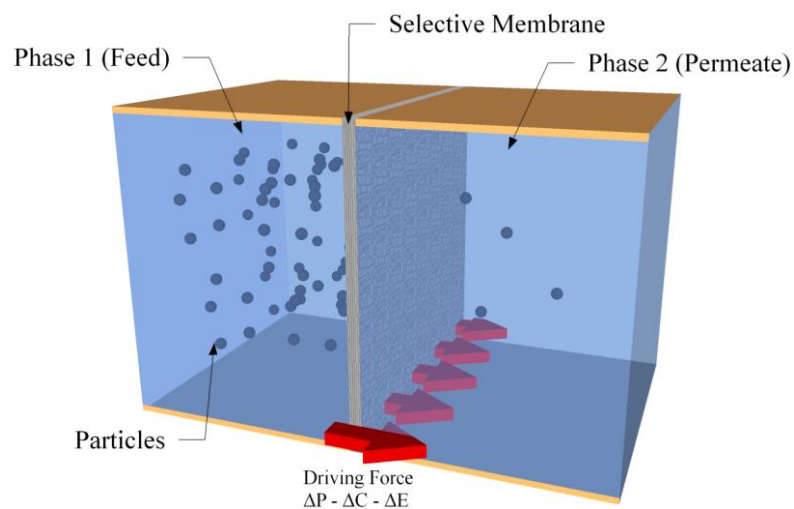


Figure 2.1. Schematic representation of a two-phase system separates by a membrane.

2.3.1. Membrane Structure

A membrane can be thick or thin, its structure can be homogeneous or heterogeneous, and transport can be active or passive. Also, membranes can be natural or synthetic, neutral or charged (Mulder 1996).

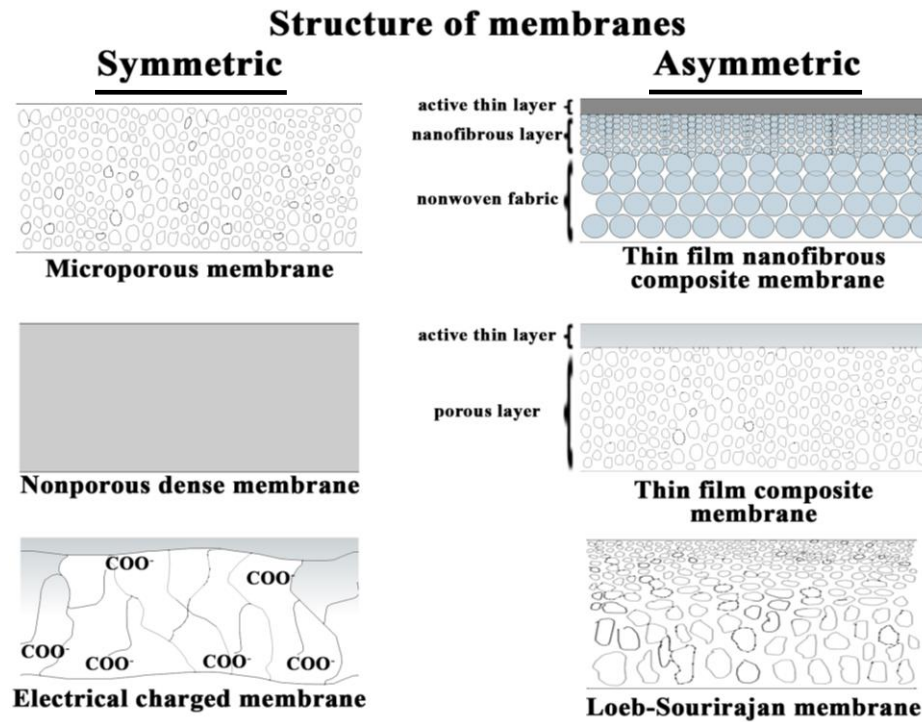


Figure 2.2. Schematic diagrams of the types of membrane

Membranes can be classified according to their cross-section views to clarify the structure of membranes. If we confine ourselves to solid synthetic membranes, two kinds of the membrane may be distinguished, i.e. symmetric and asymmetric membranes. The types of membrane are illustrated schematically in Figure 2.2 and described briefly below.

2.3.1.1. Symmetric membranes

The symmetric membranes are molecular, chemically or physically, homogeneous, and uniform in composition and structure. Microporous membrane has a rigid, highly voided structure with randomly distributed, interconnected pores on the order 0.01 – 10 μm . All particles larger than the largest pores completely reject by the microporous membranes. Nonporous, dense membranes consist of a dense film through which permeants are transported by diffusion under the driving force of pressure, concentration, or electrical potential gradient. Electrically charged membranes can be dense or microporous, but are most commonly very finely microporous, with the pore walls carrying fixed positively, or negatively charged ions (Baker 2012).

2.3.1.2. Asymmetric membranes

A breakthrough to industrial applications was the development of the asymmetric membranes. These consist of a very dense top layer or skin with a thickness of 0,1 to 0,5 μm supported by

a porous sublayer with a thickness of about 50 to 150 μm . These membranes combine the high selectivity of a dense membrane with the high permeation rate of a gaunt membrane. The resistance to mass transport is determined largely or entirely by the thin top layer (Mulder 1996). In composite membranes, the top layer and sublayer originate from different polymeric materials, and each layer can be optimized independently such as in TFNC membranes. The layer of TFNC membranes involves; nonwoven fabric, electrospun nanofibrous material and thin active layer that are produced individually and gathering together to create the filter media.

2.3.2. Interfacial polymerization

Interfacial Polymerization (IP) is a method that provides for the formation a thin layer on a porous support. Polymerization reaction occurs between two very reactive monomers at the interface of two immiscible solvents. A support layer (A) (ultrafiltration, microfiltration membrane or nanofibrous scaffold) is immersed in an aqueous solution containing a reactive monomer (B), frequently of the amine type. The wetted film is then immersed in a second bath containing a water-immiscible solvent (C), often an acid chloride. These two reactive monomers react with each other to form a dense polymeric top layer (Fig. 2.3-D).

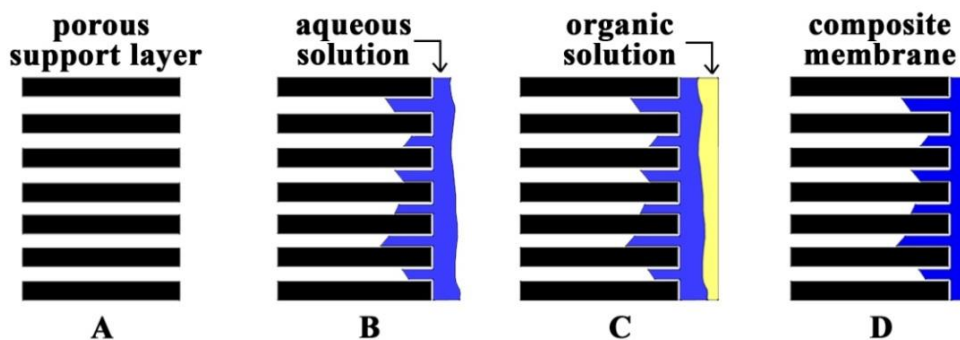


Figure 2.3. Schematic drawing of the formation of a composite membrane via IP

Heat treatment is often applied to complete the interfacial reaction and to crosslink the water-soluble monomer or pre-polymer (Mulder 1996).

2.3.3. Filtration methods

The membrane filtration process is sorted in two different methods; dead-end and cross-flow filtration. Feed solutions are applied perpendicular to membrane surface in dead-end filtration whereas feed solutions are applied horizontally to membrane surface in cross-flow filtration (Fig. 2.4). In dead-end filtration method, the membranes particularly tend to show fouling effect because of accumulation on the membrane surface. Eventually, the fouling effect ends up with

stop of filtration. Despite the dead-end, the cross-flow filtration method is reduced the fouling as far as possible and increased productivity.

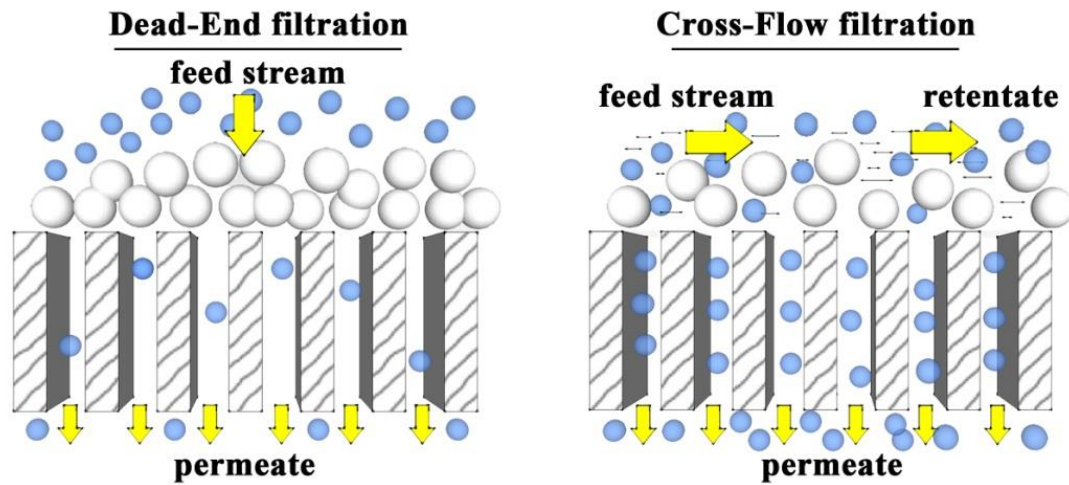


Figure 2.4. Different filtration methods

2.3.4. Membrane separation properties

The most important properties in all fabrication systems are productivity and quality. In all kind of filtration process, the quality always represents by selectivity. In liquid filtration, productivity is named by flux. The performance of a membrane crucially related to selectivity and flux. These parameters are influenced directly by the structure of the membrane such as porosity, hydrophilicity or chemical structure. Also, the content of feed solution and driving force also affect the performance of membranes.

2.4. Parameters of interfacial polymerized membranes

Interfacial polymerized (IP) membranes may contain multilayer film formed more than one-step process. Thick, porous, a nonselective substrate formed in one-step (phase inversion or electrospinning methods) for mechanical support, which is subsequently overcoated with an ultrathin selective active barrier layer on its top surface in a second step.

The formation of active barrier layer so called polyamide thin layer effects by different independent parameters (Table 2.1). The independent parameters have significant impact on the formation of polyamide thin layer in terms of final performance, morphology, physical and chemical features (Li et al. 2008; Cheng et al. 2008; Wang et al. 2010; Tang et al. 2008; Konagaya et al. 2000; Hoover et al. 2013; Sundarrajan and Ramakrishna 2013; Kao et al. 2010).

Table 2.1. Independent and dependent parameters of IP membranes

Independent Parameters	Dependent Parameters
<ul style="list-style-type: none">• Monomer solutions (Concentration, type of monomers and solvent, reactivity ratios where blends of reactants are employed, diffusion rates of the reactants)• Reaction time of monomer solutions• Drying time between reaction of monomer solutions• Post-reactions or treatments of the resulting interfacial films	<ul style="list-style-type: none">• Surface morphology of thin film• Thickness of thin film• Hydrophilicity/Hydrophobicity of thin film• Permeability of thin film membranes• Rejection of thin film membranes

These parameters were studied in another works by the different authors which is mentioned below, due to the wide application range of interfacial polymerized thin layer such as gas separation, reverse osmosis, and nanofiltration.

2.4.1. Interactions of dependent parameters and independent parameters

2.4.1.1. Type of monomer and its solutions

Various type of thin-film membranes can be prepared by interfacial polymerization on to different porous surface. Interfacially formed active barrier layers may have hydrophilic or hydrophobic groups and they may consist of rigid chemical structure according to choose of monomer and solvent type. Similarly, aromatic polyamide, polyamine and polyester membranes can be prepared using different monomers and solvent.

1,3-diaminobenzene as an aqueous reactant and formaldehyde vapor as a crosslinking agent were used to form polyamine thin layer by gas-liquid interfacial reaction. Piperazine and isophthaloyl chloride in hexane were used to prepare polyamide thin layer whereas Sorbitol and terephthaloyl chloride in hexane were used to form polyester thin layer. These aromatic thin-

layered membranes were exhibited more than 95% synthetic seawater salt (3.5%) rejection at 100 atm pressure (Cadotte et al. 1976).

As an aqueous solution, various reactants were examined to observe their influence on the final thin-layered membranes. Hydrazine, 1,2-ethanediamine, 1,3-propanediamine, 1,6-hexanediamine, 1,3-diaminobenzene, piperazine, polyethyleneimine were reacted with terephthaloyl chloride by the interfacial reaction, and in all cases involving monomeric diamines, salt rejections were far below useful levels. Only in the case of polymeric amine, polyethyleneimine, was a membrane obtained showing promise for salt rejection (Cadotte et al. 1981b).

An alternative way of making thin-layered membranes, trimesoyl chloride, cyanuric chloride, phosphorous oxychloride and isophthaloyl chloride were used as an organic solution compound by reacting Piperazine. The best result that is 99.2 % synthetic seawater rejection was obtained using cyanuric chloride. SEM studies indicated that the surface morphology of the thin-layered membranes changed as a function of acyl content (Cadotte et al. 1981b).

In the same study of Cadotte showed that base strength of the acid acceptor affected the degree of concurrent hydrolysis. Sodium hydroxide produced membranes with the lowest overall salt rejections. Weak bases such as N, N-dimethyl piperazine and sodium dihydrogen phosphate gave the highest salt rejections.

One of the important works has been done by Saha and Joshi. They investigated the effect of variation in polyamide structure of thin film composite nanofiltration membranes on flux and rejection performance. Various combinations of monomers have been prepared such as piperazine, *m*-phenylenediamine, *N*-(2-aminoethyl)-piperazine, trimesoyl chloride, isophthaloyl chloride, 3,5-diaminobenzoic acid and a mixture of diamines or acid chloride. They have shown a wide range of rejection and flux performance, and concluded that among the membranes prepared, MPD-PIP-TMC membrane at 50-50 MPD-PIP ratio displayed highest NaCl-water flux with relatively good rejection (Saha and Joshi, 2009).

Polyamide thin-layers which were interfacially polymerized under different concentrations of the same monomers indicating that their chemical compositions are almost the same. However, the changes in the concentration of monomer solutions have a direct impact on the polyamide thin-layer. This suggests that the thickness of the polyamide thin layer can be controlled by adjusting the concentration of the aqueous and organic phases (Vyas and Ray 2015).

2.4.1.2. Reaction time of monomer solutions

During the interfacial polymerization of two immiscible water based and organic based solution, reaction does not take place in the water phase, because a highly unfavorable partition coefficient for organic solution reactants (trimesoyl chloride, cyanuric chloride, phosphorous oxychloride, isophthaloyl chloride, sebacoyl chloride) limit its availability in the aqueous phase (Cadotte et al. 1976). For instance, in order for m-phenylenediamine contained in water to react with trimesoyl chloride contained in hexane, the phenylenediamine must diffuse across the water hexane interface to make reactive contact with the trimesoyl chloride. Therefore, the time of contact for porous substrate at each phases has big impact on the final polyamide thin-layer.

It is confirmed by Kong et al. that amine diffusion content was increased in contact with acid chloride phase (0 to 35 min) by the time of progress (Kong et al. 2011). Therefore, this acid chloride can then react with more incoming amine monomers, resulting in a denser and more crosslinked polyamide thin layer with a lower acid content (Jin and Su 2009). The choose of different reaction time, which could offer the possibility for control of membrane morphology (ridges and valleys, thickness, pore size) and performance (water permeability, rejection).

2.4.1.3. Drying method and time

During interfacial polymerization, an excessive amount of amine solution needs to remove from the surface of the porous substrate before reacting with organic solutions. In this stage, a rubber roller has been used to adjust the amount of amine solution (Wang et al. 2014; Kim et al. 2000; Mansourpanah et al. 2009; Yung et al. 2010). Drying method and time have not been fully defined and studied by the authors. Therefore, the detailed investigation has been done by the author within this thesis. The influence of drying method and time on the final polyamide active barrier layer were indicated in chapter 3 and 3.3.2.3.

2.4.1.4. Post reactions and treatments

To form successfully polyamide active barrier layer by interfacial polymerization using amine and acid chloride phases on the surface of the porous substrate, the curing is a necessary step to stabilize barrier layer. Heat curing is used after barrier layer formation to remove residual organic solvent from the final overall membrane and to promote additional crosslinking through dehydration of amine and carboxylic acid residues (Gosh et al. 2008). In resulting membrane tends to increase water flux and salt rejection performance during filtration. Increasing of temperature and curing time, the porosity of polyamide barrier layer is reduced by crosslinking,

hence, the water flux decrease significantly, but increase in salt rejection. However, an excessive amount of heat and curing time may damage polyamide barrier layer and porous substrate both. Optimum temperature and curing time have key factor in post treatments step (Mickols 2003; Rao et al. 2003; Rao et al. 1997).

2.5. MEMBRANE TRANSPORT THEORY

The membranes can control the rate of permeation of various species which is one of the most important properties of them. The two models are used to describe the mechanism of permeation such as pore-flow and solution-diffusion models (Fig. 2.5). In pore flow model, permeants are transported by pressure-driven convective flow through pores. Separation occurs due to one of the permeants (particles or impurities) are filtered from the pores of membranes while other permeant flows through the membranes freely. The second model is the solution-diffusion model. The membranes that have non-pores structure, in which permeants dissolve in the membrane material, then diffuse through the membrane down a concentration gradient. Permeants are separated because of differences in their solubilities in the membrane and differences in the rates at which they diffuse through the membrane (Baker 2012).

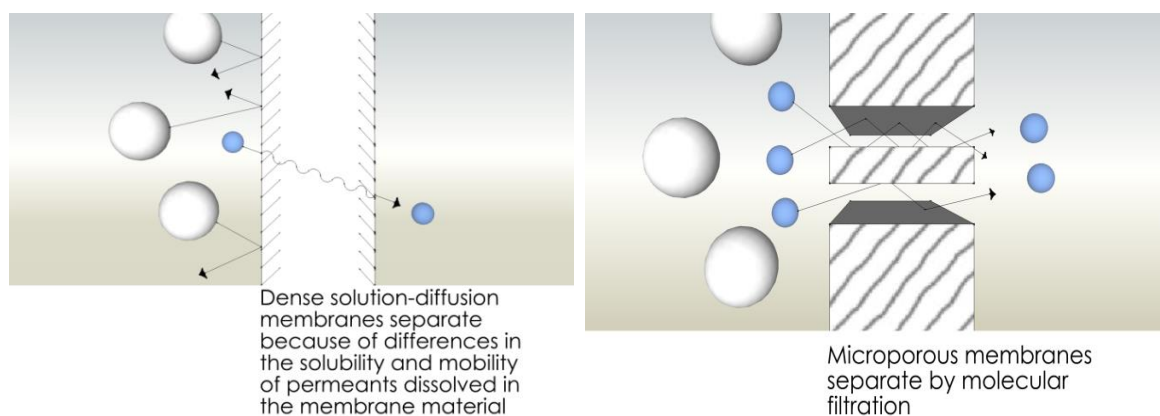


Figure 2.5. Permeants transport by pore flow and solution diffusion

Relative size and permeance of the pores are main factors to determine differences between pore-flow and solution-diffusion mechanism. The solution-diffusion model may describe by the Fick's Law (Eq. 1).

$$J_i = -D_i \frac{dc_i}{dx} \quad \text{Eq. (1)}$$

Where J_i is the rate of transfer of component i or flux and dc_i/dx is the concentration gradient of component i . D_i is called the diffusion coefficient and is a measure of the mobility of the individual molecules (Baker 2012).

The pores in the membrane are tiny spaces between polymer chains by thermal motion of the polymer chain. These pores appear and disappear on about the same time scale as the motions of the permeants traversing the membrane. On the other hand, the pore-flow model may be described by Darcy's law (Eq. 2).

$$J_i = K' c_i \frac{dp}{dx} \quad \text{Eq. (2)}$$

Where dp/dx is the pressure gradient existing in the porous medium, c_i is the concentration of component i in the medium K' is a coefficient reflecting the nature of the medium (Baker 2012).

The pores are relatively large and fixed, do not fluctuate in position or volume on the time scale of permeant motion. These pores are usually connected to one to another. The larger the individual pores, the more likely they are to be present long enough to produce pore-flow characteristics in the membrane.

It is hard to distinguish the membranes according to their average pore size due to insufficient measurement technique of membrane pores. Therefore, the measurement of the size of molecules that permeate the membranes has been adapted and determined the general groups of membranes (Fig 2.6) in below.

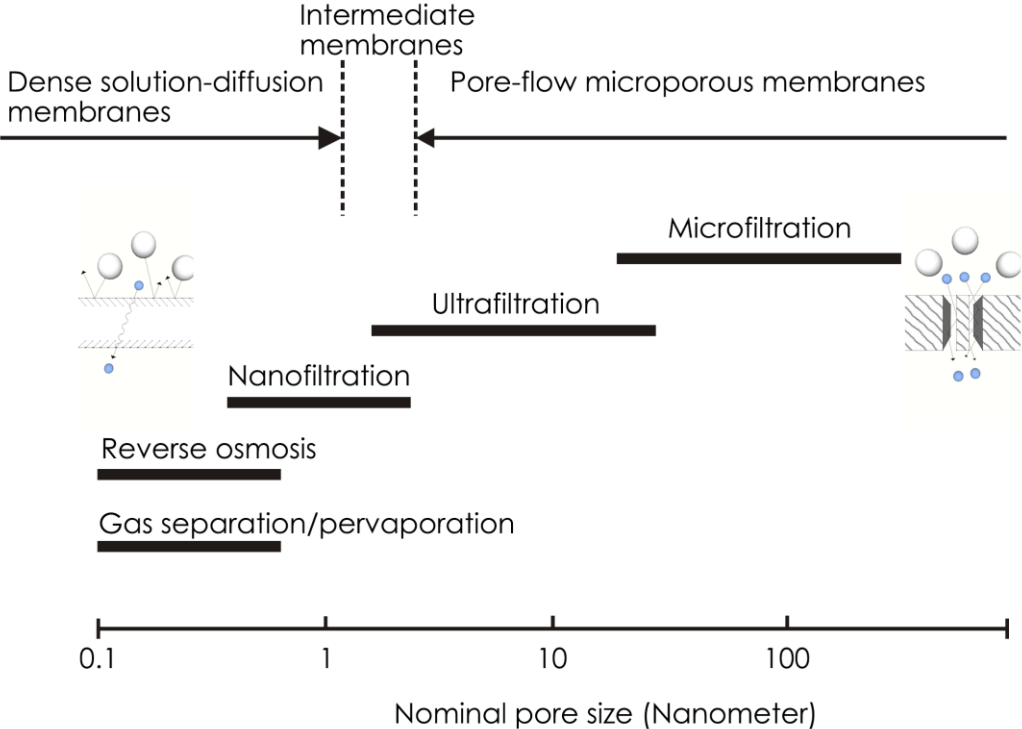


Figure 2.6 Schematic representation of the nominal pore size of membranes (Baker 2012)

- Ultrafiltration and microfiltration membranes are microporous because their pores diameter is larger than 1 – 1.5 nm and transport occurs by pore flow.
- The membranes that contain a dense selective active layer with no visible pores are reverse osmosis, pervaporation, and polymeric gas separation membranes. The pores diameter of these membranes is between 0.2 – 0.5 nm and the solution-diffusion model describes permeants transport.
- Nanofiltration membranes contain pores structure as support and dense active layer at the same time. Nanofiltration membranes are intermediate between ultrafiltration membranes due to the porous supporting structure and reverse osmosis membranes clearly dense active layer. In these membrane types contain pores with diameters between 0.5 and 1.5 nm (Baker 2012).

2.6. APPLICATION OF NANOFIBROUS SCAFFOLDS IN LIQUID FILTRATION

There are several unique features of nonwoven fabrics and nanofibrous scaffolds that are involved; the surface porosity of nanofibrous scaffolds is similar to the bulk porosity, which is closer to 80% or higher. The surface pore structures are all inter-connected throughout the layer, so there are no dead-end pores in nonwoven fabrics and nanofibrous scaffolds (Yoon et al. 2009b). According to the pore size of the materials and driven pressure, electrospun nanofibrous scaffolds have been used in microfiltration (MF), ultrafiltration (UF), (Feng et al. 2010) nanofiltration (NF), reverse osmosis (RO) and forward osmosis (FO) (Chu et al. 2012).

2.6.1. Nanofibers in microfiltration

Through the last decade, electrospun nanofibrous scaffolds in liquid filtration have taken place at microfiltration level. In one of the first practices that were the cellulose nanofiber membranes, which has fiber diameter between 200 nm - 1 μ m were prepared by electrospinning as affinity membranes (Ma et al. 2005). The nanofibrous scaffold was treated in NaOH solution in H₂O/ethanol to obtain regenerated cellulose (RC) nanofiber mesh. The Cibacron blue RC nanofiber membrane has a Cibacron blue content of 130 μ mol/g, and capture capacity of 13 mg/g for bovine serum albumin (BSA) and 4 mg/g for bilirubin. The author was worked on more or less similar study using polysulfone ultrafine fibers (diameter 1-2 μ m) (Ma et al. 2006). The filtration result of the study showed that the electrospun membranes have lower pressure drop and higher flux compared with commercial microfiltration membranes.

One of another earlier study was carried out by electrospinning of polyvinylidene fluoride into the membrane with fiber diameter approximately 380 nm (Gopal et al. 2006). The electrospun membranes were used to separate 1, 5 and 10 μm polystyrene particles. They indicated that the electrospun membranes were rejecting more than 90% of the particles from feed solutions. The results were led to the use of electrospun nanofibrous materials that best candidate the replace commercial membranes as pre-filters prior to ultrafiltration or nanofiltration to minimize the possibility of fouling. Another study of the author has used polysulfone electrospun nanofibrous scaffolds and observed the ability to remove micro-particles from solution. The membrane was able to remove 99% of 10, 8 and 7 μm particles. However, the membrane was observed to foul irreversibly by 2 and 1 μm particles on the membrane surface (Gopal et al. 2007).

In another study, the electrospun nylon-6 scaffold was prepared using electrospinning method with the fiber diameter in the range of 30-110 nm and employed as a membrane material for water filtration. The electrospun membranes separated all particles with sizes from 10 to 1 μm particles. The usage of sub-microns particles was tended to the fouling effect on the membrane surface. They indicated the importance of the influence of flow patterns such as cross-flow or through the flow to obtain better filtration performance (Aussawasathien et al. 2008).

Electrospun scaffold for microfiltration method is conducted on polysulfone and polyvinylidene fluoride with high contact angle and more hydrophobic nanofibers. High hydrophilic electrospun membranes (EM) were generated by blending with several different types of surface modifying macromolecules. The contact angle of blended EM reduced from 140° to 54° . The pure water flux of blended EM was 20 % higher than that of non-blended EM (Kaur et al. 2012a).

The poly(trimethylene terephthalate) (PTT) nanofibers with an average diameter of 145 nm for microfiltration also have been produced by wet-laid process instead of electrospinning. Heat application and blending with PP nanofibers were exposed to enhanced the mechanical properties of PTT nanofibers. The water flux and filtration efficiency have been investigated using TiO_2 suspensions with the average diameter of 100nm. It was found that the rejection performance of membranes was above 99.6 % with high flux microfiltration media (Li et al. 2013).

One of the latest studies about Solid–liquid clarification of a lignocellulosic hydrolysate and fermentation broth containing yeast cells has been investigated. The performance and fouling characteristics of electrospun polyimide nanofiber membrane were compared with commercial microfilters. All three micro filters (PES, PVDF, MCE) were showed lower flux and irreversible fouling compared the PI membrane. Moreover, PI nanofibers membranes did not show any permanent decrease in flux during cell separation or solid-liquid clarification. The authors suggested the PI nanofibers membrane would have a high potential for solid–liquid clarification and cell recycle/removal operations within a biorefinery process (Gautam et al. 2014).

The conventional electrospinning of polymeric solution has found place in liquid filtration area due to the superior physical features of nanofibers. As a conclude, the nanofibrous materials has the high filtration efficiency such as high water flux and particles rejection in microfiltration.

2.6.2. Nanofibers in ultrafiltration

Another method of membrane system so-called ultrafiltration that researchers have focused on high flux and low fouling effect using the electrospun nanofibrous material. In one of the study, a high flux and long-term performance of ultrafiltration membrane have been formed based on poly(vinyl alcohol) (PVA) electrospun nanofibrous scaffold support and PVA hydrogel coating. It was found that the electrospun scaffold fabricated by 96% hydrolyzed PVA with relatively high molecular weight exhibited excellent overall mechanical performance. They indicated that such unique hydrophilic nanofibrous composite membranes exhibited a flux rate ($130 \text{ L m}^{-2} \text{ h}^{-1}$) significantly higher than commercial UF membranes but with similar filtration efficiency (rejection rate >99.5%) (Wang et al. 2006).

In another study, an ultrafiltration membrane was produced by polyacrylonitrile electrospun nanofibrous scaffold coupled with thin top layer coating of chitosan. The prepared membrane, containing an electrospun PAN scaffold with an average diameter from 124 nm to 720 nm. Various concentration of PAN (4 to 12 %) was electrospun to form a three-tire composite membrane on the nonwoven supporting material. Three-tier composite membranes exhibited flux rates that could be an order of magnitude higher than the commercial nanofiltration filter media (e.g. NF 270 from Dow) after 1 day operation while they maintained good filtration efficiency with rejection ratios better than 99.9% (Yoon et al. 2006).

Polyaniline/polysulfone membranes have been prepared for the filtration of PANI nanofiber aqueous dispersion with PS substrate membrane. PANI nanofibers were prepared by using chemical oxidative polymerization method. The filtration performance that are permeate and rejection properties of membranes were tested using the cross-flow equipment. Pure water, PEG aqueous solution and Bovin serum albumin (BSA) aqueous solution were used as feed solution. The results indicate that PANI/PS membranes were performed higher hydrophilicity and enhancement in permeability but no changes in rejection performance. However, the antifouling properties of PANI/PS membranes showed much better performance than PS substrate during filtration of BSA solution (Fan et al. 2008).

The summarize of usage of nanofibers in ultrafiltration area that they are not capable to retain submicron particle. The surface modification or surface coating of nanofibers were crucially necessary to bring ultrafilter feature to nanofibrous layer.

2.6.3. Nanofibers in nanofiltration

As mentioned above studies, the nanofibrous scaffold itself cannot function to use in nanofiltration processes. Either mechanical properties to withstand applied high pressure or selectivity properties of nanofibrous scaffolds are not capable against to ions. In this reason, the plenty of researchers have functionalized the surface of nanofibrous scaffolds using interfacial polymerization (IP), listed below.

One of the first attempts the usage of electrospun nanofibrous in nanofiltration has been made by Ritcharoen et al. They electrospun cellulose acetate (CA) fiber mat and coated fiber surface with chitosan/sodium alginate and poly(styrene sulfonate) to obtain electrostatic multilayer. They indicated that the water flux was decreased with an increase in the number of the bilayers. For instance, they obtained that the water flux was in the range of 60 and 40 $\text{Lm}^{-2} \text{h}^{-1}$ for 15 and 25 bilayered membranes, respectively. They have found the sodium chloride solution in flux was lower than the pure water, naturally, because of osmotic pressure. As a result of the filtration process, the level of NaCl rejection from this work was in the range of 6% and 15% for 15 and 25 bilayered membranes, respectively (Ritcharoen et al. 2008).

The usage of electrospun nanofibrous scaffolds as a porous layer on nanofiltration process is taken place by electrospinning of polyacrylonitrile (PAN) nanofibers. Nanofibrous mid-layer was used as a support in a high flux thin film nanofibrous composite (TFNC) membranes. Then the active barrier layer was produced by IP of piperazine, trimesoylchloride and some additives.

The membrane performance was evaluated for nanofiltration using divalent salts (MgSO_4). They indicated that the concentration of piperazine was played a critical role in IP to optimize the flux and rejection performance. The TFNC membrane was showed higher permeate fluxes (21-42%) as well as higher rejection rates (2-22%) than those of TFC membranes (Yoon, Hsiao and Chu 2009b). In addition, TFNC membrane was exhibited 38 % permeate flux increase while maintaining rejection to that NF270 at 4.5 bar.

Another study has aimed an enhancement on the electrospun nanofibrous membranes performance of nanofiltration process. Polyethersulfone (PES) was dissolved in DMF and DMF/NMP mixture and spun onto PET nonwoven support layer. The reason of solvent mixture selection, increase the adhesion between the forming PES nanofibrous layer and PET nonwoven scaffold. Then active layer was formed onto nanofibrous scaffold surface using IP method with some surfactants additive to monomer solutions. The TFNC membranes which were prepared with surfactants additive was performed two times higher flux compared to that of NF-90 with equal salt rejection ratio, and equal flux and salt rejection performance as those of NF-270 (Yung et al. 2010).

One of the most important studies about electrospun nanofibrous composite membrane was carried out by Kaur et al. They were observed that the effect of nanofibrous structure on the thin film composite membrane and their performance in the nanofiltration process. In the first study, they have investigated the influence of fiber diameter on the filtration performance. Thus, various concentration of PAN solution was electrospun onto the nonwoven scaffold. Interfacial polymerization of polyamide thin film was formed onto PAN nanofibers. The separation performance was done using dead-end filtration cell with 2000ppm MgSO_4 feed solution. The result showed that as the fiber diameter decreased, the pore-size also decreased, and the separation of salts increased, while at the expense of flux. While the cross-sectional thickness of the electrospun layer was decreased together with smaller pore-size, it resulted in the increased flux with high salt rejection (Kaur et al. 2012b). The same author was observed the hot pressing effect on the electrospun PAN nanofibrous membrane properties and the separation of salt after interfacial polymerization. The reason for applying hot press is the increase the mechanical properties and adhesion between nanofibrous and nonwoven scaffolds. The nanofiltration result showed that the higher applied hot pressure membrane was exhibited higher rejection and lower flux than that those of TFNC membranes (Kaur et al. 2011).

The formation and preparation of nanofibers have been carried out by using needle electrospinning method in the studies which are mentioned in this section. Due to the low production rate of needle electrospinning, the large scale production of filter media or the investigation of real life performance was not possible in mentioned studies. Therefore, there is a low probability of industrial application of mentioned studies.

2.6.4. Nanofibers in reverse osmosis

The latest development has been carried out by the industrial technology research Institute based in Taiwan. They have produced high flux RO membrane modules using three layer of nonwoven fabric, polysulfone nanofibers and active polyamide thin layer. The principal application of this high-performance, low-energy-consumption membrane is desalination producing fresh water from sea water (Poly-E 2016).

2.6.5. Nanofibers in forward osmosis

The technology of forward osmosis is membrane based separation technique, and their application areas are sustainable energy, resource recovery and water production. Polyethersulfone (PES) and Polysulfone (PSf) nanofibers were collected onto PET support nonwoven layer to prepare forward osmosis membrane using electrospinning method. The MPD and TMC monomers were used to form an active barrier layer onto the fibrous supporting layer. This membrane was provided highly water flux and low salt flux (Bui et al. 2011; Tian et al. 2013).

In another study of authors were used that electrospun nylon 6,6 nanofibers due to its high hydrophilic and mechanical properties compared to other nanofibers materials. To obtain high permselectivity on forward osmosis membrane, active barrier layer were formed onto nanofibers supporting mid-layer. TFC membranes were fabricated using co-solvent such as acetone to get different water permeance and salt selectivity. These membranes were performed low salt flux compared to the HTI cellulose acetate membrane (Huang and McCutcheon 2014).

2.6.6. Improved mechanical strength of nanofibers in liquid filtration

There are many studies about improvement of mechanical properties of nanofibrous layer. Some studies were focused the change chemical structure of the nanofibers while some of them developed new mechanism of production method (Choi et al. 2004; Kaur et al. 2007; Kim et al. 2006a; Sen et al. 2004; Wang et al. 2008)

The weak mechanical properties of nanofibers and their low adhesion to nonwoven supporting layer have always been a stumbling block to prepare nanofibrous liquid filter. In many studies, the researchers have been trying to solve the mechanical problem of nanofibers.

Some of the studies were focused on increasing inter-fiber adhesion to improve the mechanical properties of membranes. The mixed solvent system (Dimethylformamide (DMF) and N-methyl-pyrrolidinone (NMP)) were used to prepare a solution of PES, then the PES polymer solution was electrospun using needle electrospinning. The different solvent mixed system contains various vapor pressure of solvents. Therefore, the nanoweb on the supporting material was still partly wetted because of the high vapor pressure of NMP, and this may lead the adhesion between fibers. The mechanical properties of PES membranes were improved significantly. However, the average fiber diameter was increased directly proportional to mechanical strength. The flux of the electrospun PES membrane was performed microfiltration performance (Yoon et al. 2009a). The same mixed solvent systems for electrospun PES membranes were mentioned above to prepare nanofiltration filter (Yung, Ma, Wang, Yoon, Wang, Hsiao and Chu 2010).

Instead of the mixed solvent system, the vapor of solvents was exposed to electrospun membranes to improve the mechanical strength. PAN and PSf in DMF solutions were spun via needle electrospinning method. Once spun, the PAN and PSf nanofibers were exposed to solvent vapor for a different period. This approach yielded smaller pore size and fiber fusion at junction points due to fiber swelling. Hence, the mechanical strength of nanofibers webs increased while the treated membranes showed lower permeability than untreated ones (Huang et al. 2013). In further studies of authors are investigated the effect of chemical modification on the improvement of mechanical properties of PAN and PSf electrospun web. The chemical modification involves coating of polydopamine (PDA) that is a hydrophilic polymer. The PDA-modified electrospun web was performed higher strength and improved hydrophilicity (Huang et al. 2014).

As a result, all mentioned attempts have been made to improve the strength and integrity of the nonwoven fabric and nanofibrous scaffolds by using solvent vapor (Huang et al. 2013), applying heat and pressure (Kaur et al. 2011) or by using different combinations of solvents to prepare polymer solutions for electrospinning (Yung et al. 2011; Yoon et al. 2009). All these alterations had negative influences on the morphology of the nanofibrous layer (e.g. the fibre diameter or nonfibrous area increased).

2.6.7. Effects of additives on the thin film composite membranes

Besides, a need for high permeance and selectivity properties, the solvent and fouling resistance membranes are also has gained attention. This is an objective of the present researchers to provide a route for the preparation of such membranes. The most appropriate method to obtain enhanced membranes is additives. ‘Many different additives can be added to the aqueous or organic phases. Additives which are commonly used in TFC membrane synthesis are surfactants, nanoparticles, acylation catalysts and phase transfer catalysts. Surfactants are added to the aqueous phase to improve the wettability of the support layer. They also decrease the surface tension at the interface, which improves the diffusion of monomers across the interface. Many possible surfactants exist, e.g. sodium dodecyl sulfate, polyethylene glycol, polyvinyl alcohol and ionic liquids’ (Alsari et al. 2001; Yamasaki et al. 2000; Sagle et al. 2009).

‘Acylation catalysts accelerate the reaction between the monomers, e.g. by removing hydrogen chloride in polyamide synthesis. Examples are sodium hydroxide, trisodium phosphate, dimethylpiperazine and triethylamine. The addition of phase transfer catalysts improves the diffusion of monomers across the interface by ion pairing with the monomers. Again, many possible phase transfer catalysts exist, e.g. tetraalkylammonium halides and phosphates, tetraalkylphosphonium halides and other ionic liquids. Yung describes the possibility of using ionic liquids as surfactants or phase transfer catalysts in interfacial polymerization, which respectively cause an increase in permeance and decrease in selectivity or a decrease in permeance and increase in selectivity. This is achieved by adding very low concentrations (< 2,5 wt%) of surfactants to the aqueous phase’ (Yung et al. 2010; Mariën et al. 2015).

‘Polymer phase-transfer catalysts are useful in bringing about reaction between a water-soluble reactant and a water-insoluble reactant (Akelah and Sherrington, 1983; Tomoi and Ford, 1988). Polymer phase transfer catalysts act as the meeting place for two immiscible reactants. For example, the reaction between sodium cyanide (aqueous phase) and 1-bromooctane (organic phase) proceeds at an accelerated rate in the presence of polymeric quaternary ammonium salts. Besides the ammonium salts, polymeric phosphonium salts, crown ethers and cryptates, poly(ethylene oxide), and quaternized polyethylenimine have been studied as phase-transfer catalysts’ (Hirao et al. 1978; Odian 2004).

2.7. APPLICATION OF LAMINATION PROCESS FOR NANOFIBERS

The applicability of nanofibrous materials as an end-product has been taken on a new meaning with invention of large-scale production method of nanofibers. New production methods and technologies have given rise to preparation of various polymeric nanofibrous fabrics that have functional properties. However, the weak mechanical properties and difficulties on the processability of nanofibers have always been crucial obstacle.

One of the biggest application areas of nanofibers are composite materials by lamination process, for instance, the functional clothes. Therefore, the potential of using electrospun nanofibrous webs for waterproof breathable materials has been investigated. Kang et al. (Kang et al. 2007) examined the feasibility of electrospinning polyurethane onto substrate fabrics to prepare waterproof breathable fabrics. Lee et al. (Lee et al. 2010) investigated the changes in mechanical properties and thermal and water transfer properties of mass-produced nanofiber web after laundering to evaluate the possibility of using nanofibers for outdoor wear. They reported that the mechanical properties of nanofiber web were sufficient for use as cloth in outdoor wear if a lamination process was used in its production.

To develop waterproof breathable materials for diverse consumer applications, electrospinning and lamination methods were combined to fabricate layered fabric systems. Yoon et al. investigated effects of lamination using various materials such as woven fabrics, nanofibers onto the breathability and waterproofness of the material (Yoon et al. 2011). Lee et al studied the lamination of PU nanofibers onto woven fabric by using two different method hotmelting and solvent laminating for use in clothing. However, they reported the physical properties of the nanofiber web may be adversely affected by the laminating process (Lee et al. 2009). Kanafchian et al. investigated influence of laminating temperature on nanofiber/laminate properties. They used hot-press method to carry out five different temperatures and nanofiber web, and reported that the nanofiber web began to damage when temperature was selected above the melting point of adhesive layer (Kanafcian et al. 2011).

In an another study, Nanofibrous mats of polyamide 6 (PA6) were deposited onto a nonwoven viscose substrate by electrospinning technique and a hot-press method using a thermoplastic resin as glue was applied to improve the adhesion of the nanofiber layer onto the textile support. They reported that the prepared samples has big potential to develop personal protective equipments against nanoparticles (Faccini et al. 2012).

2.8. MOTIVATION AND SCOPE OF THIS THESIS

In consideration of section 2.6 and 2.7, the impact of this study is filling the gap that weakness of nanofibrous materials in the application of liquid nanofiltration. Mainly, the major problems in the nanofibrous material are that weak mechanical properties, and irregular adhesion between nonwoven and nanofibrous scaffold. Lamination method of individually produced nonwoven and nanofibrous layer, rather than hot press method, has been chosen to avoid any damage to original structure of nanofibrous layer.

The main reason for choosing polyamide 6 polymer to create nanofibrous layer is indicated as;

- hydrophilic property,
- easy spinability in nanospider,
- mechanical and thermal resistance,
- considerably cheap price,
- very thin fiber diameter,
- narrow fiber diameter distribution.
- lower pore size distribution.

This thesis was directed to introduce a preparation of large scale production of mechanically robust nanofiber and nonwoven composite surface by Nanospider equipment and lamination method. Active barrier layer on the surface of nanofibrous layer has studied in detail to understand whole membrane separation characteristics (permeance and selectivity). To the best of our knowledge, this is the first work that shows usage of polyamide 6 nanofibers and bi-component nonwoven as porous surface and coating its surface with interfacial polymerized thin layer for desalination of real seawater in nanofiltration application.

Overall, this thesis will open up an opportunity for the use of nanofibrous material in industrial application of liquid nanofilter media. The understanding of PA thin active barrier layer which was breezed through by interfacial polymerization step by step, that will provide insights to the further research in liquid nanofiltration.

CHAPTER 3

FABRICATION AND OPTIMIZATION OF THIN FILM NANOFIBROUS COMPOSITE MEMBRANES FOR REMOVAL OF SALTS

3.1. INTRODUCTION

This chapter shows bi-component polypropylene/polyethylene (PE/PP) spunbond nonwoven fabric as a supporting material and electrospun nanofibrous (polyamide 6) layer as a porous surface, combining them gently under heat and pressure treatment using a lamination machine. Tensile strength and pore size distribution tests were done. Well-designed nonwoven and nanofibrous composite scaffold was used as a supporting material in an IP reaction to create a thin-film active barrier layer. Optimization of TFNC membranes was carried out in all parameters of the IP reaction such as the types of monomers, various concentrations of monomers, reaction time, drying time, and various curing temperatures. Based on the experimental results, an optimum TFNC membrane was determined according to its filtration performance (selectivity and flux) and then compared with commercial membranes under the same process parameters (e.g., feed solution, applied pressure).

3.2. EXPERIMENTAL

3.2.1. Materials

The TFNC bottom substrate was a polypropylene/polyethylene (80/20, 18g/m²) bi-component spunbond nonwoven fabric (Pegatex S BICO) from Pegas Nonwovens s.r.o. (Czech Republic). The solution used to produce the porous nanofiber layer by electrospinning consisted of polyamide 6 (PA6) (BASF B24) dissolved in acetic acid/formic acid. The selective layer of the TFNC membrane was prepared by interfacial polymerization of two immiscible phases on the porous nanofiber layer. Piperazine (PIP) and *m*-phenylenediamine (MPD) were purchased from Sigma-Aldrich and prepared in deionized water as aqueous phases, while the organic phase was prepared by dissolving trimesoyl chloride (TMC) (Sigma Aldrich) in hexane at 40 °C. The filtration performance of TFNC membranes was tested using salt solutions containing magnesium sulphate (MgSO₄) and sodium chloride (NaCl).

3.2.2. Preparation of electrospun PA6 porous nanofibrous layer

A solution of polyamide 6 (8 wt.%) was dissolved in acetic acid/formic acid at a ratio of 2/1 at 80 °C for 4 hours to produce a nanofiber layer using wire electrode electrospinning equipment (NS 1WS500U, Elmarco s.r.o, Czech Republic). Wire electrospinning is a new technique that uses an electrical force to spin nanofibers from a free surface liquid towards to the collector electrode (Fig. 3.1). A solution carriage feeds polymer solution around a moving stainless steel wire. The speed of the carriage is 245 mm/s and the rotation speed of the wire is 40.5 cm/h. High voltage suppliers are connected to the wire electrode (55 kV) and collector electrode (-10 kV). When the applied voltage exceeds a critical value, many Taylor cones are created on the surface of the wire. Polymer solution jets move toward the collector, the solvent evaporates, and the PA6 nanofibrous layer is collected on a backing paper moving in front of the collector electrode. The speed of the backing paper was 9 cm/min.

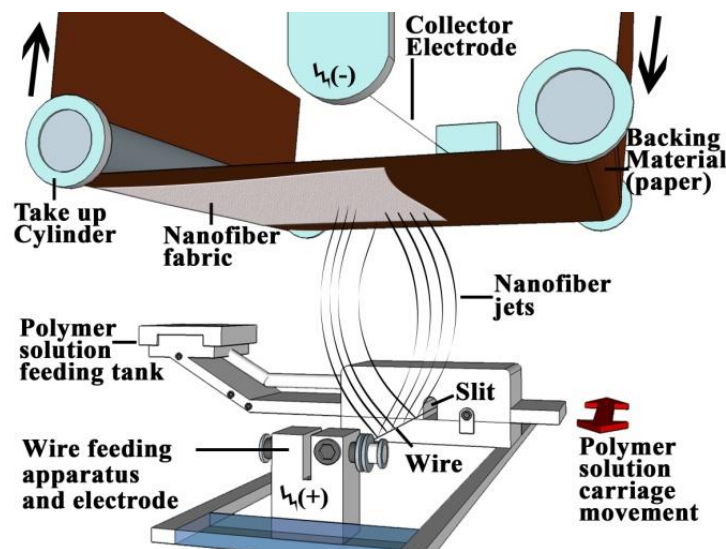


Figure 3.1. Electrospinning of PA6 nanofibers using Nanospider™ Production Line NS 1WS500U

The distance between the electrodes was 18 cm. The temperature and humidity of input air are set to 23 °C and 30% by the air-conditioning system. The volumes of air input and output are 98 and 110 m³/h respectively).

3.2.3. Lamination of nonwoven and nanofibrous materials

Bi-component spunbond nonwoven and PA6 nanofibrous fabrics were laminated using RPS-Mini fusing lamination equipment (Meyer-Germany). This process was carried out tenuously to avoid damaging the structure of the nanofibers such as the fiber diameter and pore size.

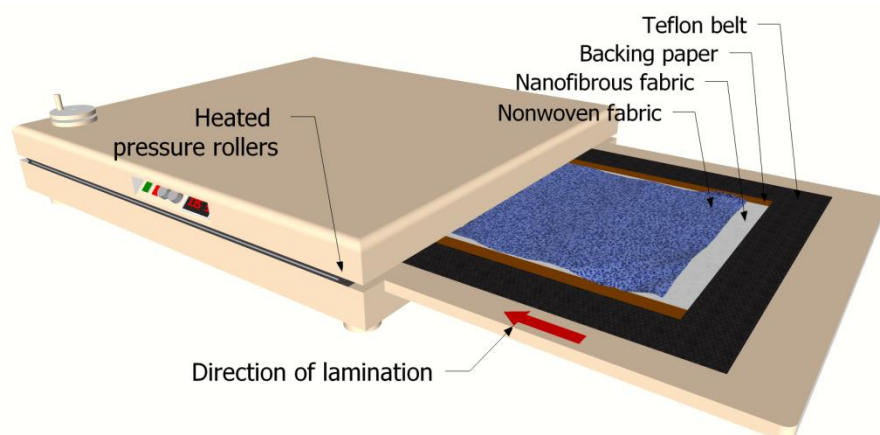


Figure 3.2. Lamination method and equipment.

PA6 nanofibrous layer was put onto PP/PE bi-component nonwoven fabric and inserted between two Teflon belts moving at 2 m/min in the lamination equipment.

The temperature was set at 135 °C because of the melting point of PE (120–130 °C). The nanofibrous layer was adhered to the nonwoven fabric at the pressure of 15 N/cm² while the PE fibers partly melted, and backing paper pilled off to obtain resulting product, which was called the nonwoven-nanofibrous composite (NNC) scaffold (Fig. 3.2).

3.2.4. Preparation and optimization of active barrier layer

Interfacial polymerization was carried out to form a polyamide active barrier layer on the NNC scaffolds. The aqueous phases were prepared by dissolving PIP and MPD in the DI water while the organic phase was prepared by dissolving TMC in the hexane. As a first step in the optimization of the barrier layer, different concentrations of monomers, 0.25, 0.5, 1.0, 2.0, and 4.0 % (w/v) were chosen to prepare aqueous phases while concentrations of 0.1, 0.2, and 0.4 % (w/v) were chosen for the organic phase. In the second step of optimization, different reaction times for the formation of the polyamide layer were investigated. NNC scaffolds were immersed in aqueous phase for 1, 3, or 5 min and immersed in organic phase for 10 s, 30 s, 1 min, 3 min, or 5 min. The third step of optimization was the investigation of the crucial drying time between two phases. After immersing the NNC scaffolds in the aqueous phase, the wetted scaffolds were left in air for 2.5, 5, 7.5, or 10 min. Moreover, in the same step, two different methods were performed: (1) the scaffolds were wetted with aqueous solutions and subsequently immersed immediately in organic solution without drying, and (2) a rubber roller was used to remove extra aqueous solution from the surface of scaffold then it was immersed in the organic solution. As a last step of optimization of the barrier layer, further processes were

applied to complete the crosslinking of the polyamide layer. After the organic solution was drained out, the thin layered NNC scaffolds (TFNC) were cured at ≈ 21 (at room temperature), 65, 70, 90, or 110 °C for 10 min each. Finally the TFNC membranes were washed and stored in DI water before the tests. The author determined all conditions of steps in this chapter unless otherwise specified.

3.2.5. TFNC membrane performance evaluation

A dead-end solvent-resistant stirred cell (Millipore-XUF 047 01) with an active filtration area of 15 cm² and capacity of 0.05 L was used for evaluation of the membrane performance (Fig. 3.3). The feed aqueous solutions were 2000 ppm NaCl and MgSO₄. The feed chamber was pressurized by nitrogen gas and tests were conducted at room temperature (≈ 21 °C) at an applied pressure of 4.8 bar. The sufficient volume of DI water was passed through the TFNC membrane to ensure stable membrane performance before testing. The conductivity of permeates was measured using a digital conductivity meter. The rejection was calculated by Eq.3.

$$\text{Rejection (\%)} = \frac{C_f - C_p}{C_f} \times 100 \quad \text{Eq. (3)}$$

where C_f and C_p are the conductivity of the feed and permeate concentrations.

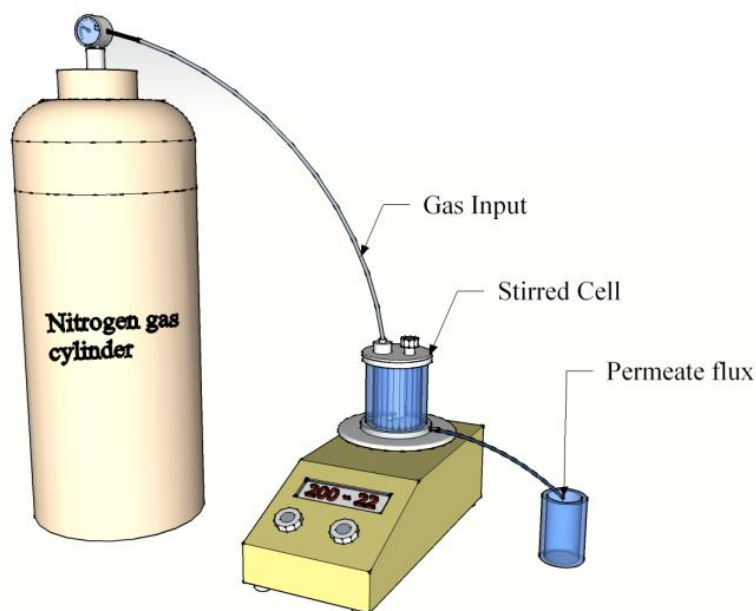


Figure 3.3. Schematic of dead-end filtration unit

3.2.6. Characterization of NNC scaffold and TFNC membrane

The NNC scaffold and TFNC membranes were dried at room temperature for 24 h and then coated with a 5 nm layer of gold using a QuorumQ150R ES sputter coater for observing of surface morphologies. The surface morphologies of the NNC scaffold and the MPD and PIP based TFNC membranes were investigated using scanning electron microscopy (Tescan-Vega3, SEM). Cross-section images were also obtained by SEM to observe the regularity of lamination and the thickness of layers. The fiber diameter was measured using NIS-Elements AR (Nikon) computer software, and the average fiber diameter of 100 different fibers was determined. Attenuated total reflectance Fourier transform infrared spectroscopy (ATR-FTIR) characterizations of the NNC scaffold and the MPD- and PIP-based TFNC membrane surfaces were made with an ATR accessory, using a Nicolet IZ10 instrument (Thermo Fisher Scientific Inc., Waltham, MA). Samples were analyzed by a reflection technique using a germanium crystal. The surface roughness of the TFNC membranes was analyzed using an atomic force microscope (JPK Nanowizard III). Measurements included average roughness (Ra), root mean square (RMS) roughness and peak-to-valley roughness (Rt). The surface hydrophilicity of the NNC scaffold and MPD and PIP based TFNC membranes was evaluated using an optical angle meter (Advex Instruments s.r.o). The contact angle was obtained from measurements of the right and left side angle of water droplets. For each sample, 60 measurements were done in different spots on the samples. No differences were found between the right and left angles of droplet; therefore, the average contact angle was calculated to define the exact value of the contact angle. The NNC scaffold was mechanically tested with a LabTest 2.050 instrument (LaborTech) and the data were evaluated using LabTest 3 software. Samples with dimensions of 50 mm × 25 mm were used for the tensile strength measurements. The pore size distribution (mean flow, bubble point, smallest pore) was determined using a capillary flow porometer. In this method, a wetting liquid is allowed to fill the pores of the NNC materials and then a nonreacting inert gas is allowed to displace the liquid from the pores. The pore size is calculated by:

$$D = 4\gamma \cos\theta / p \quad \text{Eq. (4)}$$

where D is the pore diameter, γ is the surface tension of liquid, θ is the contact angle of liquid, and p is the differential gas pressure. The measured gas pressure and flow rates allow calculate of the pore throat diameters, pore size distribution and gas permeability (Porous Materials Inc., USA).

3.3. RESULTS AND DISCUSSION

3.3.1. Characteristic of NNC scaffolds and TFNC membranes

In this chapter, production of PA6 nanofibers was carried out by Nanospider electrospinning equipment onto backing paper substrate. Then the PA6 nanofibrous layer was transferred onto PP/PE spunbond nonwoven by lamination method. Figure 3.4 illustrates the top-viewed and cross-sectioned SEM image of the NNC scaffolds. The average fiber diameter of NNC scaffolds top layer was 126 ± 29.1 nm and mean flow pore size was $0.739 \mu\text{m}$. Further features of the NNC scaffold are listed in Table 3.1.

Table 3.1. Properties of NNC scaffold

	Smallest Pore Size (μm)	Bubble Point Pore Size (μm)	Mean Flow Pore Size (μm)	Fiber Diameter (nm)
NNC scaffold	0.469	1.064	0.739	126 ± 29.1

The tensile strength test of the nonwoven, nanofibrous scaffold, and NNC scaffold were measured individually. The nanofibrous layer showed weak mechanical properties of 4.33 N/25mm (machine direction) and 4.12 N/25mm (counter-direction) while the tensile strength of the bi-component spunbond nonwoven was 14.95 N/25mm (machine direction) and 6.14 N/25mm (counter-direction). When the lamination method was applied, the tensile strength of the NNC scaffold was increased to 29.17 N/25mm (machine direction) and 14.42 N/25mm (counter-direction).

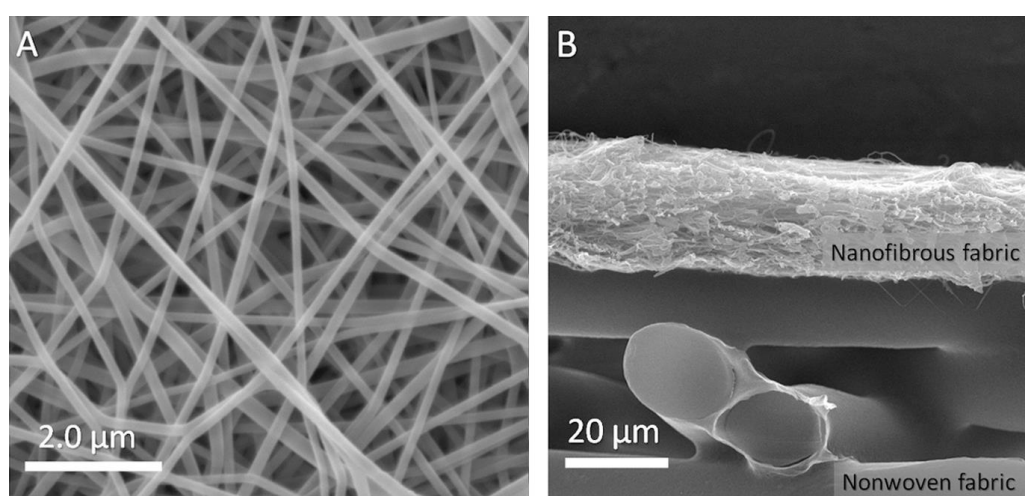


Figure 3.4. SEM images of (A) top view (nanofibers) and (B) cross-sectioned NNC scaffolds

The thicknesses of the nanofibrous scaffold and spunbond bi-component nonwoven were $38 \pm 0.5 \mu\text{m}$ and $75 \pm 1 \mu\text{m}$, respectively. After lamination of fabrics, the total scaffold thickness was $105 \pm 5 \mu\text{m}$. PA nanofibrous material on the nonwoven supporting surface and the interfacial polymerization of *m*-phenylenediamine, piperazine and trimesoyl chloride which produced the polyamide active barrier layer structures were confirmed using ATR-FTIR method (Fig. 3.5). The spectrum of NNC scaffolds surface (Fig. 3.5-1), shows typical polyamide 6 which is based on one single monomer with six carbon. The spectra of MPD-based membrane (Fig. 3.5-2) shows the absence of the acid chloride band at 1768 cm^{-1} and strong band at 1654 cm^{-1} (amide I) is present characteristic of C=O bands of an amide functional group, indicating that successful polymerization has occurred. Moreover, other bands characteristic of aromatic polyamide are also seen at 1540 cm^{-1} (amide II, C=N stretch) and 1606 cm^{-1} (aromatic ring breathing). The spectra of PIP-based membrane (Fig.3.5-3) shows strong band of C=O and aromatic ring breathing between $1660 - 1556 \text{ cm}^{-1}$. The absence of aromatic polyamide structure was observed between $1573 - 1508 \text{ cm}^{-1}$ and indicates that PIP-based membrane was arisen more linear structure in its chain during IP polymerization (Fig. 3.7). Most important difference of PIP-based membrane than MPD-based membrane is the formation of $-\text{COOH}$ group that come the hydrolysis of the unreacted carbonyl chloride. The $-\text{OH}$ (3438 cm^{-1}) which is found in both membranes proved the existence of carboxylic acid.

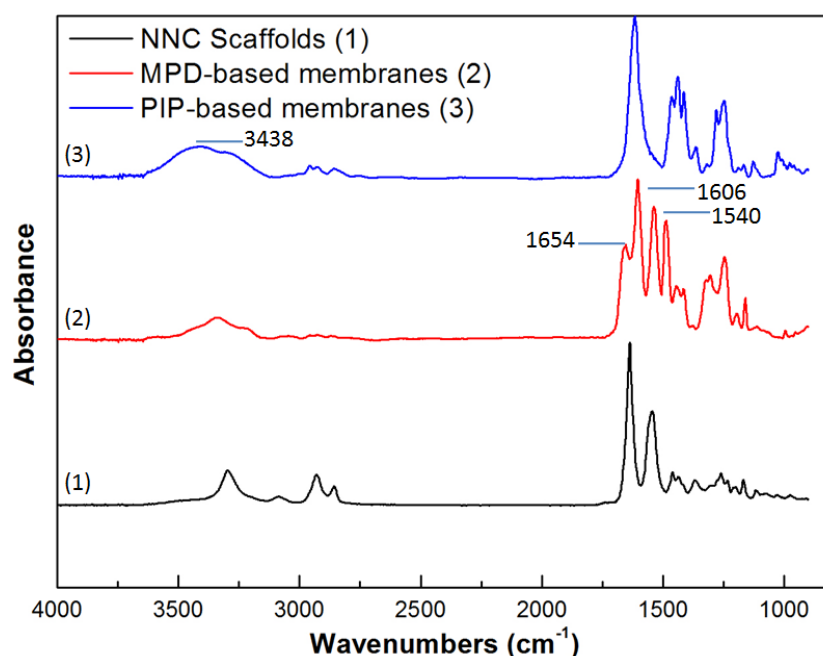


Figure 3.5. ATR-FTIR of NNC scaffold (1) and (2) 2.0–0.2 (w/v)% MPD–TMC, (3) 2.0–0.2 (w/v)% PIP–TMC

However, the amount of – OH in the PIP-based membrane is more intense than MPD-based membrane because of partial hydrolysis of unreacted acyl chloride group during IP reaction of PIP to TMC.

Table 3.2 gives the roughness properties of the NNC scaffold and MPD-based membrane (2.0 MPD and 0.2 TMC %) and PIP-based membrane (2.0 PIP and 0.2 TMC %).

Table 3.2. AFM properties of specimens

Specimens	NNC scaffold	MPD-based TFNC	PIP-based TFNC
Average Roughness (nm)	53.25 ± 5.2	22.45 ± 4.5	18.77 ± 3.8
RMS Roughness (nm)	85.17 ± 9.5	27.64 ± 4.9	23.66 ± 4.1
Peak-to-Valley Roughness (nm)	298.21 ± 12.1	161.7 ± 9.7	135.1 ± 8.5

The AFM results indicated that presence of the PA active barrier layer decreased the surface roughness of the NNC scaffold when compared with the MPD or PIP based membranes. The roughness values of the MPD-based and PIP-based membranes were almost the same.

The average contact angles of specimens are given in Table 3.3. NNC scaffold showed a slightly hydrophilic behaviour while the membranes with the active barrier layer had more hydrophilic behaviour than the NNC scaffold. In particular, the average contact angle of PIP-based TFNC membranes is 8.2°.

Table 3.3. Contact angle measurement of species

Specimens	NNC scaffolds	MPD-based membranes	PIP-based membranes
Average contact angle	62.7°	56.5°	8.2°

3.3.2. Optimization and evaluation of TFNC membranes

Interfacial polymerization was carried out to form a barrier layer by introducing an organic solution on top of the NNC (PP-PE/PA6) scaffold containing aqueous solution. One of the biggest advantages of interfacial polymerization is the absence of a requirement for

stoichiometric amounts of reactants (Kao et al. 2010). Rapid reaction is going only into interface; therefore, it is not possible to evaluate molar quantity that is reacting another. The most important reaction parameters for the optimization of the barrier layer were investigated, such as various concentrations of monomer solutions, the reaction time in solutions (contact time), drying time after immersion of scaffolds in the aqueous solution, and curing type. According to the membrane performance (flux and rejection), in each step, one of the optimum conditions was chosen and then the investigation proceeded to the next step. All experiments were carried out without extra additive (e.g., surfactant, nanoparticles) in the monomer solutions or surface modification to enhance the performance of the membranes.

3.3.2.1. Various concentration of monomer solutions

The first attempt at formation of a barrier layer on the NNC scaffold investigated various concentrations of monomer solutions [0.25, 0.5, 1.0, 2.0 and 4.0 % (w/v) aqueous solutions of PIP and MPD and 0.1, 0.2 and 0.4 % (w/v) TMC in hexane] at a constant reaction time of 3 min (aqueous solution) and 30 s (organic solution). The drying time after immersion in the aqueous solution was kept constant at 5 min. The final TFNC membrane was cured at 65 °C in an oven for 10 min. The reaction of both MPD (Fig 3.6) and PIP (Fig 3.7) monomers with TMC led to the successful formation of a dense layer on the NNC scaffold. Figure 3.8 shows the top view and cross-sectioned images of the barrier layers prepared by the IP method. Although the pattern of the nanofibers layer was visible from the surface of the SEM images of TFNC membranes, it is clear that the PIP-based TFNC membrane formed a defect-free barrier layer while the MPD-based TFNC membrane formed a spotted (dotted) barrier layer.

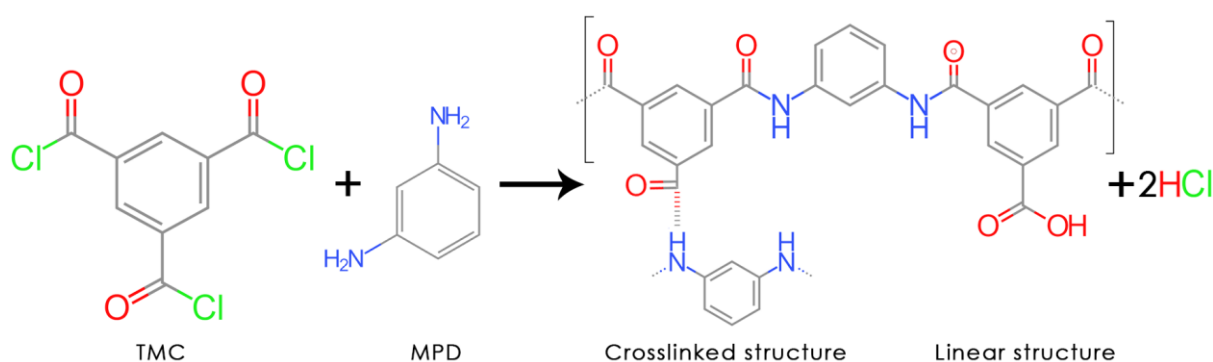


Figure 3.6. An Aromatic polyamide formed with trimesoyl chloride and *m*-phenylenediamine

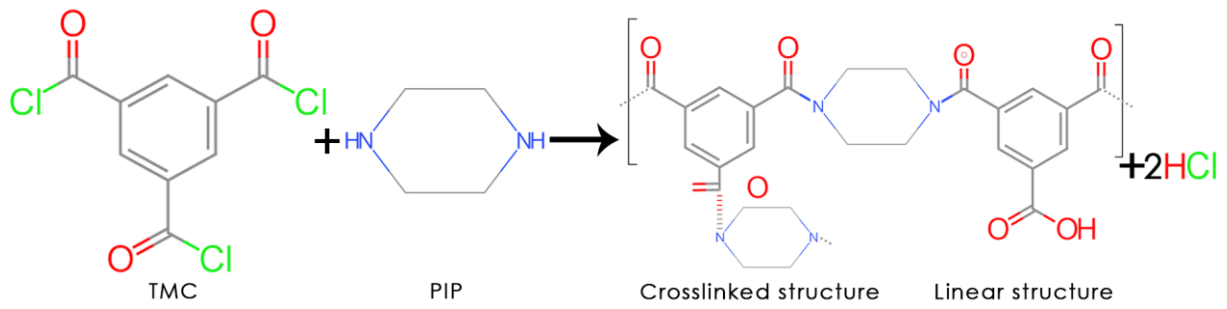


Figure 3.7. Reaction of piperazine and trimesoyl chloride to aliphatic PA

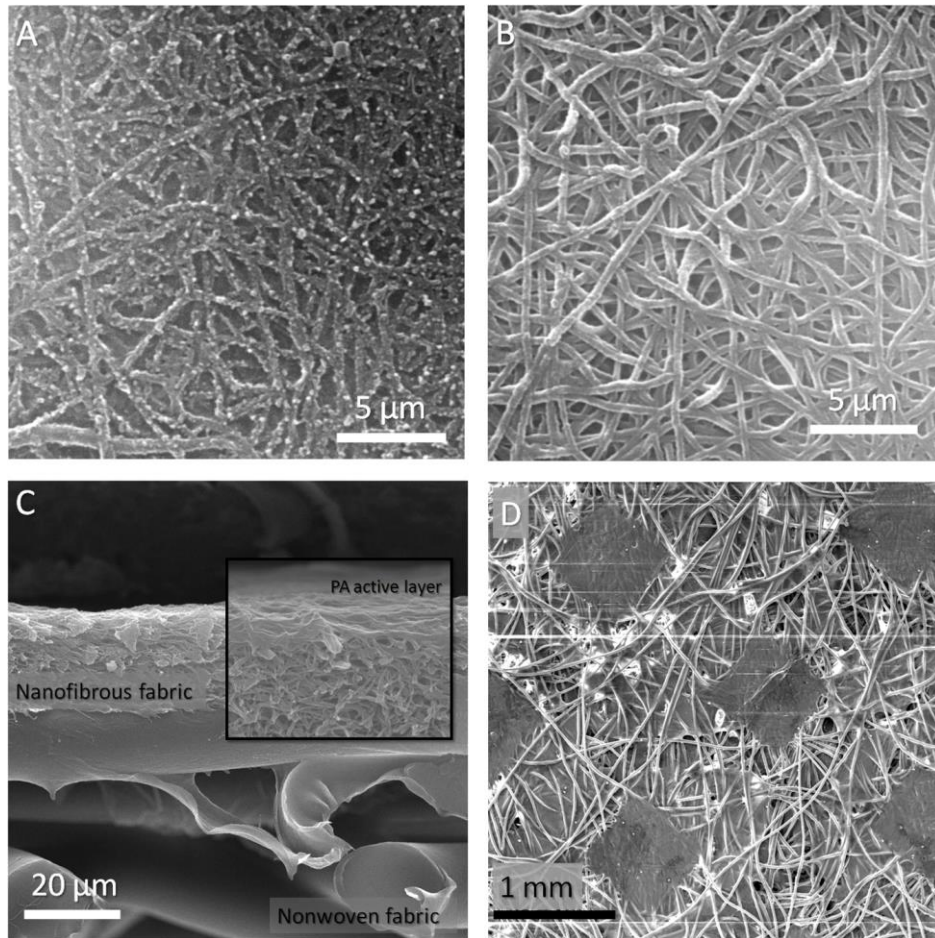
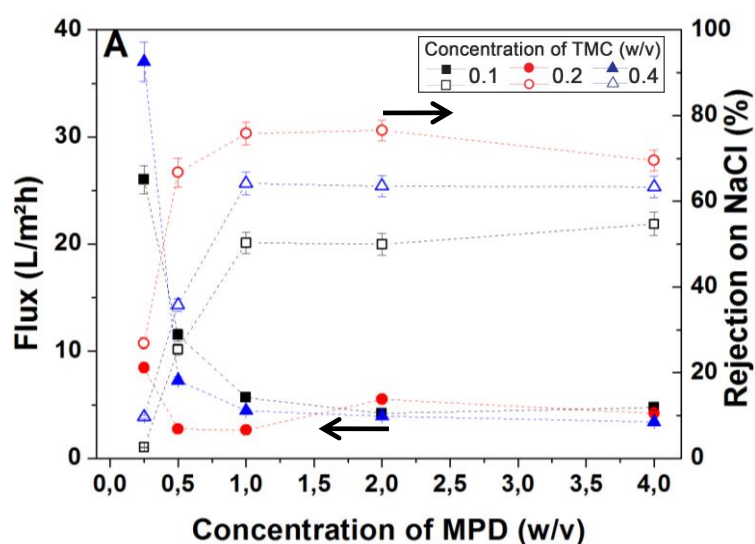


Figure 3.8. SEM images of TFNC membranes (A) 2.0–0.2 (w/v)% MPD–TMC, (B) 2.0–0.2 (w/v)% PIP–TMC, (C) cross-sectioned 2.0–0.2 (w/v)% PIP–TMC, (D) Unsuccessful polymerization of active layer on nonwoven fabric.

In Fig. 3.8.(D) shows that an active barrier layer failed to polymerization or coat the nonwoven fabric without nanofibrous scaffolds due to irregular surface and relatively bigger pore structure of nonwoven fabric. This membrane was performed zero rejection and was not investigated further in this study.

Figure 3.9 shows the NF performance (flux and rejection of NaCl/MgSO₄) of the IP of MPD-based membranes. Increasing the MPD concentration resulted generally in an increase in the rejection and a decreased flux. The lowest salt rejection was obtained when the TMC concentration was fixed at 0.1 % (w/v) because of the lack of crosslinking or the presence of cracks in the barrier layer (Fig. 3.15.A). A concentration of TMC of 0.2 % (w/v) gave the highest values for the rejection performance. For example, the combination of an MPD concentration of 2.0 % (w/v) and a TMC concentration of 2.0 % (w/v) gave a rejection of 76.5% (NaCl). However, when the TMC concentration was fixed at 0.4 % (w/v), the rejection decreased dramatically. The flux obtained with 0.4 % (w/v) TMC [and MPD < 2% (w/v)] was higher than that obtained with 0.2 % (w/v) TMC and it was lower [with MPD 2-4 % (w/v)] than that obtained with 0.2 % (w/v) TMC (Table 3.4). The reason for the higher flux and lower rejection in the initial TFNC membranes with a TMC concentration of 0.4 % (w/v) was that they had a higher acid chloride concentration and an insufficient amine concentration. Hence, the IP reaction created a defective PA active layer. The reason for the lower flux and rejection of the TFNC membranes with a TMC concentration of 0.4 % (w/v) was that the higher ratio of MPD [2-4 % (w/v)] could increase diffusion of the amine into the organic phase on the NNC scaffold during the IP reaction. Hence, the thickness of the barrier layer increased while the flux performance decreased. A higher amine or acid chloride concentration also led to the formation of brittle and disordered active barrier layers, which were allowed greater passage of salt ions (Mohan and Kullová 2013).



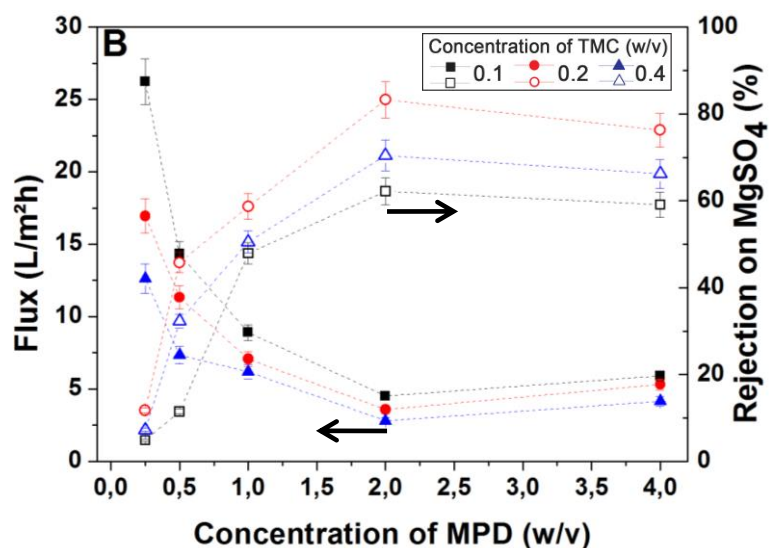


Figure. 3.9. Dependence of the flux and rejection on MPD concentration for various TMC concentrations with TFNC-based membranes using feed solutions of 2000ppm (A) NaCl and (B) MgSO₄.

A high MgSO₄ rejection of 83.2 % was obtained with the combination of 2.0 % (w/v) MPD and 0.2 % (w/v) TMC.

The NF performances of IP of PIP-based membranes are provided in Fig. 3.11. The same flux and rejection trends seen with the MPD-based membranes were also obtained with the PIP-based membranes. The PIP-based membranes showed more or less the same rejection performance as the MPD-based membranes for rejection of MgSO₄, but the rejection of NaCl, shown in Fig. 3.11.(A) was lower than that shown in Fig. 3.9.(A) at all concentrations (also see, Table 3.4). The reason of PIP-based membranes selectivity in bivalent over monovalent ions is the formation of charged PA active barrier layer on the NNC scaffolds which contains pendant carboxylic acid group (see Fig. 3.5 – ATR-FTIR). These charged carboxylic acid groups arise due to the partial hydrolysis of unreacted acyl chloride group during IP reaction (Fig. 3.10).

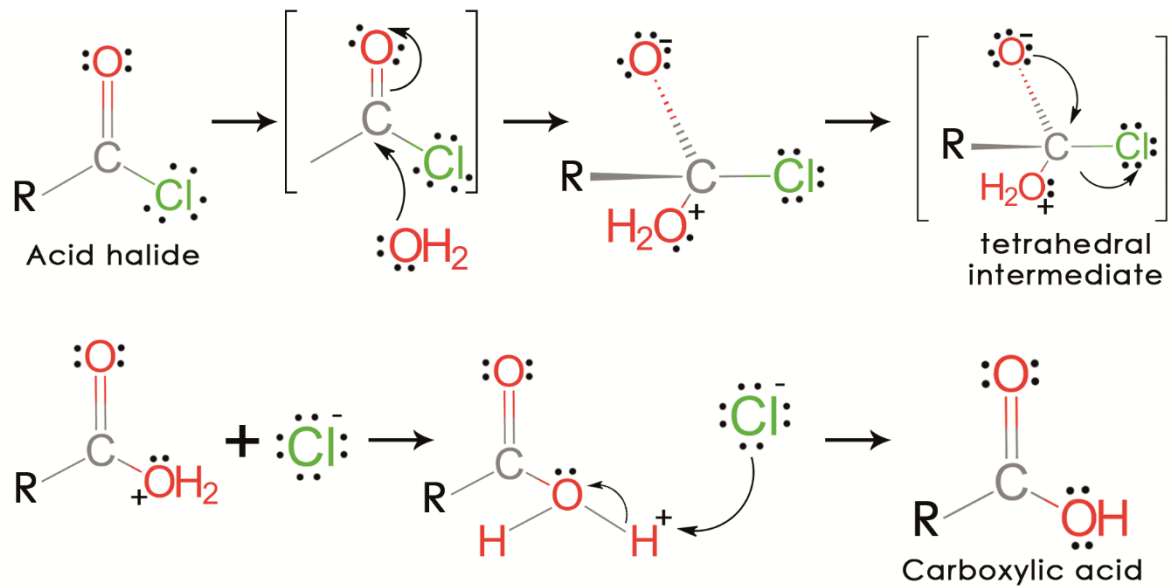
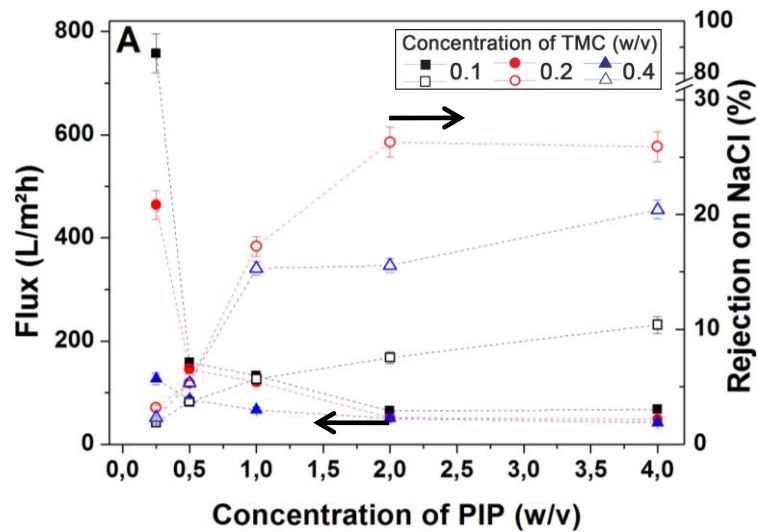


Figure 3.10. Hydrolysis of acid halides and formation of carboxylic acid

The generally accepted explanation for the selective MgSO_4 salt rejection by PIP-based membranes is the contribution of an electrostatic repulsion mechanism rather than a size exclusion mechanism (Freger 2003; Petersen 1993).



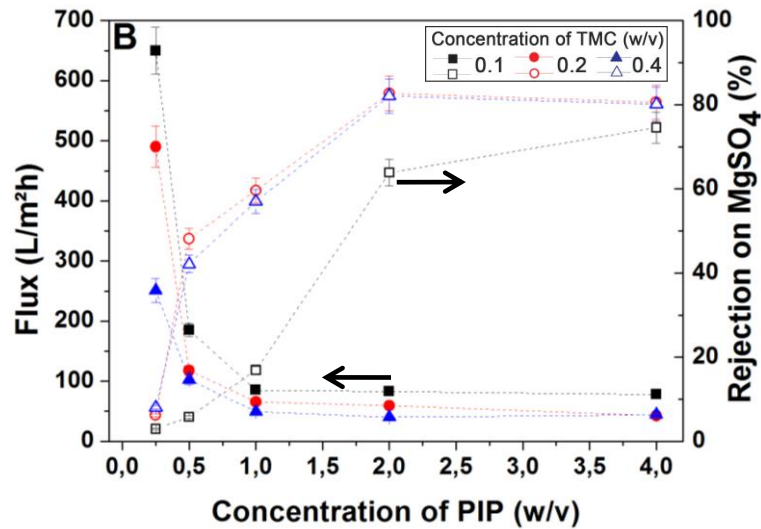


Figure 3.11. The dependence of flux and rejection on PIP concentration at various TMC concentrations in TFNC-based membranes using feed solutions of 2000ppm (A) NaCl and (B) MgSO₄.

Table 3.4. Flux and rejection performance of MPD and PIP based membranes.

Concentration of MPD-TMC % (w/v)	Flux (L m ⁻² h ⁻¹)		Rejection (%)		Concentration of PIP-TMC % (w/v)	Flux (L m ⁻² h ⁻¹)		Rejection (%)	
	NaCl	MgSO ₄	NaCl	MgSO ₄		NaCl	MgSO ₄	NaCl	MgSO ₄
0.25	26.1	26.24	2.5	4.8	0.25	757.5	650.1	1.8	2.9
0.5	11.4	14.3	25.3	11.4	0.5	158.7	185.1	3.6	5.7
1.0	5.6	8.9	50.3	47.9	1.0	132.8	85.2	5.6	16.9
2.0	4.2	4.5	49.9	62.1	2.0	64.2	82.7	7.5	63.8
4.0	4.7	5.9	54.7	59.1	4.0	67.4	77.8	10.4	74.5
0.25	8.4	16.9	26.8	11.7	0.25	463.8	490.2	3.2	6.2
0.5	2.7	11.3	66.7	45.8	0.5	145.4	117.7	5.3	48.1
1.0	2.6	7.07	75.8	58.6	1.0	120.4	65.5	17.2	59.6
2.0	5.5	3.5	76.5	83.2	2.0	51.2	59.3	26.3	82.7
4.0	4.2	5.3	69.5	76.5	4.0	48.2	42.5	25.9	80.6
0.25	37.1	12.6	9.7	7.2	0.25	126.6	251.6	2.4	8.1
0.5	7.2	7.3	35.8	32.5	0.5	86.8	102.5	5.3	42.1
1.0	4.4	6.1	64.1	50.4	1.0	66.3	49.4	15.3	57.3
2.0	3.9	2.8	63.5	70.4	2.0	49.8	40	15.5	82.2
4.0	3.3	4.1	63.3	66.2	4.0	41.9	44.2	20.4	80.1

The well-known reason for a decrease of flux while the rejection increases is that increasing monomer concentration leads to a thicker and denser active barrier layer on the NNC scaffold. Hence, the water resistivity of membranes increased and the diffusivity of water molecules through the thick active barrier layer took a longer time than that through a thinner layer, while salt ions were detained by the pores. However, a further rise in the monomer concentration (i.e., 4.0% PIP or MPD concentration) affected the barrier layer structure negatively and the rejection and flux performance decreased both.

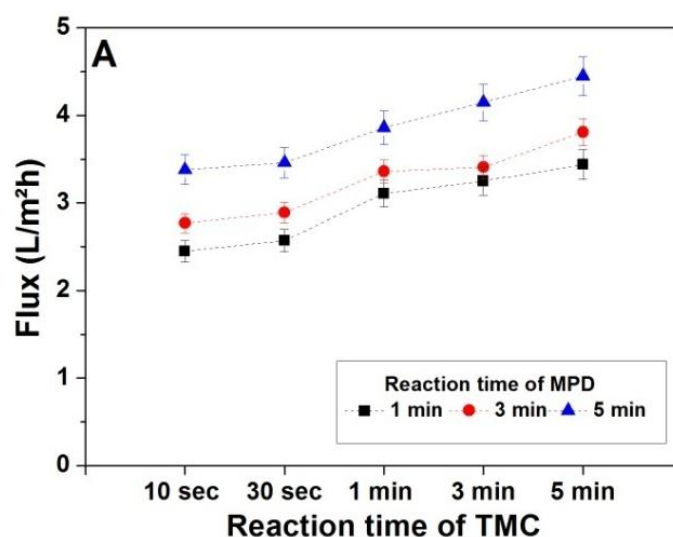
Figures 3.9 and 3.11 indicate another significant difference. The PIP-based TFNC membranes exhibited higher permeate fluxes when compared with the MPD-based TFNC membranes. The reasons for these higher permeate fluxes may be summarized as follows: (1) The amine groups in aqueous solutions can continually cross the water–hexane interface, diffuse through the already formed polyamide layer, and then come into contact with acyl chloride on the organic solvent side (Lo et al. 2013; Petersen 1993). Thus, an MPD-based active barrier layer (around 0.3 to 1.0 μm) could differ significantly in terms of thickness when compared to a layer formed from PIP (less than 0.3 μm). The presence of a thick active barrier layer on the MPD-based membranes would substantially decrease the permeate flux. (2) It is well known that secondary amines are more reactive compared to primary ones. However, the formation rate of poly(piperazineamine) active barrier layer was slow (Lo et al. 2013; Vyas and Ray, 2015; Kim et al. 2002; Saha and Joshi, 2009) despite the relatively strong basicity of this secondary amine (Petersen 1993). Probably, molecule structure of MPD is flat and the molecule structure of PIP is 3D, hence, a steric demand of PIP molecule is much higher than MPD to the large molecules that is TMC. One another speculation that piperazine ineffectively partitions in to the organic phase, tends to be tied up as the hydrochloride salt. This was due to the linear portion of the PIP-based PA active barrier layer, which possesses polar free $-\text{COOH}$ groups. The contact angle of PIP-based membranes indicated a highly hydrophilic performance when compared with MPD-based membranes. The water resistance of PIP-based membranes was noticeably low and caused a high flux of water across the entire membrane. (3) The increased surface area of the membrane is believed to have increased the flux (Freger 2003; Kwak et al. 2001). Electrospun nanofibrous materials exhibit a well known phenomenon where the numbers of nanorods or nano protrusions on the nanofibers increase the surface area of the materials (Kim et al. 2006b; Ostermann et al. 2006). Thorn-like structures were apparent in the high magnification SEM images of the nanofiber surface after the IP reaction of PIP-based membranes (Fig. 3.15.C). The directions of these thorn-like protrusions were both horizontal and vertical and they moved inward into the nanofibrous layer. Hence, we assume that the thorn-like structures increased the surface area of PIP-based membranes and provided more opportunities for contact with water, thereby paving the way for enhanced water permeability.

The results of Table 3.4 and Figure 3.9 and 3.11 were analyzed to choose optimum result from the first tests. The combination of 2.0% (w/v) MPD and 0.2% (w/v) TMC was chosen as the optimum concentration and was used in all further optimization and filtration experiments of NaCl feed solution because of the high rejection performance of monovalent salts (76.5%,

NaCl). The combination of 2.0% (w/v) PIP and 0.2 % (w/v) TMC concentrations gave a membrane with a rejection rate of 82.7% (MgSO_4), while its flux was $59.3 \text{ L m}^{-2} \text{ h}^{-1}$. The combination of 2.0% (w/v) PIP with 0.2% (w/v) TMC was chosen as the optimum concentration and used in all further optimization experiments and filtration experiments using MgSO_4 feed solution because of the high rejection of divalent salts.

3.3.2.2. Reaction time in monomer solutions (contact time)

After determination of the optimum concentrations for the TFNC membrane, the second most important parameter was investigated, namely the contact time or reaction time of the NNC scaffold in the monomer solutions. Immersion times of 1, 3 and 5 min were chosen for the aqueous solution and 10 and 30 s and 1, 3, and 5 min for the organic solutions. The drying time after immersion in the aqueous solution was kept constant at 5 min. The final TFNC membranes were cured at $65 \text{ }^\circ\text{C}$ in an oven for 10 min.



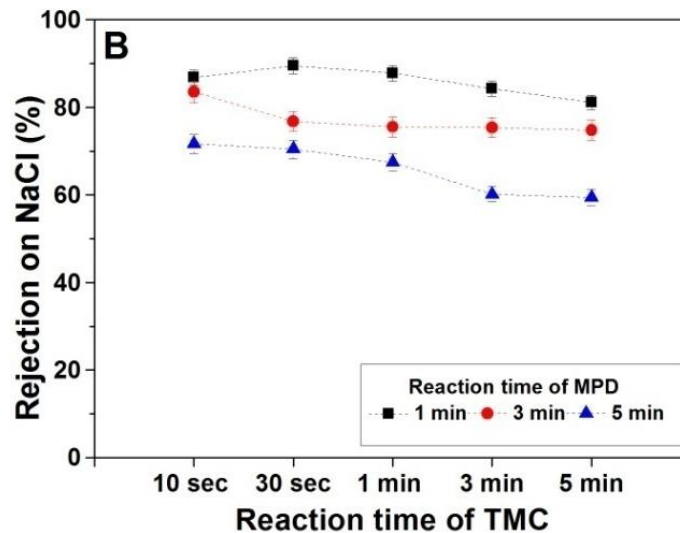


Figure 3.12. The reaction time dependence of (A) flux and (B) rejection of MPD-based TFNC membranes using the NaCl feed solutions for various reaction times.

Figure 3.12 shows the NF performance of MPD-based membranes produced at different reaction times in the solutions. The flux performance increased and rejection performance decreased as the reaction times of MPD and TMC increased. The highest value for rejection of the NaCl feed solution was obtained for the shortest reaction time with both monomers. The TFNC membrane produced by the reaction of 1 min in MPD and 30 sec in TMC solutions had a flux of $2.57 \text{ L m}^{-2} \text{ h}^{-1}$ (NaCl) and rejection of 89.5%. The reaction time for the membrane produced after 1 min in MPD and 30 sec in TMC was chosen as the optimum and used for step of curing temperature.

Figure 3.13 presents the NF performance of PIP-based membranes produced at different reaction times. The reaction time in both phases had a significant influence on the flux and rejection performance of TFNC membranes. The expected well-known phenomenon of decreasing flux and increasing rejection was not observed. Figure 3.13.(A) shows that the flux performance decreased as the reaction times of PIP and TMC increased. However, Figure 3.13.(B) shows that an increased in the reaction time with TMC enhanced the rejection performance of TFNC membranes, whereas increases in the reaction time with PIP first affected the rejection performance positively (at 10s, 30s, and 1 min for TMC) and then negatively (at 3 and 5 min for TMC).

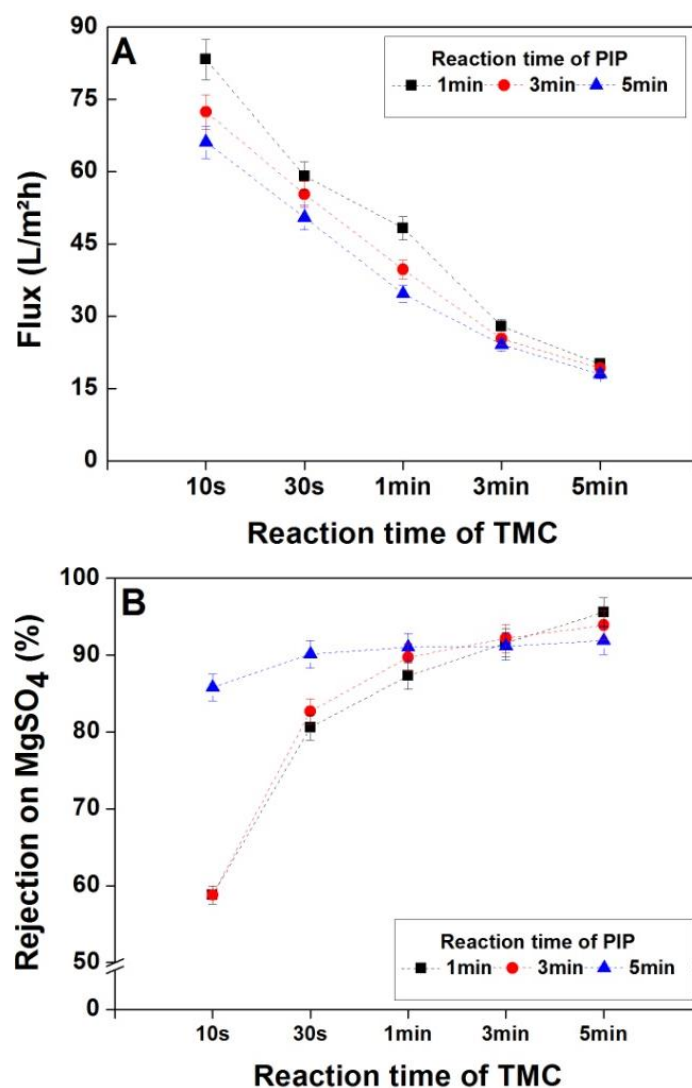


Figure 3.13. The reaction time dependence of (A) flux and (B) rejection of PIP-based TFNC membranes using the MgSO₄ feed solutions for various reaction times

For example, the TFNC membrane reacted for 5 min in PIP and TMC solutions had a flux of 16.5 L m⁻² h⁻¹ (MgSO₄) and rejection of 91.9%, while the TFNC membrane immersed for 1 min in PIP solution and for 5 min in TMC solution had a flux of 20.2 L m⁻² h⁻¹ (MgSO₄) and rejection of 95.6%. The latter membrane was called TFNC (1) and was used for comparison with commercial membranes.

The increased reaction time for both solutions led to excessive crosslinking of the monomers and formation of a thicker active barrier layer on the TFNC membrane surface, which decreased the flux performance. Excessive crosslinking also disrupted the structure of the active barrier layer, thereby decreasing its selectivity. The results shown in Figs. 3.13.(A) and 3.13.(B) indicated the possibility of an enhancement of the rejection performance without compromising the flux performance with TFNC membranes. The reaction times of 5 min in PIP solution and

30 s in TMC solution were chosen as the optimum reaction times because of the reasonable rejection and high flux performance (90.1% and 50.5L m⁻² h⁻¹, MgSO₄, respectively) and used for the next step. Figures 3.12 and 3.13 confirm the higher reaction rate of MPD monomers than PIP monomers with TMC, as indicated by the highest values of rejection with short reaction times.

3.3.2.3. Determination of drying method and time

The drying time is one of the most important parameters during fabrication of TFNC membranes. Following the immersion of the NNC scaffold in aqueous monomer solution (PIP or MPD), the nascent TFNC membranes had to be held vertically to remove excessive monomer solution. The PIP-based membranes and MgSO₄ feed solution were used to determine the drying method and time because of their higher flux performance. Different process conditions, enumerated from 1 to 6, were chosen for evaluation of their filtration performance, which is shown in Table 3.5 or Figure 3.14. In this Table, (1) represents the PIP-solution-wetted nascent scaffold was immersed in TMC solution immediately, without a drying process. In this case, the barrier layer did not attach to or properly cover the nanofiber surface (Figure. 3.15.B) and achieved zero rejection and excessive flux (Table. 3.5).

The process of squeezing excessive PIP solution from nascent NNC scaffold using a rubber roller caused the formation of an active barrier layer that showed selectivity (2).

Table 3.5. The drying method and time dependence of flux and rejection of PIP-based membranes using feed solutions of 2000ppm MgSO₄

Enumerated drying style	Flux (L m ⁻² h ⁻¹)	Rejection (%)
1	1356	0
2	57	84.9
3	56.8	86.1
4	53.1	90.2
5	55.7	88.3
6	88.1	65.7

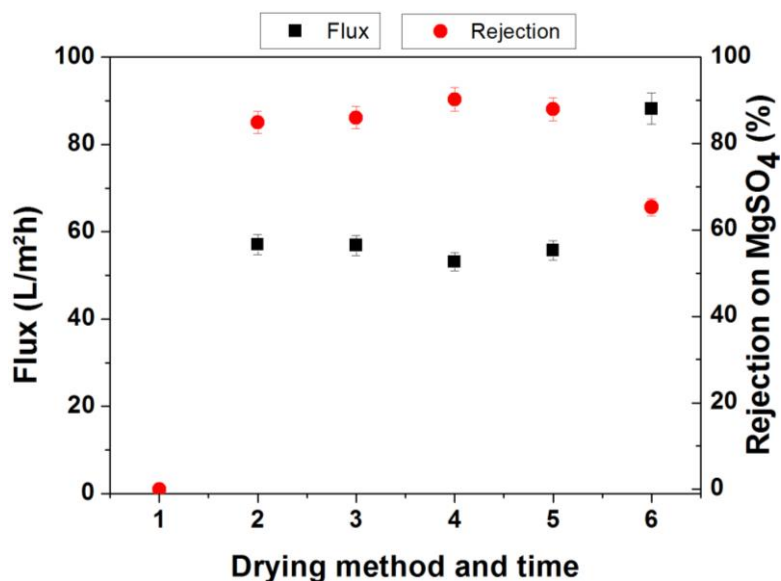


Figure 3.14. The drying method and time dependence of flux and rejection based TFNC membranes using the feed solutions MgSO₄.

1. After immersion in PIP solution, the scaffold was immediately immersed in TMC solution.
2. After immersion in PIP solution, excessive PIP solution was squeezed out with a rubber roller and then the scaffold was immediately immersed in TMC solution.
3. After immersion in PIP solution, the wetted scaffold was held vertically in air for 2.5 min and then immersed in TMC solution.
4. After immersion in PIP solution, the wetted scaffold was held vertically in air for 5 min and then immersed in TMC solution.
5. After immersion in PIP solution, the wetted scaffold was held vertically in air for 7.5 min and then immersed in TMC solution.
6. After immersion in PIP solution, the wetted scaffold was held vertically in air for 10 min and then immersed in TMC solution.

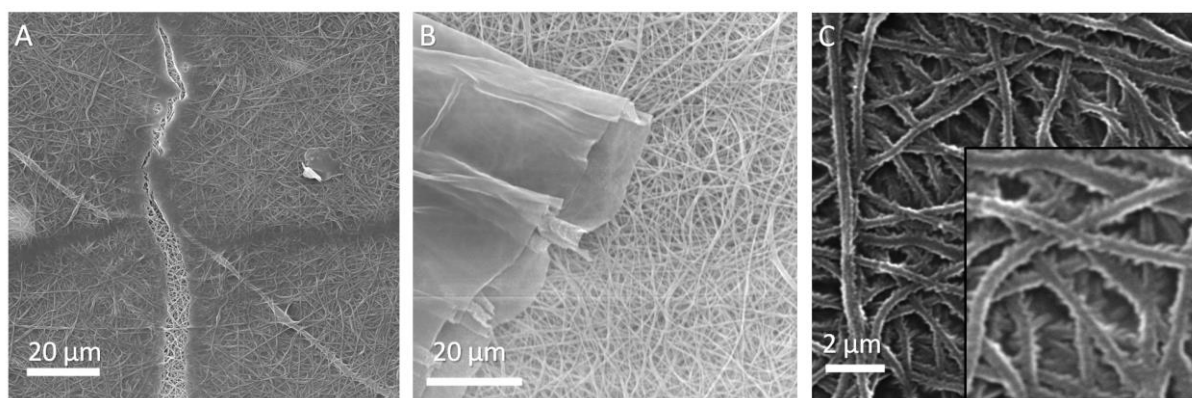


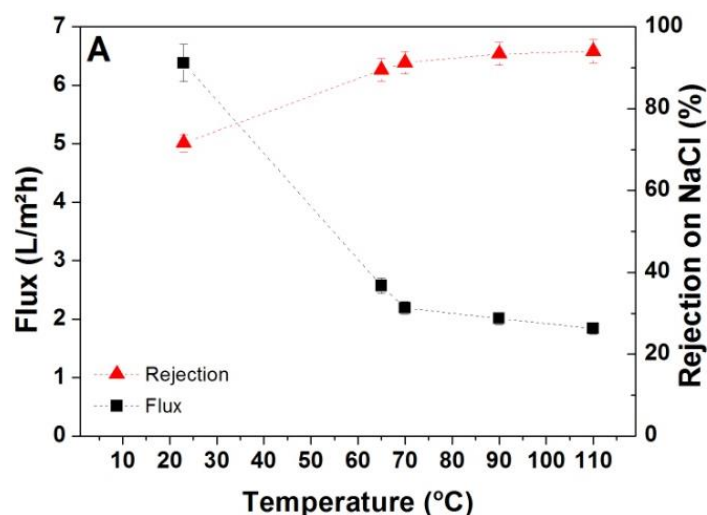
Figure 3.15. Crack(A) and unformed active layer (B) onto NNC scaffold (C) thorn-like structure on active layer

The rejection performance of TFNC membranes increased when the drying time was increased up to 5 min. After 5 min, the rejection performances decreased because the amine groups were unable to cross the water-hexane interface and come into contact with the acyl chloride on the

organic solvent side. This was due to the excessive drying of the PIP solution on the nascent NNC scaffolds (5)-(6) shown in Table 3.5 or Figure 3.14. The flux through the TFNC membranes exhibited an inherently opposite performance to that seen for rejection. Balancing the drying time of the PIP solution – at the so-called 'sweet spot' – is one important condition for the proper formation of the active barrier layer on the NNC scaffold. The optimal value for the drying time for the IP reaction between aqueous and organic solutions was determined as 5 min and was used in the final step for both PIP and MPD solutions.

3.3.2.4. Determination of curing temperature

The TFNC membranes need a curing process to complete the crosslinking of the barrier layer. This process is essentially the last step in the formation of the active barrier layer on the NNC scaffolds when there is no additional post-treatment. Following the immersion of the nascent TFNC scaffold into the TMC solution, the membranes were placed in the oven at different temperatures of ≈ 21 , 65, 70, 90 and 110 °C for 10 min. This treatment not only dries and anneals the film but also performs the crucial step of crosslinking the residual unformed active barrier layer. The temperature was not set higher than 110 °C because of the low melting point of PE (around 120–130 °C). One membrane was also kept at room temperature after immersion in the TMC solution to observe the effect of no heat treatment on the filtration performance.



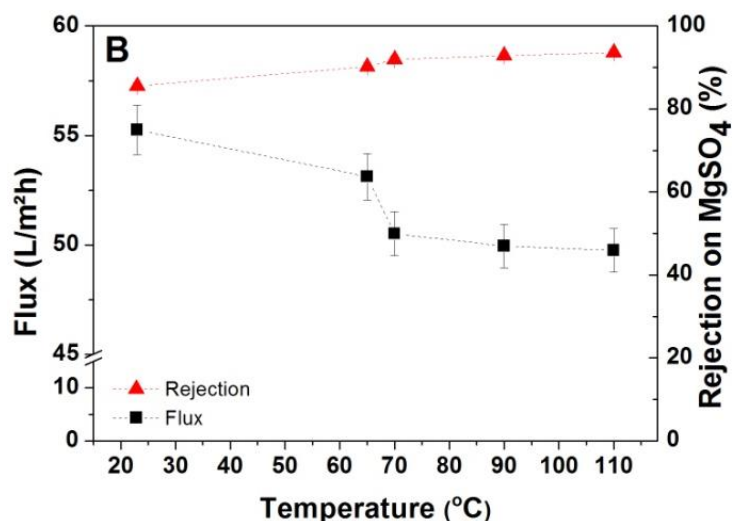


Figure 3.16. The temperature dependence of flux and rejection of (A) MPD-based membranes using the feed solutions of 2000ppm NaCl, (B) PIP-based membranes using the feed solutions of 2000ppm MgSO₄.

Figure 3.16.A shows the flux and rejection performance of TFNC membranes cured at different temperatures. A clear difference was evident between the membranes left at room temperature and those heat-treated at 65 °C, as the flux decreased from 6.38 to 2.57 L m⁻² h⁻¹ (NaCl) and the rejection increased from 71.58 to 89.5% after heating. Curing temperature increases from 70 to 90 or 110 °C caused slight decreases in the flux of TFNC membranes (2.19, 2.01 and 1.84 L m⁻² h⁻¹, respectively), whereas the rejection of the membranes increased [91.22, 93.38 and 93.57%, respectively; Fig. 3.16.(A)].

Figure 3.16.(B) shows that a flux decrease from 55.7 to 53.2 L m⁻² h⁻¹ (MgSO₄) was accompanied by a rejection increase from 85.7 to 90.22%. A curing temperature increase from 70 to 90 or 110 °C resulted in a more or less stable flux (50.51, 49.95 and 49.75 L m⁻² h⁻¹, respectively), whereas the rejection increased (91.95, 92.86 and 93.57%, respectively). The both membranes that were annealed at 110 °C were named TFNC (2) and TFNC (3) were used for comparison with commercial membranes.

3.3.2.5. Comparison with commercial membranes

The fabrication and optimization of TFNC membranes were done in four different steps. Three different TFNC membranes were determined as optimum filter samples for the separation of NaCl and MgSO₄ in feed solution and were compared with commercial Dow Filmtec membranes NF 270 and NF 90. Those commercial membranes for water treatment are polyamide thin film composite (TFC) membranes, containing three separate thin film layers. A polysulfone layer is usually cast onto a nonwoven polyester inner web that contributes to the

membrane overall structural strength. An ultrathin polyamide layer is then applied by interfacial polymerization. Thickness of this polyamide skin layer around 20 nm (Freger et al. 2002; Buch et al. 2008).

The combination of 2.0 % (w/v) MPD in DI water and 0.2 % (w/v) TMC in hexane solution with 110 °C annealing exhibited the highest NaCl separation, and this membrane was named TFNC (2). Two membranes were chosen for the separation of MgSO₄. In the second step, the various reaction times of PIP and TMC were investigated. The reaction times of 1 min in PIP and 5 min in TMC solutions exhibited the highest MgSO₄ separation with reasonable flux and named TFNC (1). Finally, in the last step, the TFNC membrane that was annealed at 110 °C in the oven was chosen as the last sample and was named TFNC (3).

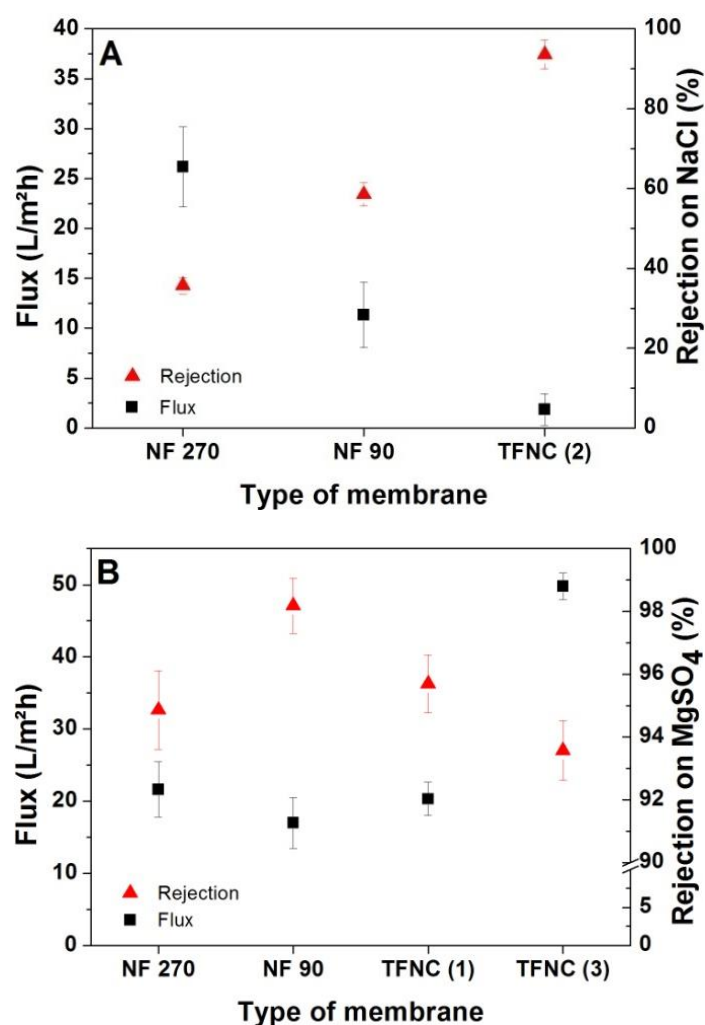


Figure 3.17. Comparison of filtration performance (A-NaCl, B-MgSO₄) between TFNC and commercial membranes at 2000ppm and 4.8 bar with dead-end filtration cell

According to Dow Filmtec sources, the NF 270 commercial membrane has a rejection capability of more than 97% for 2000 ppm MgSO_4 and a flux of around $52 \text{ L m}^{-2}\text{h}^{-1}$, while NF 90 has a rejection capability of more than 97% for 2000 ppm MgSO_4 and a flux of around $41 \text{ L m}^{-2}\text{h}^{-1}$. However, despite choosing the same process conditions in the filtration method (4.8 bar applied pressure, room temperature, stirring at 350 rpm, and 2000 ppm feed solutions in the dead-end filtration cell), NF 270 and 90 exhibited a lower flux performance than expected without showing a problem in the rejection performance (see in Figure 3.17.B). Figure 3.17.(A) illustrates that TFNC (2) exhibited higher NaCl rejection performance (93.57%) than the NF 270 and NF 90 commercial membranes (35.6 and 58.5%, respectively, NaCl) while the flux performance of TFNC (2) ($1.84 \text{ L m}^{-2}\text{h}^{-1}$) was significantly lower than the others (26.1 and $11.3 \text{ L m}^{-2}\text{h}^{-1}$, respectively). Figure 3.16.(B) illustrates that TFNC (1) exhibited a slightly higher MgSO_4 rejection performance (95.6%) than NF 270 (94.8%) and lower rejection performance than NF 90 (98.1%) while the flux performance was competitive (20.2 , 21.6 , and $16.9 \text{ L m}^{-2}\text{h}^{-1}$, respectively). In the case of TFNC (3), the MgSO_4 rejection performance (93.5%) was slightly lower than that of NF 270 and explicitly lower than that of NF 90, while the flux performance of TFNC (3) was twice as high ($49.7 \text{ L m}^{-2}\text{h}^{-1}$) as the others.

These preliminary results indicated that the optimized active barrier layer based on a well-designed nanofibrous supporting surface is suitable for use in NF membranes for separation of salt (monovalent or divalent) ions without any extra additives or modification processes.

3.4. CONCLUSION

Industrial scale PA6 nanofibrous scaffold was spun on the paper backing material than transferred on to PP/PE spunbond bi-component nonwoven fabric by using lamination methods to eliminate disadvantages factors of nanofibrous scaffold such as weak mechanical properties and poor adhesive to nonwoven surface. Lamination method was not only increased mechanical properties of NNC scaffold also created smooth surface for better interfacial polymerization.

To obtain optimum active barrier layer onto the NNC scaffold, four different basic production steps were investigated. First, different monomer concentration were prepared and IP reaction were carried out on to NNC scaffold. The TFNC membranes (2.0 - 0.2 % w/v MPD-based) chose as a first filter species which was exhibited highest NaCl salt rejection (76,5%). 2.0 - 0.2 % (w/v) PIP-based membrane was chosen as an optimum membrane for separation of MgSO_4 salt ion and proceeded to next step.

In second step of optimization of TFNC membrane, influence of different reaction time of monomer solution on the formation of barrier layer was investigated. The result was shown that even small changes in reaction time (contact) are affected directly to the membrane performances. The reaction time of 1 min in PIP solution and 5 min TMC solution chose as a second filter species [also was chosen as sample membrane named TFNC(1)] which had a flux $20,2 \text{ L m}^{-2} \text{ h}^{-1}$ (MgSO_4) and rejection 93,5 %. The reaction time of 5 min in PIP solution and 30 second in TMC solution chose as a optimum reaction time because of reasonable rejection and high flux performance (90,1 % and $50,5 \text{ L m}^{-2} \text{ h}^{-1}$, MgSO_4) and used for the next steps.

In third step, we investigated the impact of the drying time between two-monomer solution reactions on the filtration performance of TFNC membranes. Excessive aqueous solution was paved way to unformed active barrier layer. It was necessary to remove excessive aqueous solution from the surface of the NNC scaffold using a rubber roller or kept in a vertical position. The main point in this step was the drying time of wetted NNC scaffold. The drying time should neither more nor less in while wetted NNC scaffold kept in vertical position. Finally, the IP reaction was completed with the heat treatment. The annealing was carried out at 65 - 70 - 90 and 110 °C. The filtration performance made progress positively while the temperature increased. The highest NaCl and MgSO_4 rejection in this step was obtained at 110 °C value (95,6% - 93.57, respectively)[also were chosen as sample membrane named TFNC(2) - (3)].

The comparison of filtration performance between TFNC and commercial membranes were indicated that optimization of TFNC membranes were successfully carried out by using conventional methods of IP and TFNC membranes were able to compete against to commercial membranes. This chapter usually contented to physically optimization of the membranes (pore size or thickness of active layer) because there were no extra chemically additive in solutions or modification of membranes to change structure of active layer.

The next chapter will be contained the chemically optimization of TFNC membranes to increase monovalent and bivalent salts rejection and flux performance.

CHAPTER 4

ENHANCEMENT FILTRATION PROPERTIES OF THIN FILM NANOFIBROUS COMPOSITE MEMBRANES

4.1. INTRODUCTION

The optimization of TFNC membranes based on nonwoven and nanofibrous materials were carried out in Chapter 3. The different parameters of interfacial polymerization were investigated to form an active layer onto NNC scaffolds without any additive. In the previous chapter, the optimization of TFNC membranes was investigated using $MgSO_4$ and $NaCl$ feed solutions in the filtration process.

It is noticed from the previous chapter that MPD-based membranes were performed low flux with reasonable monovalent ($NaCl$) salt rejection. Moreover, the PIP-based membranes were performed high rejection rate for divalent ($MgSO_4$) salt ions. However, the permeate flux performance of MPD-based membranes and rejection rate of PIP-based membranes were still insufficient.

Based on previous chapter results, the aim of this chapter was to eliminate the negative side of the filtration performance of MPD and PIP based TFNC membranes such as low permeate flux of MPD-based TFNC membranes. Moreover, we expected higher divalent salt ions rejection (more than 98 % rejection) and permeate flux performance from the PIP-based TFNC membranes. The one of best and easiest way to improve the filtration performance of TFNC membranes is the addition of acid acceptor (base – tertiary amine) (Li et al. 2015; Xiang et al. 2014; Xiang et al. 2013) and surfactants (ionic liquids) (Mansourpanah et al. 2011).

Petersen has reported that to obtain higher rejection performance in PIP-based membranes, the presence of an acid acceptor was necessary in aqueous solution, on the other hand; this is not the case for MPD-based membranes (Petersen 1993). As we mentioned in the previous chapter, the formation rate of PIP aqueous solution into the TMC solution was rather low, needs a higher concentration of the acyl halide along with the acid acceptor to promote PA active barrier layer. In the case of MPD-based membranes, the high portion of tertiary amine content acts as a built-in acid acceptor. Hermans has proved that usage of tertiary amine base was necessary to obtain high rejection rate together with surfactants. However adding each of them separately has not improved the performance (Hermans et al. 2015). Mansourpanah has indicated that adding

different kind of surfactants (anionic, cationic and non-ionic) affects the filtration performance and morphology of the active barrier layer. They reported increasing of surfactant concentrations in aqueous PIP solutions usually decreases rejection and increases permeate flux with some exceptions (Mansourpanah et al. 2009).

In this chapter, the effects of adding acid acceptor and surfactants in the aqueous MPD and PIP solutions were investigated on the performance of TFNC membranes such as salt ions rejection and permeate flux. The four kind of salt (MgSO_4 , NaCl , CaCl_2 , Na_2SO_4) were used in this chapter as feed solutions. The filtration performances were examined for the extended period process to determine the performance of TFNC membranes under the long-term utilization in dead-end filtration cell. The presence of a residual compound of TFNC membranes in the permeate side was investigated, which might be released in the permeate water such as MPD, PIP, TMC, TEA, NaOH, surfactants during the filtration. Therefore, liquid chromatography equipment was used to observe the condition of permeate water. Finally, TFNC membranes were used to desalinate the real seawater, which was provided from the Mediterranean Sea.

4.2. EXPERIMENTAL

4.2.1. Materials

Laminated PP/PE Nonwoven and PA6 Nanofibrous scaffolds (NNC) were used as supporting materials, PIP and MPD for aqueous solution and TMC for the organic solution were used to form an active barrier layer on to NNC. Triethylamine (TEA) from Sigma-Aldrich, sodium hydroxide (NaOH) and sodium phosphate (Na_3PO_4) were chosen for acid acceptor materials. Triton-X (Sigma-Aldrich) was used as non-ionic surfactants, and Synferol AH 1241 was used as an anionic surfactant. MgSO_4 , NaCl , CaCl_2 salts as feed solutions were provided from Penta s.r.o. (CZE) moreover, Na_2SO_4 from Lachema, Brno (Chemapol).

4.2.2. Preparation of enhanced TFNC membranes

The laminated PP/PE bi-component spunbond nonwoven and the PA6 nanofibrous web were used as supporting material to create enhanced TFNC membranes. To form an active barrier layer, interfacial polymerization were carried out using MPD and PIP monomers for an aqueous solution while TMC was used for organic solutions.

To prepare the PIP-based TFNC membranes, different concentration of TEA [0.25, 0.5, 1.0, 2.0, 4.0 % (w/v)] were added in certain amount of PIP [2.0 % (w/v)] aqueous solution while

the concentration of TMC were [0.2 % (w/v)]. When the concentration of TEA determined according to best filtration performance, the certain amount of NaOH and Na₃PO₄ [1.0 % (w/v)] were added in [2.0% (w/v) PIP + TEA] aqueous solution and filtration performance were tested again. The reaction times for aqueous (1min) and organic solutions (5min, and 45sec) were determined. The drying time between the solutions was determined 5 min. Curing temperature and time were 110 °C and 10 min in the incubator.

MPD-based membranes were prepared using acid acceptor [TEA, 2.0% (w/v)] and surfactants [non-ionic – anionic liquid, 0.2% (w/v)]. The concentrations of MPD [2.0% (w/v)] and TMC [0.2 % (w/v)] were kept constant in all aqueous and organic solutions. The IP reaction for MPD-based membranes was carried out under the same condition such as the drying, curing time and curing temperature that was mentioned above for PIP-based membranes except the reaction times. The reaction time for MPD aqueous solution was decided 1 min whereas the reaction time for an organic solution was decided 30 sec.

4.2.3. Liquid chromatography analysis

Prepared MPD and PIP based membranes were used to find out any residual compound release from the membranes to the permeate side such as MPD, PIP, TMC, TEA or surfactants. Therefore, the membranes were set into dead-end filtration cell and only pure water was used as a feed solution. The permeate water samples were stored in a vial that is special glassware for liquid analysis. The permeate water samples were taken separately at first 1h of filtration, then between 2nd - 3rd hours of filtration and 4th - 5th hours of filtration. The existence of residual chemicals that could be released from the membranes itself during the pure water filtration experiments were investigated using ABSciex 3200 QTRAP mass spectrometer and a Dionex Ultimate 3000 liquid chromatography.

The amount of salt ions (Na⁺, Ca⁺², K⁺, Mg⁺², Cl⁻, SO₄⁻, NO₂⁻, NO₃⁻) in the original feed seawater and filtered seawater were carried out ion chromatography analysis using ICS-90 Dionex.

4.2.4. Characterization of enhanced TFNC membranes

The surface morphologies of enhanced MPD and PIP based TFNC membranes were investigated using scanning electron microscopy (Tescan-Vega3 SEM). Attenuated total reflectance Fourier transforms infrared spectroscopy (ATR-FTIR) characterization of the MPD

and PIP based TFNC membrane surfaces were made with ATR accessory, using a Nicolet IZ10 (Thermo Fisher Scientific Inc., Waltham, MA). Analysis of samples was carried out by reflection technique using a Germanium crystal. The surface hydrophilicity of NNC scaffold and MPD and PIP based TFNC membranes were evaluated by optical angle meter (Kruss Drop Shape Analyzer DS4).

4.2.5. Molecular weight cut-off (MWCO) test using aqueous PEG solutions

Molecular weight cut-off refers to the lowest molecular weight solute (in daltons) in which 90% of the solute is retained by the membrane (Web source - Library 2016), or the molecular weight of the molecule that is 90% retained by the membrane. The MWCO of MPD and PIP based membranes were evaluated with polyethylene glycol aqueous feed solutions, contain 1000 ppm PEG with different molecular weights (Sigma-Aldrich; Mn: 200, 400, 600). The permeants and feed solutions were analyzed using total organic carbon (TOC) analyzer (Direct measurement method - Analytik Jena Multi N/C 2100S - Germany). The filtration performance of PEG solutions was tested using dead-end filtration cell.

4.2.6. Evaluation of filtration performance

The dead-end filtration cell was used to investigate filtration performance of enhanced MPD and PIP based TFNC membranes. All filtration experiments were performed for hours to observe long term and fouling performance of TFNC membranes, on the contrary of filtration experiments in previous chapter. The experiments were done using pure water and salt solutions as a feed water for example 2000ppm MgSO₄, NaCl, CaCl₂ and Na₂SO₄ solutions. The rejection performance was calculated by equation 3, using conductivity meter.

4.3. RESULTS AND DISCUSSION

4.3.1. Characteristic of enhanced TFNC membranes

In this chapter, the PIP and MPD based TFNC membranes were prepared by adding various additives to the aqueous solutions. The addition of acid acceptor such as TEA, NaOH and Na₃PO₄ to the aqueous solution has a significant effect on the surface morphology of the PIP-based TFNC membranes (Fig 4.1).

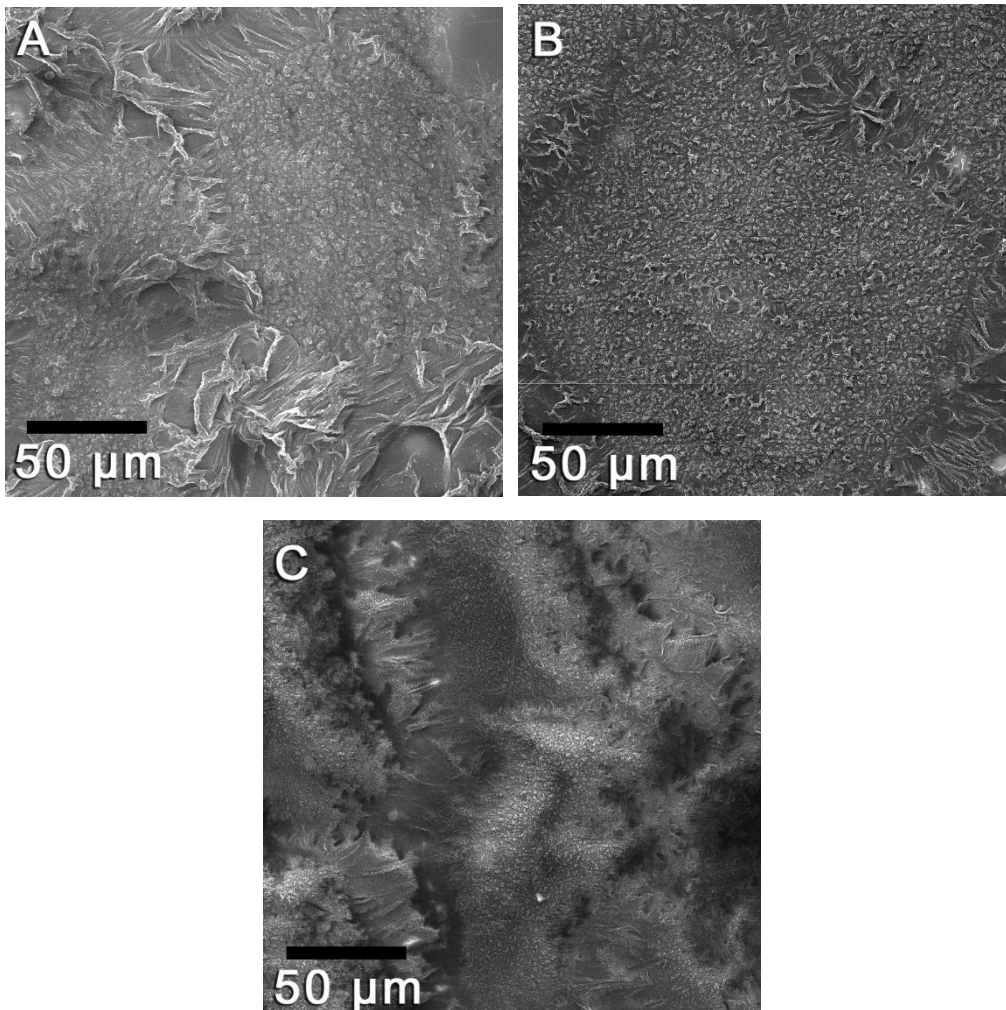


Figure 4.1. Surface images of PIP-based membranes which were prepared (A) 4 % w/v TEA, (B) TEA+NaOH and (C) TEA+ Na_3PO_4 in aqueous solutions.

It is obvious from the SEM images in Figure 4.1 that the fibrous pattern of top active barrier layer disappeared and formed typical ridge and valley PA active barrier structure on the NNC scaffold. It was the proof that the formation rate of PIP monomer increased towards the TMC monomer due to the presence of TEA. Hence, more PIP molecules reacted with TMC molecules and created thicker PA active layer.

Surface morphology of the MPD-based membranes that were prepared with the addition of acid acceptor and surfactant to the aqueous solution were illustrated in Figure 4.2.

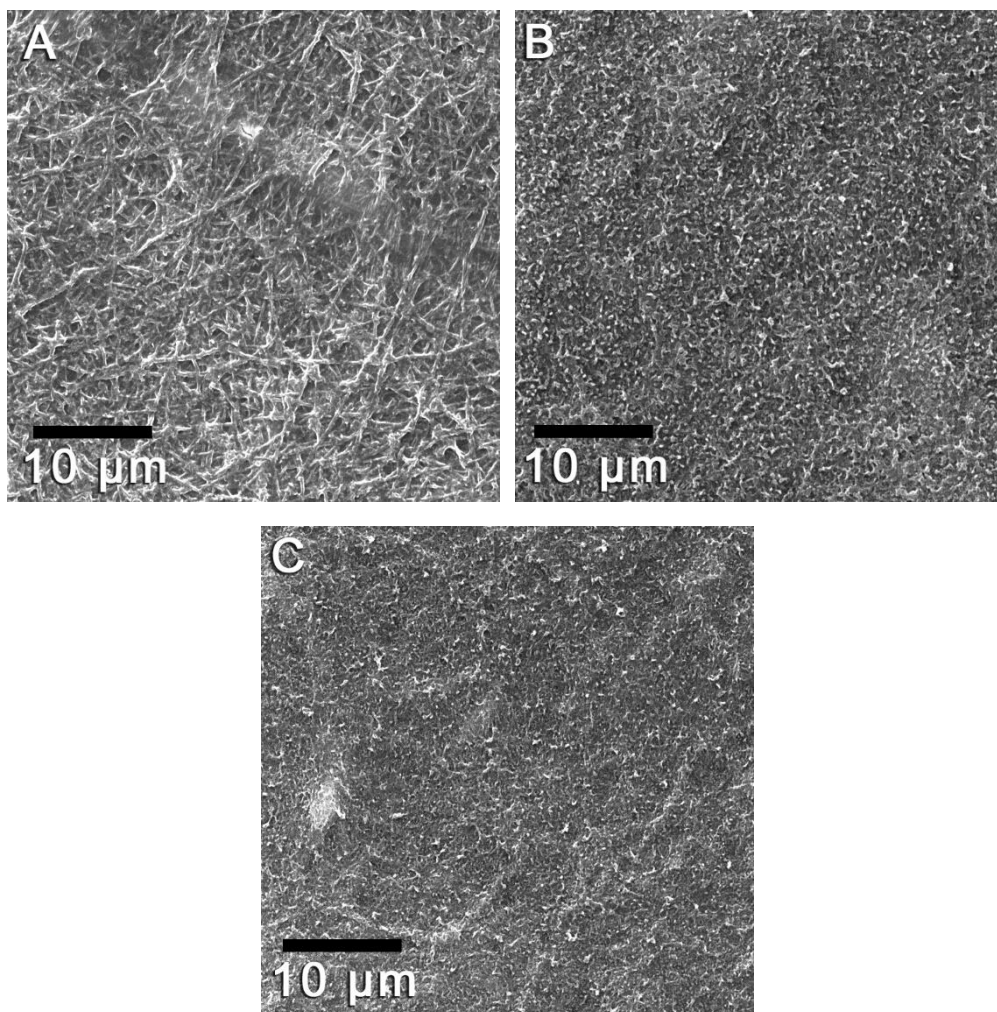


Figure 4.2. Surface images of MPD-based membranes which were prepared (A) 2 % w/v TEA, (B) TEA+Synferol AH and (C) TEA+Triton-X in aqueous solutions.

The addition of only TEA in the aqueous solution did not affect the surface morphology of MPD-based membranes (Fig.4.2.A). The fibrous pattern is clearly visible. However, the addition of surfactants in the aqueous solution affected the active layer and formed ridge and valley structure (Fig. 4.2.B-C). Moreover, the surface structures of MPD-based membranes prepared with surfactants were smooth and homogenous according to PIP-based membranes. It is well known fact that the high concentration of surfactant has tendency of micelle structure (the value of critical micelle concentration for Synferol AH 1241 is 8.2 mM and for Triton X-100 surfactant is 0.22 mM). It was reported that the micelle structure reduces the interaction between the polymer chains for establishment of the polymer-surfactant complex (Rahimpour et al. 2007; Mansourpanah et al. 2011) therefore, the concentration of surfactants were kept as less as possible. The chemical structure of Triton X-100 and Synferol AH 1241 were given in Figure 4.3.

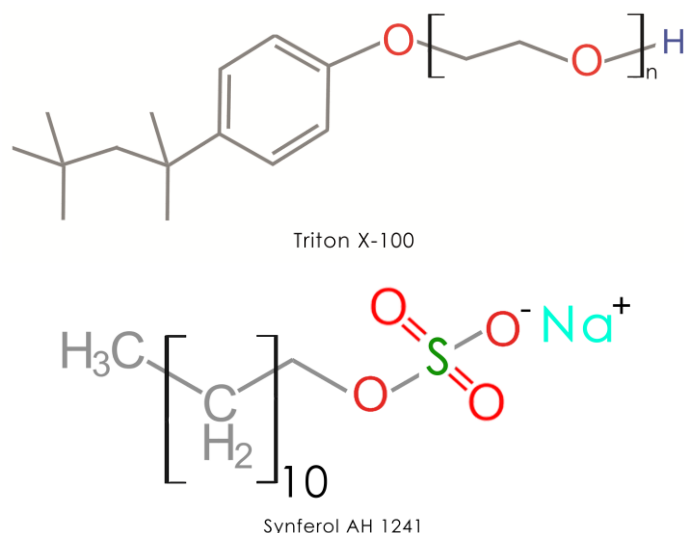


Figure 4.3. The chemical structure of surfactants.

The FTIR spectrums of the obtained PIP-based PA active layers on the NNC scaffold were shown in Figure 4.4. The strong and broad signals around a wavelength of 3405 cm^{-1} were observed with the addition of NaOH and Na₃PO₄, which was assigned to the carboxylic acid group or hydroxyl group on the surface of the active layer. However, for the membranes coated with PIP-TEA, the same bond seems weaker. A strong band at 1620 cm^{-1} is an indicator of the C=O bond of an amide functional group for all three membranes.

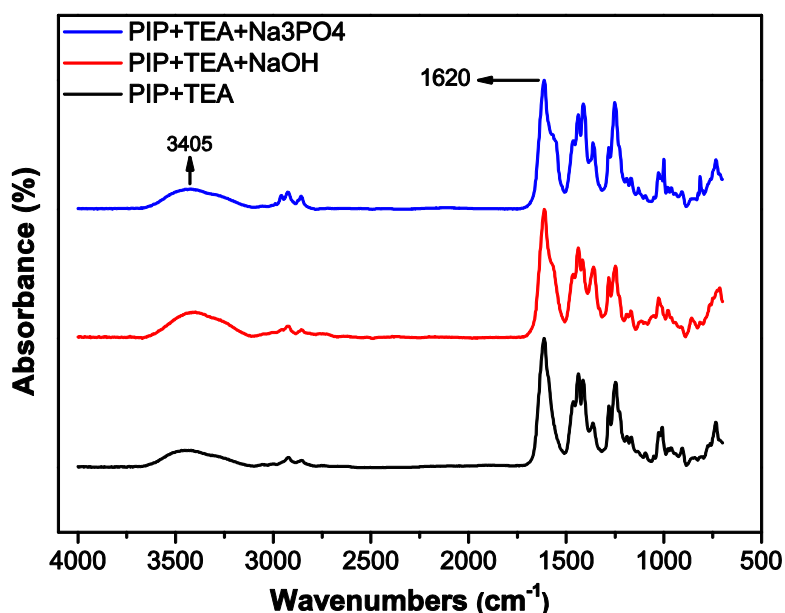


Figure 4.4. ATR-FTIR of PIP-based TFNC membranes active layer prepared using additives.

The FTIR spectrums of the prepared MPD-based PA active layers on the NNC scaffold were given in Figure 4.5. The one of the characteristic properties of MPD-based membranes were

seen at 1650 cm^{-1} and 1550 cm^{-1} which are represented C=C bond of the phenyl ring and amide II, respectively.

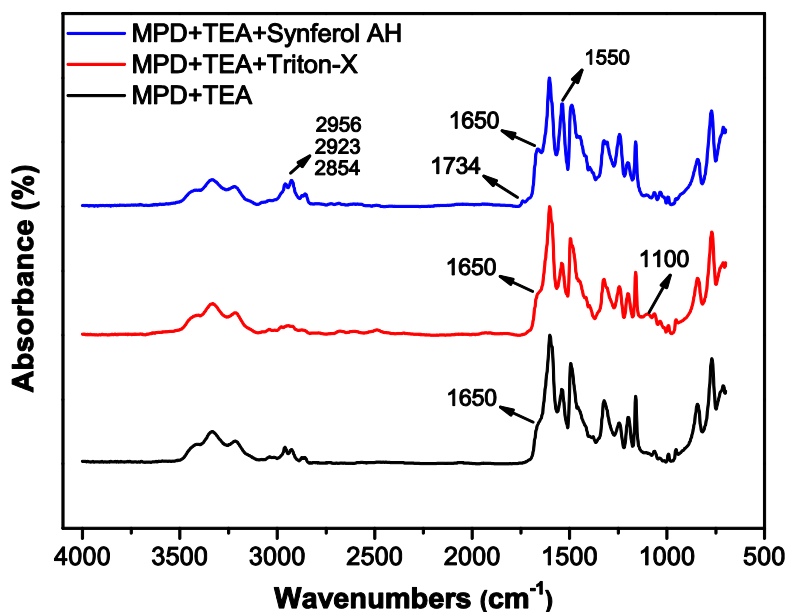


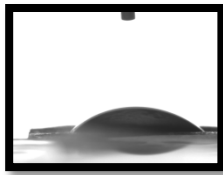
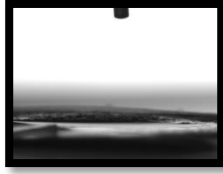

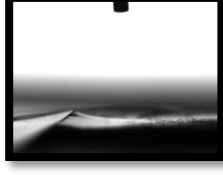
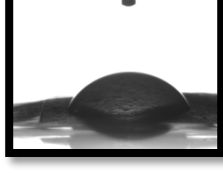

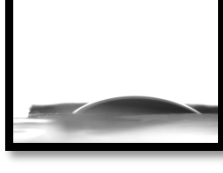
Figure 4.5. ATR-FTIR of MPD-based TFNC membranes active layer prepared using additives.

The existence of non-ionic liquid (Triton-X 100) may be proved by breeding of infrared absorption at 1100 cm^{-1} . The C-H stretching region for anionic liquid (Synferol AH) can be observed a medium peak at 2956 cm^{-1} (asymmetric CH_3), 2923 cm^{-1} (asymmetric CH_2) and 2854 cm^{-1} (symmetric CH_3) (Khan 2011). The other peaks which were observed after 1000 cm^{-1} , indicated C-H bonds in aromatics groups.

The existence of additive in interfacial polymerization reaction such as surfactants or phase transfer catalysts helps the movement of monomers from aqueous phase to organic phase. TEA, synferol AH 1241 and triton X-100 draft to PIP and MPD monomers and carry to interface where they react with TMC monomer. Then, interfacial polymerization reaction continues itself.

The surfactants are not only serve as a phase transfer catalysis, they also have big impact onto hydrophilicity of the overall membranes. The surface hydrophilicity of prepared PIP and MPD based TFNC membranes were given in Table 4.1.

Table 4.1. Contact angle properties of TFNC membranes (type of membrane specified with reaction time)

Membranes	Contact angle	Images of water droplet
PIP (1min) + TEA + TMC (5min)	25±1.67	
PIP (1min) + TEA + TMC (45sec)	0	
PIP (1min) + TEA + NaOH + TMC (45sec)	0	
PIP (1min) + TEA + Na ₃ PO ₄ + TMC (45sec)	0	
MPD (1min)+ TEA + TMC (30sec)	48±3.2	
MPD (1min) + TEA + Triton + TMC (30sec)	36±1.91	
MPD (1min) + TEA + Synf + TMC (30sec)	21±1.64	

The measurement of contact angles of PIP-based membranes showed super hydrophilic behavior with the existence of acid acceptors (TEA, NaOH, Na₃PO₄). The PIP+TEA based membranes that were prepared in longer reaction with an organic solution (5 min), showed

slightly higher contact angle values than usual PIP-based membranes. However, the PIP-based membranes, which were prepared with the addition of acid acceptor and under short reaction condition, performed super hydrophilic behavior with 0° (Drelich and Chibowski 2010).

The measurement of the contact angle of MPD-based membranes was showed that the addition of acid acceptor and surfactants in aqueous solution have the crucial effect to the surface hydrophilicity of active barrier layer. The contact angle of additive-free MPD-based membranes was 56.5° (see Table 3.3) as shown in previous chapter. The existence of surfactants decreased the surface resistivity against to water and the contact angle of enhanced MPD-based membranes became 48° , 36° and 21° .

Pure water permeate analysis was carried out to investigate any residual chemicals release to permeate side using liquid chromatography analysis. The result of the obtained permeate water analysis after pure water filtration using MPD and PIP based membranes shows that there was no signal of PIP, MPD, TMC or surfactants in the permeate water. However, we confirmed the existence of TEA in the permeate water after pure water filtration. The permeate water was contained 2.4 mg/L at first 1 hour. The same filtration between 2nd and 3rd hours was shown that the amount of TEA in the permeate water decreased to 0.2mg/L. Finally, at the end of the 5 hours filtration, TEA was found in the permeate water (0.1mg/L).

4.3.2. Filtration Performance of Enhanced PIP-based TFNC membranes

In the previous chapter, PIP and MPD based thin film nanofibrous membranes were prepared and optimized via filtration process by using $MgSO_4$ and $NaCl$ solutions. The main limitations of the membranes are low salt rejection and low permeate flux performance. Therefore, to increase rejection performance of PIP-based membranes, TEA, $NaOH$ and Na_3PO_4 were added in aqueous solution as an acid acceptor and IP reaction carried out on the NNC scaffold.

First, the effects of various TEA concentrations on the rejection performance of PIP-based TFNC membranes were investigated using divalent salt ($MgSO_4$ and Na_2SO_4). According to results of Chapter 3, the best rejection of $MgSO_4$ salts (95.6 %) obtained with TFNC (1) membrane. Therefore, the same IP reaction parameters were chosen which were used to prepare TFNC (1) membrane. The IP reactions were carried out with immersing NNC scaffolds for 1 min in aqueous solution and 5 min in organic solution. Then membranes were cured at $110^\circ C$ for 10 min. The filtration performance of PIP-based membranes with an additive of TEA was illustrated in Figure 4.6.

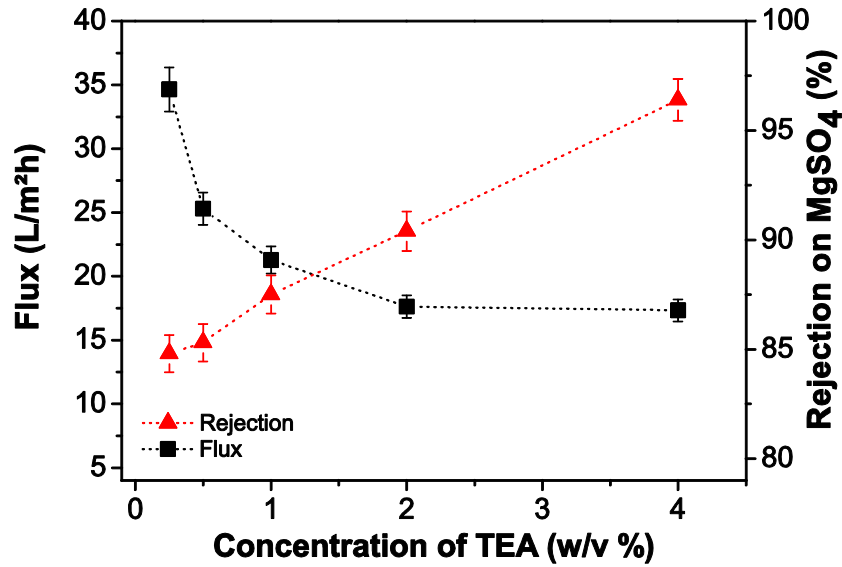


Figure 4.6. Effects of TEA concentration on MgSO₄ rejection and flux performance of PIP-based membranes at 2000ppm and 4.8 bar with dead-end filtration cell.

The membranes, which were synthesized with a lower concentration [0.25 to 2 % (w/v)] of TEA showed poor performance. The addition of TEA did not improve the membrane performance except at 4% (w/v) concentration of TEA. The MgSO₄ rejection rate of the PIP-based membrane with 4% (w/v) TEA was 96.48%, that is slightly higher than TFNC (1) membrane while the flux performance was 17.43 L m⁻²h⁻¹. The same rejection and flux performance trend were obtained in filtration process of Na₂SO₄ (Fig. 4.7).

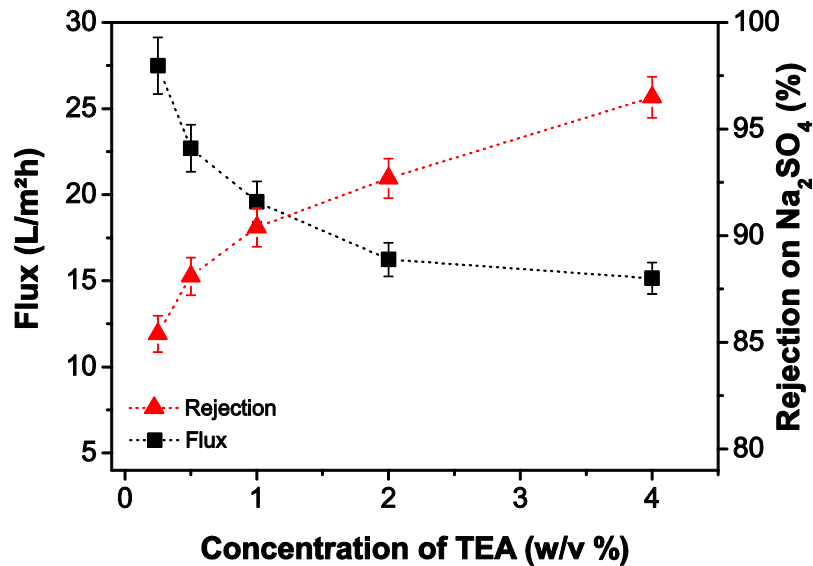


Figure 4.7. Effects of TEA concentration on Na₂SO₄ rejection and flux performance of PIP-based membranes at 2000ppm and 4.8 bar with dead-end filtration cell.

The highest Na₂SO₄ rejection rate of PIP-based membranes was obtained at the highest concentration of TEA (96.5 % - 15.18 L m⁻²h⁻¹). However, the flux performance of the PIP-

based membranes was still quite low, and rejection performances were insufficient. The reason of low flux might be the longer reaction time of organic solution during the IP reaction, hence the formed thicker PA active barrier layer on to NNC scaffold. To increase the flux performance of the PIP-based membranes, the formation of PA active barrier layer were investigated by using various reaction time of organic solution such as at 3 minute and then 45 second.

The effects of the different reaction time of organic solutions of PIP-based membranes with 4% (w/v) TEA addition on flux and rejection performance were illustrated in Figure 4.8.

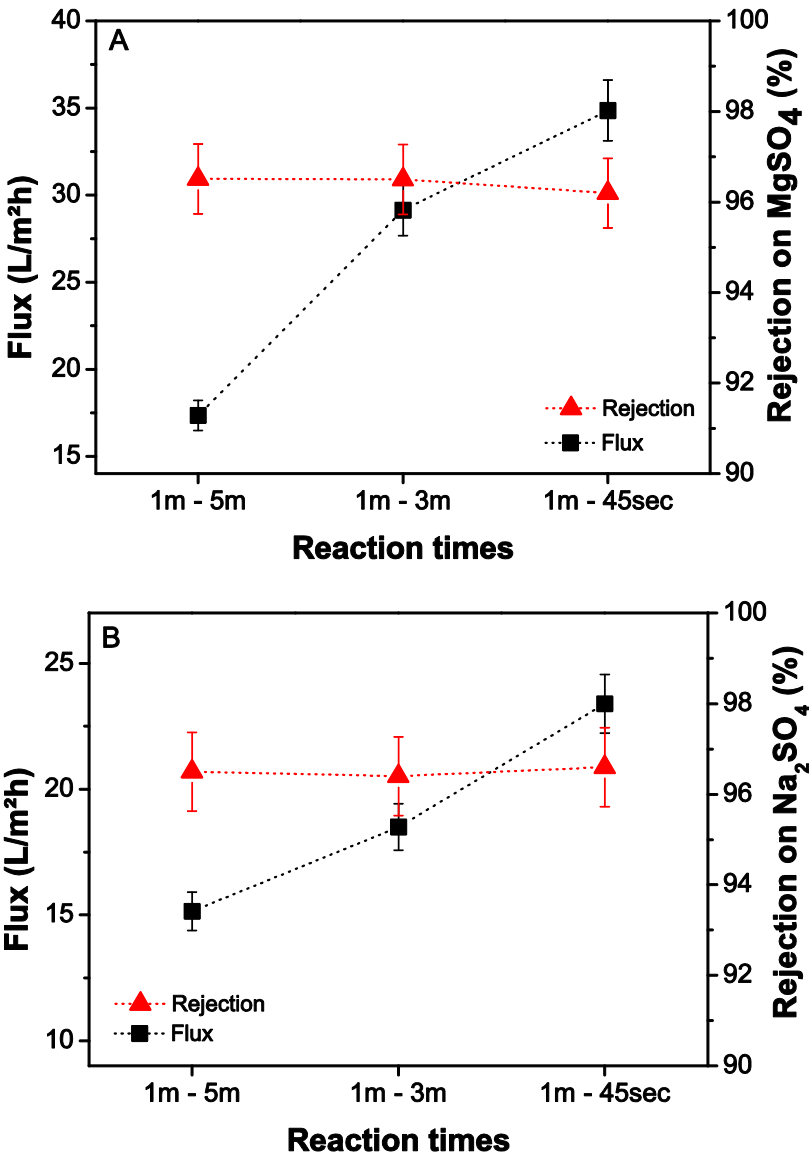


Figure 4.8. Effects of the different reaction time of organic solution on (A) MgSO₄, (B) Na₂SO₄ rejection and flux performance of PIP+TEA based membranes at 2000ppm and 4.8 bar with dead-end filtration cell.

Figure 4.8 obviously indicates that the reaction time of organic solution has a crucial impact on the filtration performance of TFNC membranes. The presence of acid acceptor (TEA) yielded higher partition coefficient of PIP. Hence the formation rate of PIP became higher. Thereby, the high reaction time of organic solution became unnecessary for the formation of PA active barrier layer. Even, short reaction time can form thinner PA active layer successfully, hence, the flux performance were increased without adversely affecting to salt rejection. The cross-sectioned images of PIP+TEA based membranes which were prepared 1min - 5min and 1min - 45 sec reaction time, are illustrated in Figure 4.9.

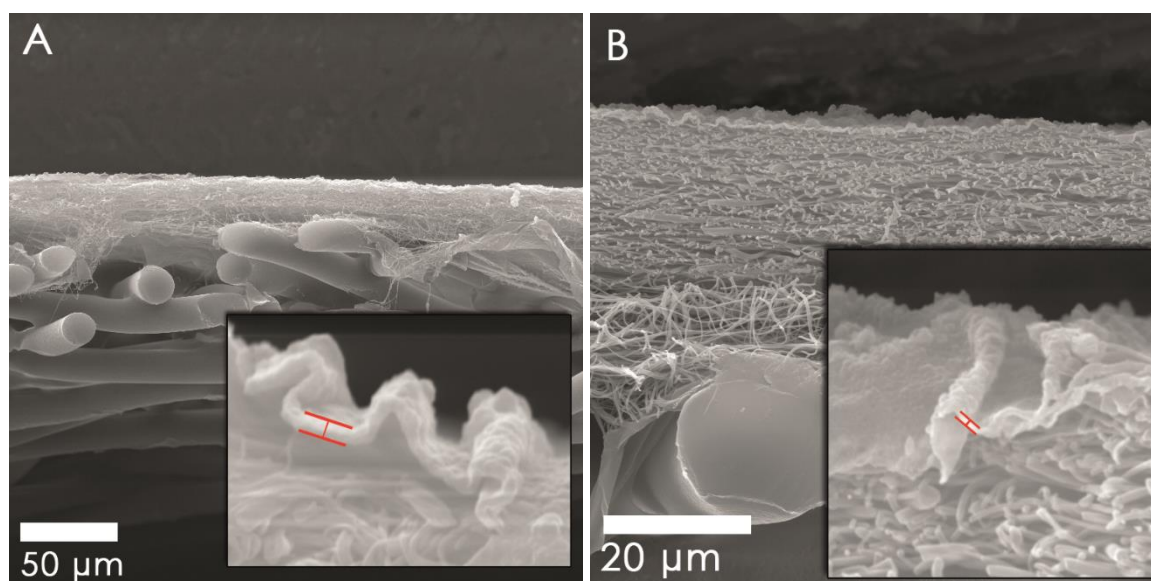


Figure 4.9. Cross-sectioned images of PIP+TEA based membranes that were prepared (A) 1m-5m and (B) 1m-45sec reaction time.

Thickness measurement of active layer showed that the thickness of PIP+TEA based membrane, which was prepared under 1min-5min reaction time, was 398.21 nm. Other side thickness of PIP+TEA based membrane, which was prepared under 1min-45sec reaction time, was 97.2 nm. The obtained flux performance of PIP+TEA (1min+45sec) based membrane was $34.8 \text{ L m}^{-2}\text{h}^{-1}$ while the rejection of MgSO_4 performance was 96.2 % (Fig. 4.8.A). The flux performance was obtained $23.4 \text{ L m}^{-2}\text{h}^{-1}$ in filtration of Na_2SO_4 while the rejection performance was 96.6 % (Fig. 4.8.B).

The second limitation of PIP-based TFNC membranes was the low rejection performance against to divalent salt (lower than 98%). To increase rejection performance of PIP-based TFNC membranes, strong base such as 1.0% (w/v) NaOH and Na_3PO_4 were used as secondary acid

acceptors. The filtration performance of 2.0% (w/v) PIP + 4% (w/v) TEA based membranes with the addition of strong base given in Figure 4.10.

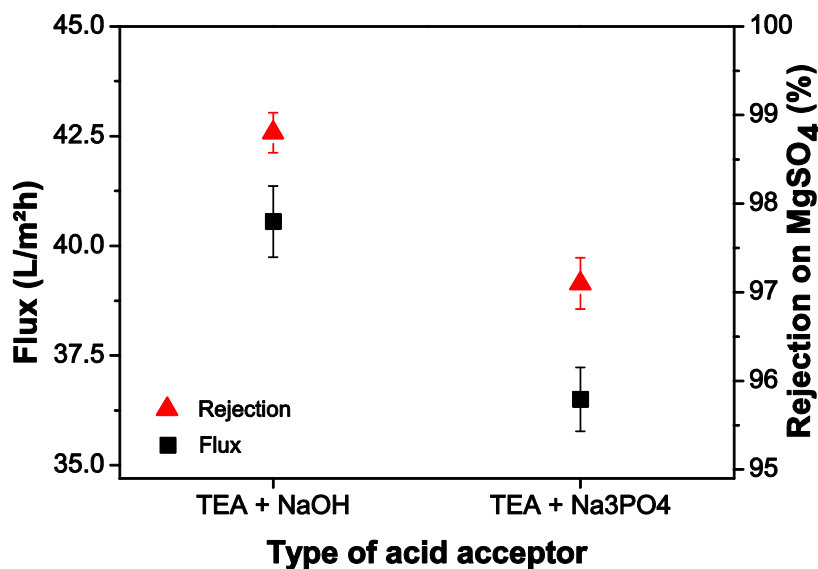


Figure 4.10. Effects of different acid acceptor on MgSO₄ rejection and flux performance of PIP-based membranes at 2000 ppm and 4.8 bar with dead-end filtration cell.

It is obvious from Figure 4.8 that the addition of 1.0% (w/v) bases gave the highest MgSO₄ salt rejection while the flux performance increased dramatically. Particularly, the sodium hydroxide additive in the aqueous solution has a crucial impact on the filtration of divalent salt. The rejection rate of PIP+TEA+NaOH based TFNC membrane was 98.8 % with 40.5 L m⁻²h⁻¹ flux performance. The TFNC membrane prepared PIP+TEA+Na₃PO₄ was performed slightly lower rejection and flux performance (97.1 % and 36.5 L m⁻²h⁻¹, respectively).

It is mentioned previous chapter that the selectivity of TFNC membranes based on poly(piperazine amide) was due to the contribution of electrostatic repulsion mechanism more than size exclusion mechanism. The main reason of electrostatic repulsion mechanism was due to the presence of carboxylic acid group on the chain structure of active barrier layer. The FTIR spectrum analyzes of PIP-based membrane indicated high intense of the carboxylic acid bond at 3438 cm⁻¹ (Fig. 3.5). However, in Figure 4.4 the PIP+TEA based membrane indicates the lowest strength of the band at 3405 cm⁻¹ which is represented to the carboxylic acid group on the membrane chain structure. The reason for a lower ratio of carboxylic acid on PIP+TEA based membranes may be explained by role of TEA in the PIP aqueous solution during the IP reaction. Besides being an acid acceptor, TEA can also act as a catalyst in the IP reaction and make PIP amine more reactive towards to acyl chloride. Therefore, the amount of carboxylic acid group decreased in the chain structure of PA active barrier layer of PIP+TEA based

membrane. This was also proved the reason of the low filtration performances of PIP+TEA based membrane in Figure 4.6 and 4.7 against to divalent salts. Moreover, the addition of NaOH was increased the intensity of carboxylic acid group on the chain structure of PIP+TEA+NaOH based membrane and performed the highest divalent salts rejection. The intensity of carboxylic acid group in the PIP+TEA+NaOH based membrane was proved with the highest peak at 3405 cm^{-1} in Figure 4.4. As a result, the addition of TEA in the aqueous solution was not enough to prepare poly(piperazine amide) TFNC membrane. The addition of base was also necessary to obtain high performance against to divalent salts.

The filtration processes in the extended period were carried using a PIP+TEA+NaOH based membrane. First, the filtration process was carried out using distilled water to determinate pure water permeate flux and level of compaction of the membrane (Fig. 4.11).

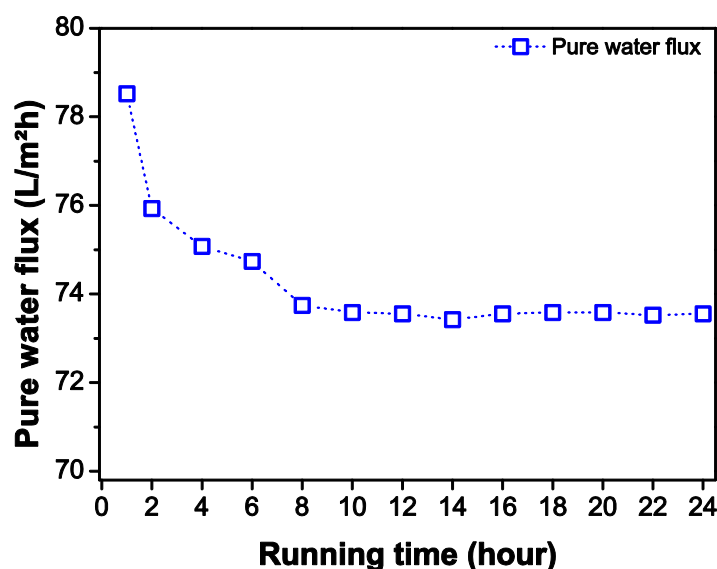


Figure 4.11. Observation of filtration process in an extended period of PIP+TEA+NaOH membrane using pure water at 4.8 bar.

In the early filtration stage of all of the membrane, the determination of the pure water flux is necessary in order for the membranes to reach a steady state. In this thesis, trans-membrane pressure was applied to all of the prepared membranes for compaction. Once the membranes reach a steady state using pure water, the filtration process was carried out for the feed solutions. Figure 4.11 shows the pure water flux of PIP+TEA+NaOH based membranes for 24 hours. The filtration of the pure water flux began with $78.5\text{ L m}^{-2}\text{h}^{-1}$ and was then decreased to 75.9 and $74.7\text{ L m}^{-2}\text{h}^{-1}$. Stable flux averaging $73.5\text{ L m}^{-2}\text{h}^{-1}$ was obtained after 6 hours. The differences between the steady state and third-hour flux were not so significant ($1.2\text{ L m}^{-2}\text{h}^{-1}$). It is also seen

from Figure 4.11 that the amount of compaction on the PIP-based membranes was almost negligible.

After the steady state of the PIP+TEA+NaOH-based membrane was determined and attained using pure water, feed solution experiments were carried out for an extended period. Four kinds of salts, that is, $MgSO_4$, $NaCl$, $CaCl_2$ and Na_2SO_4 were chosen for the feed solution. The properties of salt solutions are given in Table 4.2 and the filtration performances of the four kinds of solution are illustrated in Figure 4.12.

Table 4.2. Properties of salt that were used for feed solutions.

Type of salts	Conductivity (ms/cm)	pH	Part per million (ppm)
$MgSO_4$	2.21	5.59	2000
Na_2SO_4	5.74	6.87	2000
$NaCl$	3.52	6.15	2000
$CaCl_2$	3.62	5.75	2000

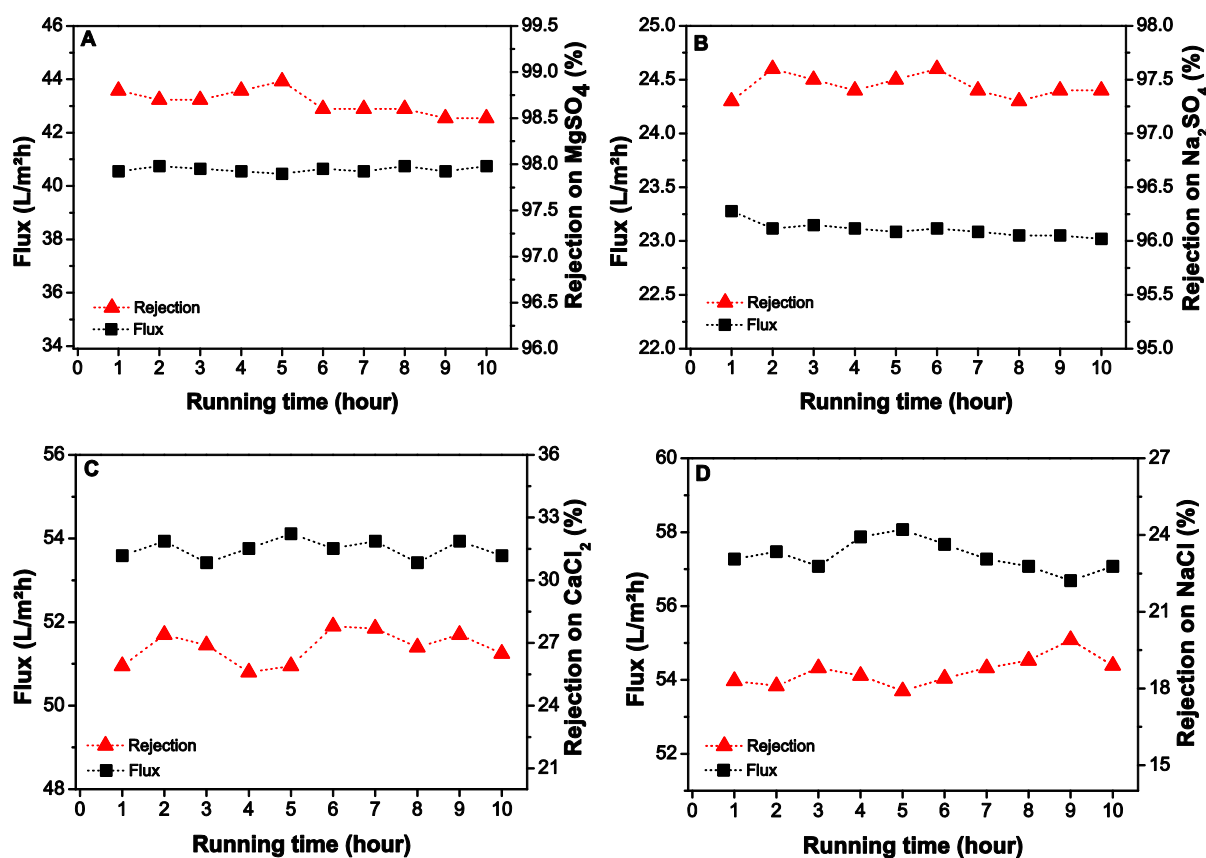


Figure 4.12. Extended filtration of (A) $MgSO_4$, (B) Na_2SO_4 , (C) $CaCl_2$ and (D) $NaCl$ feed solutions at 2000ppm and 4.8 bar using dead-end cell.

The flux and rejection performance are shown for the filtration of feed solutions in all of the graphs in Figure 4.12. In Figure 4.12(B), the flux performance showed a decreasing trend, which means that the PIP+TEA+NaOH-based membrane showed slightly fouling behaviour during the filtration of the Na₂SO₄ feed solution. Eventually, the PIP+TEA+NaOH-based membrane showed a high rejection performance for divalent salts. Inherently, the retained monovalent salt ratios were low

4.3.3. Filtration Performance of Enhanced MPD-based TFNC membranes

In consideration of previous chapter, the MPD-based membranes performed relatively low permeate flux performance (1.84 L m⁻²h⁻¹) as a nanofiltration membrane [TFNC (1)]. Besides, the rejection performance of that membrane was not reasonable (93.57%). To increase permeate flux and rejection performance of MPD-based membranes, TEA and surfactants such as Synferol AH 1241 anionic, Triton X-100 non-ionic liquids were added to the aqueous solution, then IP reaction carried out on the NNC scaffold. TFNC (2) membrane preparation parameter was taken as a reference to prepare enhanced MPD-based membranes such as 1 min and 30 sec reaction time in aqueous and organic solution respectively. Then membranes were cured at 110 °C for 10 min. First, the pure water flux of MPD-based membranes was investigated using distilled water at 4.8 bar with dead-end filtration cell (Fig. 4.13). The filtration performances of MPD-based membranes were tested using NaCl and CaCl₂ feed solution (Fig. 4.14).

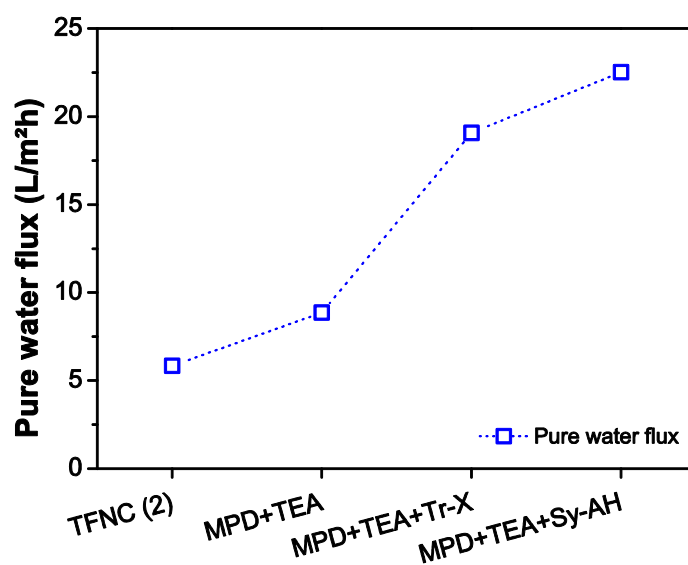
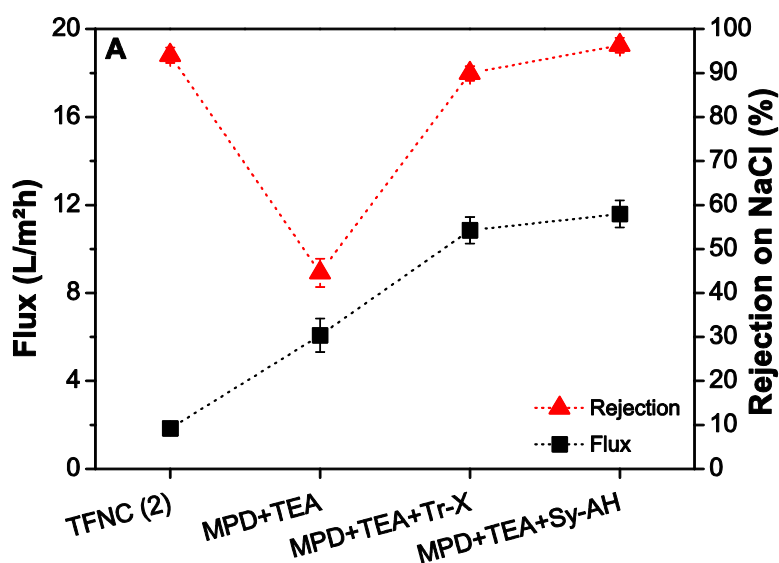


Figure 4.13. Pure water fluxes performance for MPD-based membranes.

The acid acceptor and surfactants as an additive in the aqueous solution of MPD have significant effects on the pure water flux performance of the membranes. MPD+TEA ($7.6 \text{ L m}^{-2} \text{ h}^{-1}$) based membrane was performed slightly higher pure water flux than TFNC (2) ($5.8 \text{ L m}^{-2} \text{ h}^{-1}$) whereas MPD+TEA+Sy-AH ($22.5 \text{ L m}^{-2} \text{ h}^{-1}$) based membrane was performed almost 4 times higher.

The monovalent salt rejection performance of MPD based membranes is given in Figure 4.14. The flux performance of MPD-based membranes which was prepared with additives showed increment dramatically. The permeate flux of MPD+TEA+Sy-AH ($11.5 \text{ L m}^{-2} \text{ h}^{-1}$) based membrane was 6 times higher than TFNC(2) ($1.84 \text{ L m}^{-2} \text{ h}^{-1}$) membrane without compromising rejection performance. The rejection performance of MPD+TEA+Sy-AH (96.3 %) based membrane was slightly higher than TFNC(2) (93.57 %) membrane. The MPD+TEA+Tr-X based membrane showed slightly lower rejection (89.1 %) and significantly higher flux performance ($10.8 \text{ L m}^{-2} \text{ h}^{-1}$) than TFNC (2). The thin film composite membranes containing surfactants has been performed superior performance compared with the membranes prepared without surfactant addition (Kuehne et al. 2001). The most common surfactants Triton-X 100 (non-ionic liquid), sodium dodecyl sulphate (anionic liquid) and cetyl trimethyl ammonium bromide (cationic liquid) were studied many times by researchers (Alsari et al. 2001; Tsai et al. 2000; Wang et al. 1998). However, it is still kind a question that the presence of different properties of surfactant during IP process might really improve the properties of PA active layer and what underlying mechanism involved in the changes.



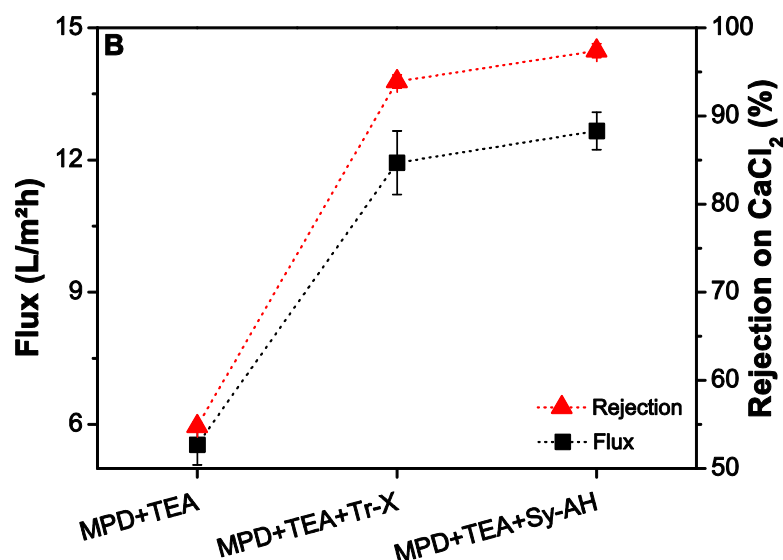


Figure 4.14. Effects of different additive on (A NaCl, (B) CaCl₂ rejection and flux performance of MPD-based membranes at 2000ppm and 4.8 bar with dead-end filtration cell.

The effects of additives on the filtration performance can be explained according to our characterization results. The hydrophilicity of MPD based membranes was improved significantly with the addition of surfactants (see Table 3.3 and 4.1). The reasons of high hydrophilicity can be summarized as follows. (1) The addition of surfactants especially anionic liquid was increased the amount of hydrogen bond and hydrophilic ionic molecules (polar group) in the chain backbone of PA active layer. The FTIR spectrum analyzes were supported this idea (Fig 4.4), (2) PA active layer of MPD+TEA+Surfactants based membranes were created smooth and uniform surface morphology. Thus, nanosize ridge and valley pattern was yielded the increase surface area (contact area) for feed solutions (see Figure 4.2.B.C).

Wittbecker and Morgan demonstrated that adding anionic liquids is equivalent to increase the amine concentration in the aqueous solutions (Wittbecker and Morgan 1959). This may be the reason of the highest monovalent salt rejection, in the presence of Synferol AH (anionic liquid), the PA active layer became denser. We also assumed that due to the existence of Synferol AH anionic liquid, negative charge increased on the PA active layer chain structure, Na⁺ ions are absorbed on the membrane surface and created an ion deposited layer. Therefore, the MPD+TEA+Sy-AH based membrane surface charge is covered by Na⁺ ions and led to increment in Na⁺ rejection.

As it is seen in both graphs of Figure 4.14 that MPD+TEA based membrane was performed the lowest rejection performance against to monovalent salt while the flux performance was also

low. Effects of the addition of TEA on the MPD based membrane performance has not been clarified yet. It was initially mentioned by Cadotte that adding an acid acceptor in the MPD based membrane system does not provide any advantage (Cadotte 1981; Cadotte et al. 1980). A study of Hermans was in agreement with Cadotte (Hermans, Bernstein, Volodin and Vankelecom 2015). In another study about the effect of TEA on the TFC membranes that adding TEA or increasing the concentration of TEA affected both lower flux and rejection performance (Kim et al. 2002).

It is well known that the partition coefficient of MPD is already high enough in the interfacial formation of an aromatic PA active layer. Therefore, the presence of TEA can be yield to inhibited interfacial reaction (Kim, Jegal and Lee 2002). We believe that only TEA additive for MPD based membranes affects negatively for forming of PA active layer. The formation of PA active barrier layer was not completed on the surface of NNC scaffold during the IP reaction. The defects, which were smaller than micro dimension, were able to observed by SEM image (Fig. 4.15).

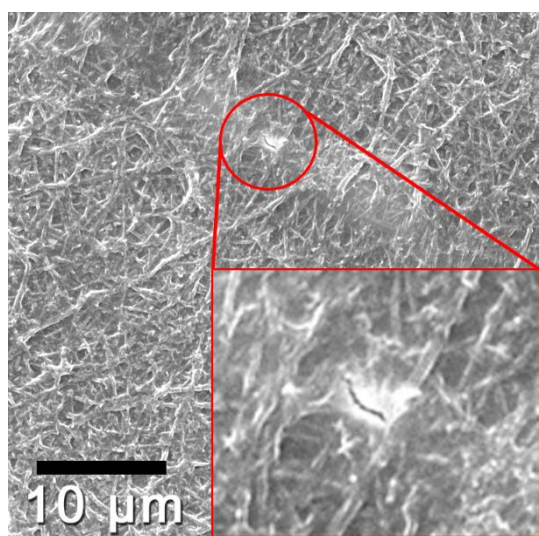


Figure 4.15. A nanosize crack on the surface of MPD+TEA based membrane.

Figure 4.15. shows that the crack on the PA active layer of MPD+TEA based membrane and were explained the reason of slightly higher flux and significantly lower rejection than TFNC(2) membrane.

In the sight of monovalent salts filtration experiments that are mentioned above, MPD+TEA+Sy-AH based membrane was chosen for the filtration of the extended period. The pure water filtration over an extended period is shown in Figure 4.16.

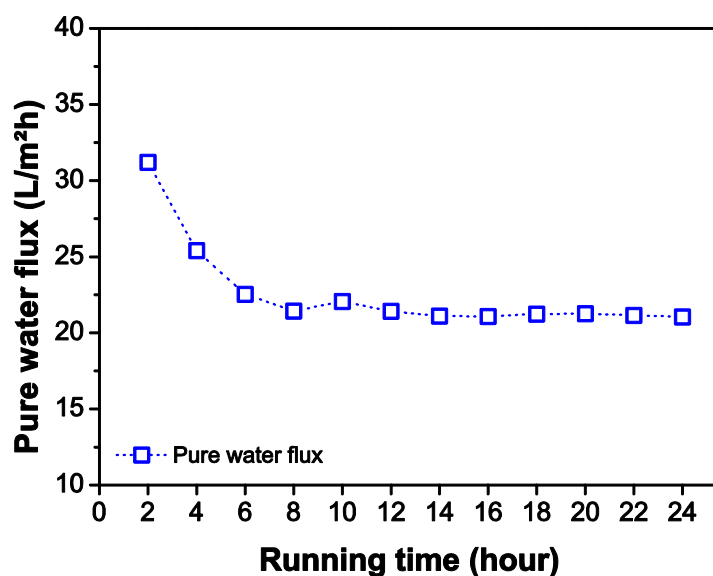


Figure 4.16. Observation of filtration process in extended period of MPD+TEA+Sy-AH membrane using pure water at 4.8 bar.

The MPD+TEA+Sy-AH based membrane began with considerably high pure water flux; after a while the pure water flux becomes stable and reaches a steady state. The pure water flux began around $31.2 \text{ L m}^{-2}\text{h}^{-1}$ and then reached a steady state at $22.3 \text{ L m}^{-2}\text{h}^{-1}$ after 6 hours. The membrane compaction is crucial for the NF and RO membranes and depends on the applied pressure and type of membrane (Manito Pereira et al. 2006; Persson et al. 1995). Flux performance can drop significantly, especially in reverse osmosis membranes, (McGovern et al. 2015). Figure 4.11 and 4.16 showed that compaction rate of the TFNC membranes is substantially low due to the advantages of the fibrous structure of the supporting layer.

The filtration experiments of different salts-based feed solutions for the MPD+TEA+Sy-AH-based membrane are given in Figure 4.17. The rejection rates of divalent salts were higher than 98 %, and were around 96 - 97 % for monovalent salts. The flux performance of the MPD+TEA+Sy-AH-based membrane showed a slightly decreasing trend. This may be explained by the concentration polarization due to the usage of dead-end filtration cell.

A specific amount of feed water was used in each experiment, and the circulation of feed water was impossible in the dead-end filtration system. As the water molecules diffuse through the TFNC membrane, the salt ion is retained and concentration of feed water continuously increases. Due to the fact that the ratio of salt ions increased rapidly, concentrated feed solutions accumulate on the surface of membrane and lead salt leakage or fouling. Moreover, the osmotic pressure of the feed water increases proportionally to the concentration of feed solution. For

this reason, the flux of feed water tended to decrease during filtration using MPD-based membranes.

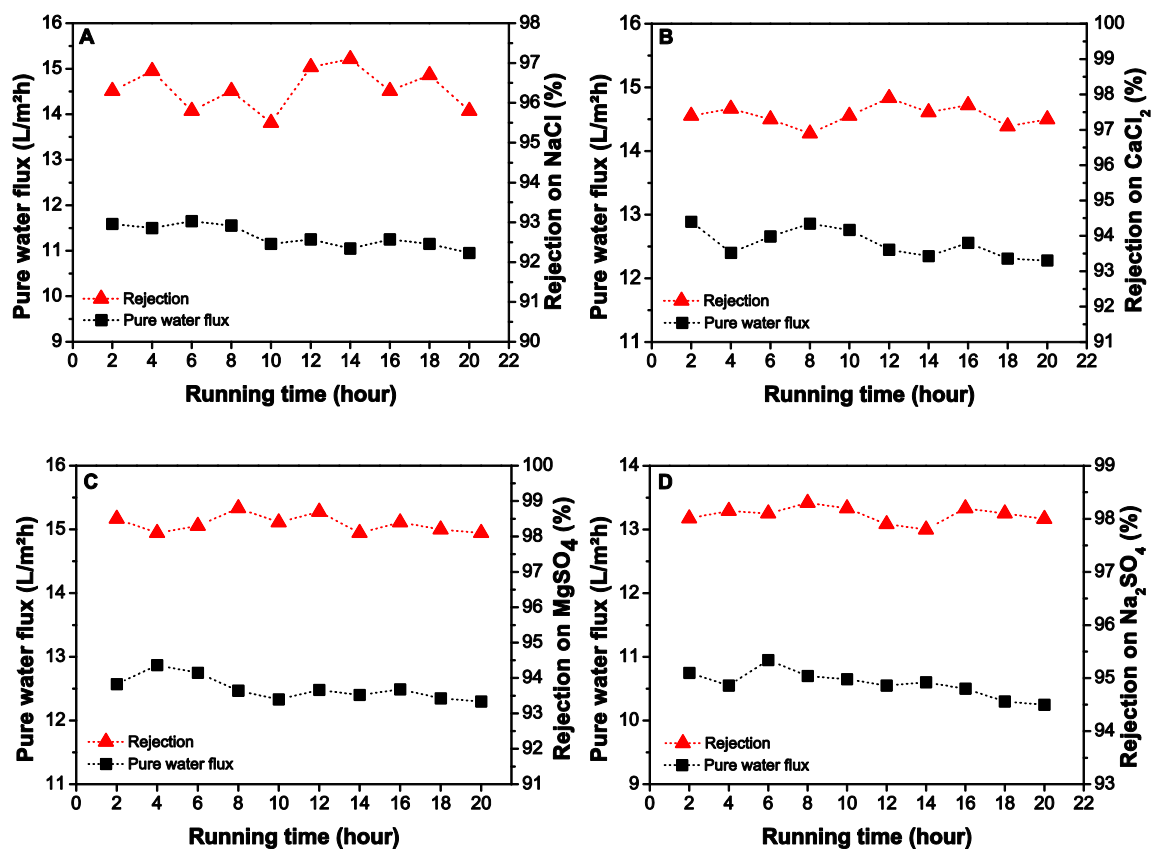


Figure 4.17. Extended filtration of (A) NaCl, (B) CaCl₂, (C) MgSO₄ and (D) Na₂SO₄ feed solutions at 2000ppm and 4.8 bar using dead-end cell.

4.3.4. Determination of Molecular weight cut-off of the TFNC membranes

The filtration of different molecular weight aqueous PEG solution was carried out using dead-end filtration to determine the MWCO of the TFNC membrane. Table 4.3 gives the PEG rejection values of the PIP+TEA+NaOH-based TFNC membrane, and MPD+ TEA+Synferol-based TFNC membrane. 1000 ppm PEG with molecular weight 200, 400 and 600 feed solutions were used in filtration experiment.

Table 4.3. The rejection values of TFNC membranes using PEG feed solutions

Membranes	PEG-200	PEG-400	PEG-600
PIP+TEA+NaOH	61.5 %	91.1 %	98.9
MPD+TEA+Sy-AH	97.3 %	98.9 %	99.6

It was found that the MWCO of the PIP+TEA+NaOH based membrane was 400 Da (the rejection rate is 91.1 %). The average solution diameter of PEG-400 was 1.8 nm, which means the effective pore size of PIP+TEA+NaOH based membrane around 1.8 nm. MPD+TEA+Sy-AH based membrane was performed high PEG-200 rejection rate (97.3 %). The average solution diameter of PEG-200 was 1.3 nm (200 Da) that means the effective pore size of MPD+TEA+Sy-AH based membrane was lower than 1.3 nm (Lin et al. 1987). As a result of TOC analysis that PIP+TEA+NaOH based membrane was able to retain the compounds which have maximum average molecular weight 400 g/mol. On the other side, MPD+TEA+Sy-AH based membrane was able to retain compound which has a molecular weight less than 200 g/mol.

4.3.5. Analysis of real seawater filtration

The desalination of seawater using membrane technology is a promising technique, which essentially requires more than one-step to produce drinkable water such as pre-filtration, microfiltration and softening. The results ion-exchange chromatography analysis and conductivity measurements show that the amount of main dissolved salt ions and conductivity of the seawater were extremely high for NF membrane process (Table 4.4).

Table 4.4. Main dissolved ions in Mediterranean seawater sample

Cations	mg/L
Na ⁺	11741
Mg ⁺²	1447
Ca ⁺²	433
K ⁺	411
Anions	mg/L
Cl ⁻	21384
SO ₄ ⁻²	2357
NO ₂ ⁻	<100
NO ₃ ⁻	<100
Conductivity of seawater	53.2 ms/cm

The primarily filtration experiment was carried out using PIP+TEA+NaOH and MPD+TEA+Sy-AH based membranes by measuring the conductivity of the permeate water only (Fig. 4.18).

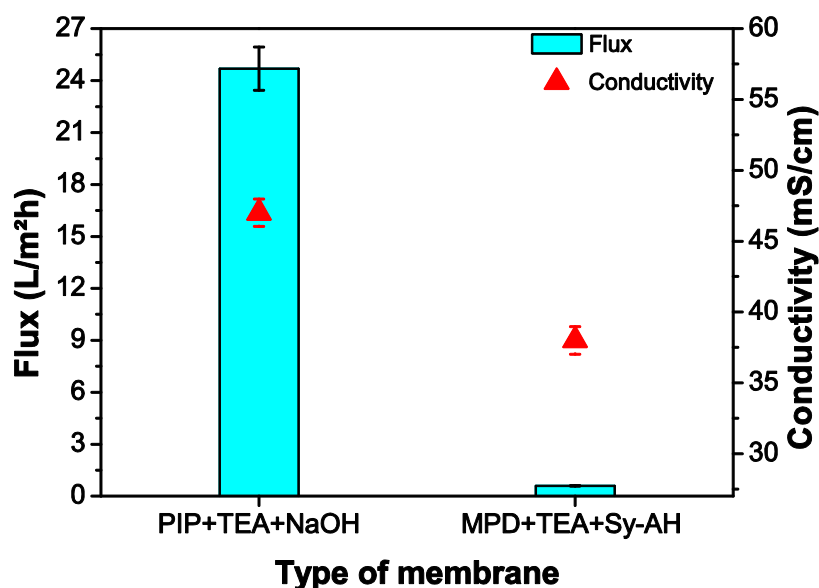


Figure 4. 18. The filtration experiment of seawater using different membrane and dead-end cell at 4.8 bar.

The results in Figure 4.18 show that the conductivity value of permeate water dropped from 53.2 mS/cm to 47 mS/cm and 38 mS/cm, respectively, while the flux performance was 24.6 L m⁻²h⁻¹ and 0.65 L m⁻²h⁻¹, respectively. It is clear that the PIP- and MPD-based membranes remained incapable of retaining an excessive amount of salt ions in the seawater all at once. For this reason, the same feed seawater was circulated and was used more than once while the same membrane was fixed on the dead-end cell.

The filtration experiment of circulated seawater started with the PIP-based membranes and was repeated six times. Subsequently, the same permeate water was used as feed water using the MPD-based membranes and was repeated two times (Fig. 4.19). The flux performance of the PIP+TEA+NaOH based membranes in the filtration of seawater was higher compared to the MPD+TEA+Sy-AH based membranes. Moreover, the flux performance of PIP-based membranes increased after each filtration process, while the conductivity of the feed seawater decreased. The conductivity of the feed seawater remained stable after the fifth (32.5 ms/cm) and sixth (32.0 ms/cm) filtration (Fig. 4.19.A). It was understood that after four filtration cycles using the PIP-based membranes there was none or only trace amounts of divalent salt ions in the feed seawater.

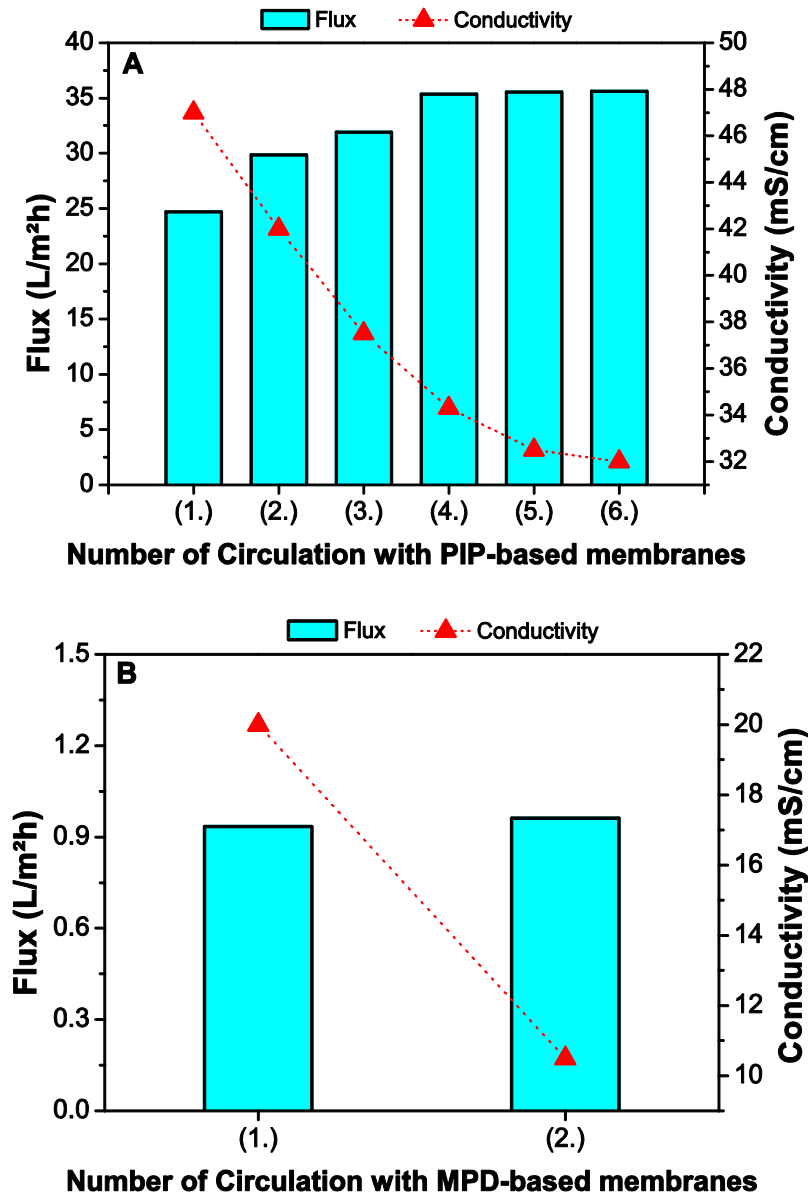


Figure 4.19. Circulated filtration of seawater using (A) PIP and (B) MPD based membranes

Further filtration was continued with MPD+TEA+Sy-AH based membrane using pre-filtered feed seawater, which had a conductivity 32.0 mS/cm (Fig. 4.19.B). In the first attempt of filtration, the conductivity dropped to 20 mS/cm while the flux performance was 0.935 L m⁻²h⁻¹, which was slightly higher than shown in Figure 4.18. During the second filtration of the feed seawater, the conductivity decreased to 10.5 mS/cm while the flux performance was more or less same (0.965 L m⁻²h⁻¹).

After the second attempt at MPD-based filtration, the conductivity of obtained permeate water was 10.5 mS/cm which means that approximately 80 % of salt ions were retained from the seawater using TFNC membranes by dead-end filtration. The analysis of the ion-exchange

chromatography was carried out again, and the amounts of salt ions in the filtered water are given in Table 4.5.

Table 4.5. Amount of ions in the filtered seawater sample [permeate (2.) in Figure 4.19]

Cations	mg/L
Na ⁺	2554
Mg ⁺²	5.3
Ca ⁺²	39.4
K ⁺	85.3
Anions	mg/L
Cl ⁻	3620
SO ₄ ⁻²	<100
NO ₂ ⁻	<100
NO ₃ ⁻	<100
Conductivity of seawater	10.5 mS/cm

It is clear from Figure 4.19 that the rejection ratio of salt ions from seawater was dependent on the number of repetitions of the circulated feed seawater using the dead-end filtration method. We firmly believed that there was a chance to retain rest of the salt ions from the obtained seawater permeants by increasing the circulation time. However, the flux performance of MPD-based membranes dropped extremely. It was not reasonable to proceed with the filtration of seawater experiment using a dead-end filtration cell and then so we limited the circulation times of feed seawater to two using MPD-based membrane.

4.3.6. Conclusion

The key advantage of the nanofiltration membranes is high permeate flux compared to reverse osmosis membranes. For this reason, flux performance of TFNC membranes, which was prepared in Chapter 3, was not reasonable. Improvements of those TFNC membranes performances, especially flux performances were required critically.

In this chapter, not only the flux performances but also rejection performances of MPD- and PIP-based membranes were significantly high using an acid acceptor and surfactants. The addition of TEA as an acid acceptor is necessary for the formation of poly(piperazine amide). The presence of TEA increased the formation rate of PIP monomer to the TMC monomers. However, one of the main properties of poly(piperazine amide) active layer that an electrostatic

repulsion mechanism lost influence in the presence of TEA. For this reason, divalent salts rejection performances of PIP-based membranes were too low with the additive of TEA alone while the flux performance of the membrane was increased. A Strong base (NaOH) were added as a second additive to the aqueous solution and poly(piperazine amide) active barrier layer formed onto NNC scaffold. The highest divalent rejection performance was obtained using the PIP+TEA+NaOH-based membrane, which was on average 98.8% MgSO_4 and 97.4 % Na_2SO_4 . Even though, the effect of the dead-end filtration method proved to be a disadvantage, the pure water flux and permeate flux of PIP+TEA+NaOH based membrane were high, that is, $73.5 \text{ L m}^{-2}\text{h}^{-1}$ and $40.5 \text{ L m}^{-2}\text{h}^{-1}$, respectively.

On the other side, the MPD-based membrane that was prepared in the previous chapter performed too low flux performance. The additive of acid acceptor and surfactants were used to increase flux performance of MPD-based membranes. The additive of TEA did not improve any filtration performance, besides; TEA had a negative influence and decreased the filtration features of the MPD-based membranes. The MPD-based membrane showed high flux and rejection performance with the addition of an anionic surfactant (Synferol AH) and TEA. The highest monovalent rejection performance was recorded with the MPD+TEA+Sy-AH-based membrane, which had an average of 97.4% CaCl_2 and 96.3 % NaCl . The pure water flux and permeate flux of MPD+TEA+Sy-AH based membrane were high, that is $22.5 \text{ L m}^{-2}\text{h}^{-1}$ and $12.5 \text{ L m}^{-2}\text{h}^{-1}$, respectively.

The analysis of MWCO of the TFNC membranes was indicated that the effective pore size of MPD+TEA+Sy-AH was less than 1.3 nm while the effective pore size of PIP+TEA+NaOH was around 1.8 nm. The results of MWCO values have matched the performance of salt ions rejection (divalent or monovalent).

The filtration experiments of the real seawater indicated that the TFNC membranes were not able to retain a sufficient amount of salt ions at the first attempt. For this reason, the combination of circulated feed seawater was used to retain a higher amount of salt ions. As a result, 80 % of the salt ions were retained from the original seawater. The results of the ion-exchange chromatography analysis of the original and obtained permeate water matched the conductivity values.

One of the other advantages of the TFNC membranes were revealed by liquid chromatography analysis of permeate water. The results of the analysis showed that the amount of the residual

chemical, which might be released from the membrane itself, was not observed except the trace amount of TEA (0.1 mg/L after 5 hours pure water filtration).

CHAPTER 5

GENERAL CONCLUSION

Electrospinning has been already adapted to industrial production by the new technological equipment, and production of electrospun nanofibrous layers has become easier than ever before. Unfortunately, weak mechanical properties of electrospun layers have been delaying to find a place in the final product. The most convenient way to use electrospun nanofibrous materials is to combine nanofibrous materials with another material or surface. However, its easy-deformable structure has limited the manipulation of nanofibrous material.

In this thesis, the mechanical issues of nanofibrous materials is overcome by a lamination method. It is essential to avoid any damage to the nanofibrous structure during the lamination process. Therefore, choosing of lamination technique has also a significant impact on the final structure of supporting material. The polyamide 6 nanofibrous layer, which was prepared in large scale electrospinning equipment, was transferred gently onto polypropylene/polyethylene bi-component spunbond nonwoven fabric under heat and pressure treatment using a lamination machine. The prepared nonwoven and nanofibrous scaffold showed excellent adhesion and high mechanical strength. The thin film nanofibrous composite membranes exhibited high mechanical properties and resisted an applied pressure of 4.8 bar in all of the filtration experiments.

It was necessary to cover NNC scaffold surface with thin active barrier layer before use it in the liquid filtration for separation of salt ions. Therefore, polyamide active barrier layer was formed onto NNC scaffold via interfacial polymerization method. The first attempt of formation of PA active layer performed promising flux and rejection performance when MgSO_4 and NaCl used for the feed solutions. Thin film nanofibrous composite membranes, which were optimized by various IP reaction parameters, were able to compare with the commercial membranes without any complex additives or modifications. The TFNC membranes were used as a media filter in all filtration process without having any mechanical problems.

The further work was related to the improvement of filtration performance of TFNC membranes. The basic two additives (surfactants and acid acceptor) had a significant effect on filtration performance of the TFNC membranes. Surfactant-added membranes reached to highest rejection and flux values, which were obtained in this thesis.

Poly(piperazine amide) based membrane were able to retain divalent salt ions (more than 98%) due to the electrostatic repulsion mechanism of the active layer. Poly(*m*-phenylenediamine) based membrane was able to retain both monovalent and divalent salt ions (around 96% – 98%) due to the size exclusion mechanism.

At the first attempt of desalination of real seawater was failed to retain sufficient amount of salt ions due to the high salt content of the feed seawater and incapable filtration with the dead-end cell. This problem was overcome using the feed seawater repeatedly. TFNC membranes performed that they were capable of retaining a high amount of salt from seawater. However, the low flux performance due to the dead-end filtration method was only the biggest obstacle against to TFNC membranes during the filtration of seawater. TFNC membranes were retained 80% of salt ions from seawater.

The one of the main advantage of the usage of nanofibrous membranes as supporting material instead of phase-inverted membranes is the economic side of productions. The phase-inverted membranes usually need high concentrated solutions (15 – 30 % wt.) which are also expensive polymers (PVDF, PES, PSF). We indicated that the low concentration of polymers (8 % wt.) was enough to obtain 150 nm fiber diameters and less than 1 μ average pore size for the formation of PA active barrier layer. Also the water consumption (becomes waste water) as a nonsolvent in the polymer, solvent and nonsolvent system in phase inversion method that is another issue.

Only one case the speed of production of phase inversion method can be faster than electrospinning method due to the rapid reaction between solvent and nonsolvent system. However, with high technology equipment of electrospinning equipment provides large (industrial) amount of product at less time. The electrospinning system can gather nonwoven and nanofibrous materials in one-step than lamination method and interfacial polymerization can be applied continually after spinning.

This thesis indicated that electrospun nanofibres are promising candidates for use as new high-performance nanofiltration membranes due to their high flux and ion rejection.

There are several ideas to do for future work in the sight of this thesis. Those ideas have brought the new questions together with them:

1. Using the cross-flow filtration equipment and investigating its effects on the filtration performance.

2. Varying the type of lamination method obtain better supporting material and filtration properties. There are many ways to combine nonwoven and nanofibrous materials such as dot lamination and using adhesive webs, etc.
3. Using a different kind of polymers observe the effect on the filtration performance.
4. Using the additive of the complex compound into aqueous and organic solutions and studying its effects on the filtration performance.
5. Using the different area weight of nonwoven or nanofibrous fabric and observing the effects of filtration performance.

REFERENCES

- AKALEH, A., D.C. SHERRINGTON Recent developments in the application of functionalized polymers in organic synthesis. *Polymer*, 24/1983(11), 1369-1386.
- ALSARI, A. M., K. C. KHULBE AND T. MATSUURA The effect of sodium dodecyl sulfate solutions as gelation media on the formation of PES membranes. *Journal of Membrane Science*, 7/15/ 2001, 188(2), 279-293.
- ANTON, F. Process and apparatus for preparing artificial threads. In.: US Patents US 1975504 A, 1934.
- AUSSAWASATHIEN, D., C. TEERAWATTANANON AND A. VONGACHARIYA Separation of micron to sub-micron particles from water: Electrospun nylon-6 nanofibrous membranes as pre-filters. *Journal of Membrane Science*, 5/1/ 2008, 315(1-2), 11-19.
- BAKER, R. W. *Membrane Technology and Applications*. Edition ed.: Wiley, 2012. ISBN 9781118359693.
- BUCH, P.R., D. J. MOHAN, A.V.R. REDDY Preparation, characterization and chlorine stability of aromatic-cycloaliphatic polyamide thin film composite membranes. *Journal of Membrane Science* 309/2008(1-2), 36.
- BUI, N.-N., M. L. LIND, E. M. V. HOEK AND J. R. MCCUTCHEON Electrospun nanofiber supported thin film composite membranes for engineered osmosis. *Journal of Membrane Science*, 12/1/ 2011, 385-386, 10-19.
- CADOTTE, J. E. Interfacially synthesized reverse osmosis membrane. In.: US Patents US 4277344 A, 1981.
- CADOTTE, J. E., R. J. PETERSEN, R. E. LARSON AND E. E. ERICKSON A new thin-film composite seawater reverse osmosis membrane. *Desalination*, 1980/01/01 1980, 32, 25-31.
- CADOTTE, J. E., K.E. COBAIN, R.H. FORESTER, and R. J. PETERSEN Continued Evaluation of In Situ-Formed Condensation Polymers for Reverse Osmosis Membranes. available from National Technical Information Center, Springfield, VA, Report No. PB-253/193, April 1976.
- CADOTTE, J. E., R. S. KING, R. J. MAJERLE AND R. J. PETERSEN Interfacial Synthesis in the Preparation of Reverse Osmosis Membranes, *Journal of Macromolecular Science: Part A - Chemistry: Pure and Applied Chemistry*. 15/51981b, 727-755.
- CHEN, G., S. LI, X. ZHANG, S. ZHANG Novel thin-film composite membranes with improved water flux from sulfonated cardo poly(arylene ether sulfone) bearing pendant amino groups. *Journal of Membrane Science*, 310/2008, 102-109.
- CHU, B., B. S. HSIAO, D. FANG, K.S. KIM High flux and low fouling filtration media. In US Patent, US 8222166 B2. New York, 2012.
- CHOI, S.-S., Y. S. LEE, C. W. JOO, S. G. LEE, et al. Electrospun PVDF nanofiber web as polymer electrolyte or separator. *Electrochimica Acta*, 11/30/ 2004, 50(2-3), 339-343.
- COOLEY, J.F. Apparatus for electrically dispersing fluids. In: US Patent, US692631, Boston, 1902.

DARRELL, H. R. AND C. IKSOO Nanometre diameter fibres of polymer, produced by electrospinning. *Nanotechnology*, 1996, 7(3), 216.

DRELICH, J. AND E. CHIBOWSKI Superhydrophilic and Superwetting Surfaces: Definition and Mechanisms of Control. *Langmuir*, 2010/12/21 2010, 26(24), 18621-18623.

FACCINI, M., C. VAQUERO, D. AMANTIA Development of protective clothing against nanoparticle based on electrospun nanofibers. *Journal of Nanomaterials*, Volume 2012 (2012), Article ID 892894, 9 pages.

FAN, Z., Z. WANG, M. DUAN, J. WANG, et al. Preparation and characterization of polyaniline/polysulfone nanocomposite ultrafiltration membrane. *Journal of Membrane Science*, 3/5/ 2008, 310(1–2), 402-408.

FENG, C., K. C. KHULBE, T. MATSUURA Recent progress in the preparation, characterization, and applications of nanofibers and nanofiber membranes via electrospinning/interfacial polymerization. *Journal of Applied Polymer Science*, 115/2010, 756-776.

FREGER, V. J. GILRON, S. BELFER. TFC polyamide membranes modified by grafting of hydrophilic polymers: an FT-IR/AFM/TEM study. *Journal of Membrane Science*, 209/2002(1), 283–292.

FREGER, V. Nanoscale Heterogeneity of Polyamide Membranes Formed by Interfacial Polymerization. *Langmuir*, 2003/05/01 2003, 19(11), 4791-4797.

GAUTAM, A. K., C. LAI, H. FONG AND T. J. MENKHAUS Electrospun polyimide nanofiber membranes for high flux and low fouling microfiltration applications. *Journal of Membrane Science*, 9/15/ 2014, 466, 142-150.

GILBERT, G. AND MOTTELAY, P.F. William Gilbert of Colchester, physician of London: On the load stone and magnetic bodies, John Wiley and Sons, 368/1893 accessed 17th September 2016.

GOPAL, R., S. KAUR, C. Y. FENG, C. CHAN, et al. Electrospun nanofibrous polysulfone membranes as pre-filters: Particulate removal. *Journal of Membrane Science*, 2/15/ 2007, 289(1–2), 210-219.

GOPAL, R., S. KAUR, Z. MA, C. CHAN, et al. Electrospun nanofibrous filtration membrane. *Journal of Membrane Science*, 9/15/ 2006, 281(1–2), 581-586.

GOSH, A.K., B.H. JEONG, X. HUANG, E. M.V. HOEK Impacts of reaction and curing conditions on polyamide composite reverse osmosis membrane properties. *Journal of Membrane Science*, 311/2008, 34-45.

HERMANS, S., R. BERNSTEIN, A. VOLODIN AND I. F. J. VANKELECOM Study of synthesis parameters and active layer morphology of interfacially polymerized polyamide–polysulfone membranes. *Reactive and Functional Polymers*, 1// 2015, 86, 199-208.

HIRAO, A., S. NAKAHAMA, M. TAKAHASHI, et al. Additive effect of poly(ethylene oxide), 3.Retardation effect of poly(ethylene oxide) in the reduction of aldehydes and ketones with sodium borohydride. *Macromolecular Chemistry and Physics*, 179/1978, 2343-2347.

HOOVER, L.A., J. D. SCHIFFMAN, M. ELIMELECH Nanofibers in thin-film composite membrane support layers: Enabling expanded application of forward and pressure retarded osmosis. *Desalination*, 308/2013,73-81.

HUANG, L., J. T. ARENA, S. S. MANICKAM, X. JIANG, et al. Improved mechanical properties and hydrophilicity of electrospun nanofiber membranes for filtration applications by dopamine modification. *Journal of Membrane Science*, 6/15/ 2014, 460, 241-249.

HUANG, L., S. S. MANICKAM AND J. R. MCCUTCHEON Increasing strength of electrospun nanofiber membranes for water filtration using solvent vapor. *Journal of Membrane Science*, 6/1/ 2013, 436, 213-220.

HUANG, L. AND J. R. MCCUTCHEON Hydrophilic nylon 6,6 nanofibers supported thin film composite membranes for engineered osmosis. *Journal of Membrane Science*, 5/1/ 2014, 457, 162-169.

JIN, Y., Z. SU, Effects of polymerization conditions on hydrophilic groups in aromatic polyamide thin films. *Journal of Membrane Science*, 330/2009, 175-179.

JIRSAK, O., F. SANETRNIK, D. LUKAS, V. KOTEK, et al. Method of nanofibres production from a polymer solution using electrostatic spinning and a device for carrying out the method. In.: US Patents, 2005.

JIRSÁK, O. AND L. C. WADSWORTH *Nonwoven Textiles*. Edition ed.: Carolina Academic Press, 1999. ISBN 9780890899878.

KANAFCHIAN, M., M. VALIZADEH, A. K. HAGHI A study on the effects of laminating temperature on the polymeric nanofiber web. *Korean Journal of Chemical Engineering*, 28/2011(2), 445-448.

KANG, Y. K., C. H. PARK, J. KIM, and T. J. KANG Application of electrospun polyurethane web to breathable water-proof fabrics. *Fibers and Polymers*, 8/2007(5), 564–570.

KAO, S.T., S.H. HUANG, D.J. LIAW, W.C. CHAO Interfacially polymerized thin-film composite polyamide membrane: positron annihilation spectroscopic study, characterization and pervaporation performance. *Polymer Journal*, 42/2010, 242-248.

KAUR, S., R. BARHATE, S. SUNDARRAJAN, T. MATSUURA, et al. Hot pressing of electrospun membrane composite and its influence on separation performance on thin film composite nanofiltration membrane. *Desalination*, 9/15/ 2011, 279(1–3), 201-209.

KAUR, S., Z. MA, R. GOPAL, G. SINGH, et al. Plasma-Induced Graft Copolymerization of Poly(methacrylic acid) on Electrospun Poly(vinylidene fluoride) Nanofiber Membrane. *Langmuir*, 2007/12/01 2007, 23(26), 13085-13092.

KAUR, S., D. RANA, T. MATSUURA, S. SUNDARRAJAN, et al. Preparation and characterization of surface modified electrospun membranes for higher filtration flux. *Journal of Membrane Science*, 2/15/ 2012a, 390–391, 235-242.

KAUR, S., S. SUNDARRAJAN, D. RANA, T. MATSUURA, et al. Influence of electrospun fiber size on the separation efficiency of thin film nanofiltration composite membrane. *Journal of Membrane Science*, 3/1/ 2012b, 392–393, 101-111.

- KHAN, R. Supported TritonX-100 Polyaniline Nano-Porous Electrically Active Film onto Indium-Tin-Oxide Probe for Sensors Application. *Advances in Chemical Engineering and Science*, 2011, 2011(1), 140-146.
- KIM, G. M., R. LACH, G. H. MICHLER, P. POTSCHEKE, et al. Relationships between phase morphology and deformation mechanisms in polymer nanocomposite nanofibres prepared by an electrospinning process. *Nanotechnology*, Feb 28 2006a, 17(4), 963-972.
- KIM, I.-C., J. JEGAL AND K.-H. LEE Effect of aqueous and organic solutions on the performance of polyamide thin-film-composite nanofiltration membranes. *Journal of Polymer Science Part B: Polymer Physics*, 2002, 40(19), 2151-2163.
- KIM, I.-D., A. ROTHSCHILD, B. H. LEE, D. Y. KIM, et al. Ultrasensitive Chemiresistors Based on Electrospun TiO₂ Nanofibers. *Nano Letters*, 2006/09/01 2006b, 6(9), 2009-2013.
- KIM, C.K., J.H. KIM, I.J. ROH, J.J. KIM The changes of membrane performance with polyamide molecular structure in the reverse osmosis process. *Journal of Membrane Science*, 165/2000, 189-199.
- KONAGAYA, S., H. KUZUMOTO, O. WATANABE. New reverse osmosis membrane materials with higher resistance to chlorine. *Journal of Applied Polymer Science*. 75/2000, 1357-1364.
- KONG, C., T. SHINTANI, T. KAMADA, V. FREGER, T. TSURU Co-solvent-mediated synthesis of thin polyamide membranes. *Journal of Membrane Science*, 384/2011, 10-16.
- KUEHNE, M. A., R. Q. SONG, N. N. LI AND R. J. PETERSEN Flux enhancement in TFC RO membranes. *Environmental Progress*, 2001, 20(1), 23-26.
- KWAK, S.-Y., S. G. JUNG AND S. H. KIM Structure-Motion-Performance Relationship of Flux-Enhanced Reverse Osmosis (RO) Membranes Composed of Aromatic Polyamide Thin Films. *Environmental Science & Technology*, 2001/11/01 2001, 35(21), 4334-4340.
- LEE, S., D. KIMURA, A. YOKOYAMA, K. H. LEE, J. C. PARK, and I. S. KIM The effects of laundering on the mechanical properties of mass-produced nanofiber web for use in wear. *Textile Research Journal*, 79/2009 (12), 1085-1090.
- LEE, S., D. KIMURA, K. H. LEE, J. C. PARK, and I. S. KIM The effect of laundering on the thermal and water transfer properties of mass-produced laminated nanofiber web for use in wear. *Textile Research Journal*, 88/2010(99), 1085-1090.
- LI, M., D. WANG, R. XIAO, G. SUN, et al. A novel high flux poly(trimethylene terephthalate) nanofiber membrane for microfiltration media. *Separation and Purification Technology*, 9/15/ 2013, 116, 199-205.
- LI, W., L. LOU, Y. HAI, C. FU, et al. Polyamide thin film composite membrane using mixed amines of thiourea and m-phenylenediamine. *RSC Advances*, 2015, 5(67), 54125-54132.
- LI, L.S, X. ZHANG, G.ZHENG. Polyamide thin film composite membranes prepared from isomeric biphenyl tetraacyl chloride and m-phenylenediamine. *Journal of Membrane Science*, 315/2008, 20-27.
- LIBRARY, C.-P. T. *Laboratory Filtration Selection Guide*. In., 2016, vol. 2016.

LIN, J. K., M. R. LADISCH, J. A. PATTERSON AND C. H. NOLLER Determining pore size distribution in wet cellulose by measuring solute exclusion using a differential refractometer. *Biotechnol Bioeng*, Jun 1987, 29(8), 976-981.

LO, R., A. BHATTACHARYA AND B. GANGULY Probing the selective salt rejection behavior of thin film composite membranes: A DFT study. *Journal of Membrane Science*, 6/1/ 2013, 436, 90-96.

MA, Z., M. KOTAKI AND S. RAMAKRISHNA Electrospun cellulose nanofiber as affinity membrane. *Journal of Membrane Science*, 11/15/ 2005, 265(1-2), 115-123.

MA, Z., M. KOTAKI AND S. RAMAKRISHNA Surface modified nonwoven polysulphone (PSU) fiber mesh by electrospinning: A novel affinity membrane. *Journal of Membrane Science*, 3/15/ 2006, 272(1-2), 179-187.

MANITO PEREIRA, A. A., J. M. TIMMER AND J. J. KEURENTJES Swelling and compaction of nanofiltration membranes in a non-aqueous environment. *Desalination*, 2006 2006, 200(1-3), 381.

MANSOURPANAH, Y., K. ALIZADEH, S. S. MADAENI, A. RAHIMPOUR, et al. Using different surfactants for changing the properties of poly(piperazineamide) TFC nanofiltration membranes. *Desalination*, 4/15/ 2011, 271(1-3), 169-177.

MANSOURPANAH, Y., S. S. MADAENI AND A. RAHIMPOUR Fabrication and development of interfacial polymerized thin-film composite nanofiltration membrane using different surfactants in organic phase; study of morphology and performance. *Journal of Membrane Science*, 11/1/ 2009, 343(1-2), 219-228.

MARIËN, H., I. VANKELECOM, S. HERMANS Improved method for synthesis of polyamide composite membranes. Katholieke Universiteit Leuven Ku Leuven Research & Development, In: Patent WO2016070247 A1, 2015.

MCGOVERN, RONAN KILLIAN, D. MCCONNON, V. LIENHARD AND H. JOHN 2015. The effect of very high hydraulic pressure on the permeability and salt rejection of reverse osmosis membranes. In *Proceedings of the 2015 IDA World Congress on Desalination and Water Reuse*, San Diego, California, USA2015 International Desalination Association.

MICKOLS, W.E., Composite membrane and method for making the same. In: US Patent 6,562,266, 2003.

MOHAN, D. J. AND L. KULLOVÁ A study on the relationship between preparation condition and properties/performance of polyamide TFC membrane by IR, DSC, TGA, and SEM techniques. *Desalination and Water Treatment*, 2013/01/01 2013, 51(1-3), 586-596.

MORTON, W.J. Method of dispersing fluids. In: US Patent US705691, Newyork, 1902.

MULDER, M. *Basic Principles of Membrane Technology*. Edition ed.: Springer, 1996. ISBN 9780792342472.

NORTON, C.L. Method of and apparatus for producing fibrous or filamentary material. In: US Patent US2048651, Massachusetts, 1936.

ODIAN, G., *Principles of Polymerization*, Fourth Edition. John Wiley & Sons, Inc., Hoboken, New Jersey. Chapter 9, 2004, p 770.

OSTERMANN, R., D. LI, Y. YIN, J. T. MCCANN, et al. V2O5 Nanorods on TiO2 Nanofibers: A New Class of Hierarchical Nanostructures Enabled by Electrospinning and Calcination. *Nano Letters*, 2006/06/01 2006, 6(6), 1297-1302.

PERSSON, K. M., V. GEKAS AND G. TRÄGÅRDH Study of membrane compaction and its influence on ultrafiltration water permeability. *Journal of Membrane Science*, 4/14/ 1995, 100(2), 155-162.

PETERSEN, R. J. Composite reverse osmosis and nanofiltration membranes. *Journal of Membrane Science*, 1993/08/12 1993, 83(1), 81-150.

RAO, A.P., S.V. JOSHI, J.J. TRIVEDI, C.V. DEVMURARI, V.J. SHAH Structure–performance correlation of polyamide thin film composite membranes: effect of coating conditions on film formation. *Journal of Membrane Science*, 211/2003, 13-14.

RAO, A.P., N.V. DESAI, R. RANGARAJAN Interfacially synthesized thin film composite RO membranes for seawater desalination. *Journal of Membrane Science*, 124/1997, 263-272.

RIBEIRO, J. *Desalination Technology: Survey and Prospects*. Edition ed.: IPTS, 1996.

RITCHAROEN, W., P. SUPAPHOL AND P. PAVASANT Development of polyelectrolyte multilayer-coated electrospun cellulose acetate fiber mat as composite membranes. *European Polymer Journal*, 12// 2008, 44(12), 3963-3968.

SAGLE, A.C., E.M. VAN WAGNER, H. JU, B.D. MCCLOSKEY, B.D. FREEMAN, M.M. SHARMA PEG-coated reverse osmosis membranes: desalination properties and fouling resistance, *Journal of Membrane Science*, 340/2009, 92-108.

SAHA, N.K., S.V. JOSHI Performance evaluation of thin film composite polyamide nanofiltration membrane with variation in monomer type. *Journal of Membrane Science*, 342/2009, 60-69.

SEN, R., B. ZHAO, D. PEREA, M. E. ITKIS, et al. Preparation of Single-Walled Carbon Nanotube Reinforced Polystyrene and Polyurethane Nanofibers and Membranes by Electrospinning. *Nano Letters*, 2004/03/01 2004, 4(3), 459-464.

SUNDARRAJAN, S AND S. RAMAKRISHNA New directions in nanofiltration applications — Are nanofibers the right materials as membranes in desalination?. *Desalination*, 308/2013, 198-208.

TANG, B., X. HUO, P. WU. Study on a novel polyester composite nanofiltration membrane by interfacial polymerization of triethanolamine (TEOA) and trimesoyl chloride (TMC) I. Preparation, characterization and nanofiltration properties test of membrane, *Journal of Membrane Science*, 320/2008, 198–205.

TIMOTHY H., G. AND G. KRISTINE M. Nanofiber Webs from Electrospinning In *Proceedings of the Nonwovens in Filtration - Fifth International Conference*, Stuttgart, Germany, March 2003.

TSAI, H. A., L. D. LI, K. R. LEE, Y. C. WANG, et al. Effect of surfactant addition on the morphology and pervaporation performance of asymmetric polysulfone membranes. *Journal of Membrane Science*, 8/15/ 2000, 176(1), 97-103.

TIAN, M., C. QIU, Y. LIAO, S. CHOU, R. WANG Preparation of polyamide thin film composite forward osmosis membranes using electrospun polyvinylidene fluoride (PVDF) nanofibers as substrates. *Separation and Purification Technology*, 118/2013, 727-736.

The Industrial Technology Research Institute. PolyE membrane technology aims to combat worsening fresh-water crisis worldwide. *Journal of Membrane Science*, 2/2016 p.10.

TOMOI, M. and W. T. FORD Polymeric phase transfer catalysts, Chapter 5 in *Synthesis and Separations Using Functional Polymers*, D. C. Sherrington and P. Hodge, eds., Wiley, New York, 1988.

WANG, D.-M., F.-C. LIN, T.-T. WU AND J.-Y. LAI Formation mechanism of the macrovoids induced by surfactant additives. *Journal of Membrane Science*, 5/13/ 1998, 142(2), 191-204.

WANG, X., D. FANG, K. YOON, B. S. HSIAO, et al. High performance ultrafiltration composite membranes based on poly(vinyl alcohol) hydrogel coating on crosslinked nanofibrous poly(vinyl alcohol) scaffold. *Journal of Membrane Science*, 7/5/ 2006, 278(1-2), 261-268.

WANG, X., K. ZHANG, M. ZHU, B. S. HSIAO, et al. Enhanced Mechanical Performance of Self-Bundled Electrospun Fiber Yarns via Post-Treatments. *Macromolecular Rapid Communications*, 2008, 29(10), 826-831.

WANG, H., L. LI, X. ZHANG, S. ZHANG. Polyamide thin-film composite membranes prepared from a novel triamine 3,5-diamino-N-(4-aminophenyl)-benzamide monomer and m-phenylenediamine. *Journal of Membrane Science*, 353/2010, 78-84.

WANG, X., T.M. YEH, Z. WANG, R. YANG, R. WANG, H. MA, B. S. HSIAO, B. CHU Nanofiltration membranes prepared by interfacial polymerization on thin-film nanofibrous composite scaffold. *Polymer*, 55/2014, 1358-1366.

WIKIPEDIA. drinking water. In., 2015, vol. 2015.

WITTBECKER, E. L. AND P. W. MORGAN Interfacial polycondensation. I. *Journal of Polymer Science*, 1959, 40(137), 289-297.

XIANG, J., Z. XIE, M. HOANG, D. NG, et al. Effect of ammonium salts on the properties of poly(piperazineamide) thin film composite nanofiltration membrane. *Journal of Membrane Science*, 9/1/ 2014, 465, 34-40.

XIANG, J., Z. XIE, M. HOANG AND K. ZHANG Effect of amine salt surfactants on the performance of thin film composite poly(piperazine-amide) nanofiltration membranes. *Desalination*, 4/15/ 2013, 315, 156-163.

VYAS, B.B., P. RAY. Preparation of nanofiltration membranes and relating surface chemistry with potential and topography: Application in separation and desalting of amino acids. *Desalination*, 362/2015, 104-116.

YALCINKAYA, B., AND F. CENGIZ-CALLIOGLU. The effect of supporting material type on the nanofiber morphology. In *3rd International Conference on Nanocon*. Brno, Czech Republic: Tanger, 2011.

YALCINKAYA, B., F. CENGIZ CALLIOGLU AND F. YENER Measurement and analysis of jet current and jet life in roller electrospinning of polyurethane. *Textile Research Journal*, March 27, 2014 2014.

YALCINKAYA, B., F. YENER, F. CENGIZ-CALLIOGLU AND O. JIRSAK. Effect of concentration and salt additive on Taylor cone structure. In *4th International Conference on Nanocon*. Brno Czech Republic: Tanger, 2012, p. 200-203.

YALCINKAYA, F., B. YALCINKAYA AND O. JIRSAK Influence of Salts on Electrospinning of Aqueous and Nonaqueous Polymer Solutions. *Journal of Nanomaterials*, 2015, 2015, 12.

YAMASAKI, A. R. K. TYAGI, A. E. FOU DA, K. JONNASON, and T. MATSUURA Effect of Surfactant as an Additive on the Formation of Asymmetric Polysulfone Membranes for Gas Separation. *Membrane formation and modification*, Chapter 6. 744/20087-95.

YENER, F. AND B. YALCINKAYA. Electrospinning of polyvinyl butyral in different solvents. In *e-Polymers*. 2013, vol. 13, p. 229.

YOON, K., B. S. HSIAO AND B. CHU Formation of functional polyethersulfone electrospun membrane for water purification by mixed solvent and oxidation processes. *Polymer*, 6/19/ 2009a, 50(13), 2893-2899.

YOON, K., B. S. HSIAO AND B. CHU High flux nanofiltration membranes based on interfacially polymerized polyamide barrier layer on polyacrylonitrile nanofibrous scaffolds. *Journal of Membrane Science*, 1/20/ 2009b, 326(2), 484-492.

YOON, K., K. KIM, X. WANG, D. FANG, et al. High flux ultrafiltration membranes based on electrospun nanofibrous PAN scaffolds and chitosan coating. *Polymer*, 3/22/ 2006, 47(7), 2434-2441.

YOON, B., AND S. LEE Designing waterproof breathable materials based on electrospun nanofibers and assessing the performance characteristics. *Fibers and Polymers*, 12/2011(1), 57-64.

YUNG, L., H. MA, X. WANG, K. YOON, et al. Fabrication of thin-film nanofibrous composite membranes by interfacial polymerization using ionic liquids as additives. *Journal of Membrane Science*, 12/1/ 2010, 365(1-2), 52-58.

ZELNY, J. The electrical discharge from liquid points and a hydrostatic method of measuring the electric intensity at their surfaces. *Physical Review*, 3/2/ 1914, 69-91